NOTICE

The quality of this microfiche is heavily dependent upon the quality of the original thesis submitted for microfilming. Every effort has been made to ensure the highest quality of reproduction possible.

If pages are missing, contact the university which granted the degree.

Some pages may have indistinct print especially if the original pages were typed with a poor typewriter ribbon or if the university sent us a poor photocopy.

Previously copyrighted materials (journal articles, published tests, etc.) are not filmed.

Reproduction in full or in part of this film is governed by the Canadian Copyright Act, R.S.C. 1970, c. C-30. Please read the authorization forms which accompany this thesis.

THIS DISSERTATION
HAS BEEN MICROFILMED
EXACTLY AS RECEIVED

AVIS

La qualité de cette microfiche dépend grandement de la qualité de la thèse soumise au microfilmage. Nous avons tout fait pour assurer une qualité supérieure de reproduction.

S'il manque des pages, veuillez communiquer avec l'université qui a conféré le grade.

La qualité d'impression de certaines pages peut laisser à désirer, surtout si les pages originales ont été dactylographiées à l'aide d'un ruban usé ou si l'université nous a fait parvenir une photocopie de mauvaise qualité.

Les documents qui font déjà l'objet d'un droit d'auteur (articles de revue, examens publiés, etc.) ne sont pas microfilmés.

La reproduction, même partielle, de ce microfilm est soumise à la Loi canadienne sur le droit d'auteur, SRC 1970, c. C-30. Veuillez prendre connaissance des formules d'autorisation qui accompagnent cette thèse.

LA THÈSE A ÉTÉ
MICROFILMÉE TELLE QUE
NOUS L'AVONS REÇUE

UNIVERSITÉ D'OTTAWA
UNIVERSITY OF OTTAWA

PYROLYSIS OF METHANE

by

Chin-Jung Chen, M.Sc.

A thesis submitted to the School of Graduate Studies in partial fulfillment of the requirements for the degree of Ph.D. in Chemistry

UNIVERSITY OF OTTAWA

OTTAWA, CANADA, 1976

ACKNOWLEDGMENTS

This work was conducted under the direction of Professor M. H. Back and Dr. R. A. Back (NRC), whose encouragement, assistance and constant interest throughout the course of study are most gratefully appreciated. With deep gratitude I wish to thank them for their patience, understanding, and readiness for discussion in preparing this thesis. Appreciation is also due to the staff of the National Research Council for sharing their broad scientific knowledge and valuable assistance. I also wish to express my sincere acknowledgment to Professor K. J. Laidler for his teaching on the Theories of Chemical Kinetics.

TABLE OF CONTENTS

LIST OF TABLES

LIST OF FIGURES

ABSTRACT

The pyrolysis of methane was studied in a static system over the pressure range 25 to 740 Torr and at temperatures of 995, 1038, 1068 and 1103 K. It was concluded that the initial stages of the reaction can be described by a simple homogeneous, nonchain radical mechanism,

[1] $CH_4 \rightarrow CH_3 + H$

[2] $H + CH_4 \rightarrow H_2 + CH_3$

[3] $2CH_3 \rightarrow C_2H_6$

[4] $CH_3 + C_2H_6 \rightarrow CH_4 + C_2H_5$

[5] $C_2H_5 \rightarrow C_2H_4 + H$

Initial rates of the reaction were measured, based on analysis of hydrogen, ethane and ethylene and the first-order rate constant for reaction [1] was found to be pressure dependent. A model of unimolecular decomposition was proposed based on RRKM theory. Comparison of previous shock tube and flow system data at temperatures up to 2200K showed good agreement with values calculated from this model. It was concluded that in all previous shock tube studies the initial dissociation was in its pressure-dependent region, and that in almost all of the studies carried out in conventional static and flow systems, rates of the reaction were measured in the region where autocatalysis was important.

The rate constant for the hydrogen abstraction reaction,

reaction 4, was measured at 880, 995, 1038 and 1068 K. The results were in good agreement with previous studies in different systems, and provide additional evidence that the Arrhenius activation energy for this reaction is temperature-dependent over the range 300-1200 K.

A mechanism was proposed to account for the observed reaction products up to all of the C_3 hydrocarbons. Possible reactions causing autocatalysis were explored.

A technique was developed to monitor the formation of the carbon film during the pyrolysis of methane. This method was capable of measuring a deposit of carbon equivalent to less than one mono-layer of graphite on the walls of the reaction vessel. Application of this method may provide useful information in studies of hydrocarbon pyrolysis.

CHAPTER ONE: INTRODUCTION

I. General introduction.

The mechanism of the pyrolysis of methane has been the subject of study by many investigators. Methane is the simplest and most stable hydrocarbon. One might expect that its decomposition would also be simple and easy to interpret. Although the results of many studies have been reported over the past 100 years we are still far from understanding the mechanism of the reaction. Since there are only C-H bonds in methane its decomposition requires a relatively high temperature compared to other paraffins which dissociate through the rupture of a C-C bond. The initial conversion to ethane and hydrogen is rapidly followed by successive dehydrogenation steps. Although a general picture was well established for the over-all reaction,

$$2CH_4 \xrightarrow{-H_2} C_2H_6 \xrightarrow{-H_2} C_2H_4 \xrightarrow{-H_2} C_2H_2 \xrightarrow{-H_2} \frac{2}{n}C_n$$

the reaction products other than C_2 hydrocarbons have never been carefully measured nor have the individual reactions involved been established. All the products of higher C number are less stable than methane and the secondary and tertiary reactions become important even at very low conversions. The pyrolysis thus becomes a complex system and a satisfactory understanding of it has proved extremely difficult.

II.. Static System.

Between 1863 and 1869, Berthelot (1a) made a comprehensive study of the pyrolyses of hydrocarbons. He postulated that a hydrocarbon would never directly be resolved into its elements, but that the reaction would always involve either a polymerization or a coalition of two or more molecules to form a fused hydrocarbon with elimination of hydrogen. These fused molecules would in turn undergo a series of similar reactions until carbon appeared as the final product. From Berthelot's generalization, the methane pyrolysis can be written as follows,

$$2CH_4 \rightarrow C_2H_6 + H_2$$

$$C_2H_6 \rightarrow C_2H_4 + H_2 \quad \text{or} \quad 2C_2H_6 \rightarrow C_4H_{10} + H_2$$

$$C_2H_4 \rightarrow C_2H_2 + H_2 \quad \text{or} \quad 2C_2H_4 \rightarrow C_4H_6 + H_2$$

$$\text{and} \quad \eta C_2H_2 \rightarrow \tfrac{\eta}{3}C_6H_6 \rightarrow \tfrac{\eta}{5}C_{10}H_{10} \rightarrow \tfrac{\eta}{5}C_{10} + \eta H_2$$

From today's view point, even though Berthelot's theory might appear insufficient and inaccurate it does express the general character of the methane decomposition in the gas phase.

Following earlier work by several investigators (1), Kassel (2) made a thorough kinetic study of the pyrolysis of methane in the temperature range 973-1123 K. From the measurement of pressure change, the rate was obtained after a short induction period. It was concluded that the primary reaction was homogeneous and kinetically first-order with E = 79.4 kcal/mole and A = 5×10^{11}/sec. By comparing the estimated heats of reactions, Kassel considered

methylene formation as the primary reaction followed by its reaction with methane to form ethane,

$$CH_4 \rightarrow CH_2 + H_2$$

$$CH_2 + CH_4 \rightarrow C_2H_6$$

Increasing the S/V ratio 20-fold did not have any effect on the reaction rate. Kassel also observed that the reaction rate was greatly retarded by the addition of hydrogen.

Kodama (3) investigated the induction period by observing the pressure change and found that it was quite reproducible if the reaction vessel was conditioned by introducing air into it to burn off carbon. He observed that the induction period was reduced by increasing pressure of methane or increasing temperature, and was increased by increasing S/V ratio. If the pyrolysis took place in a carbon coated vessel the induction period was greatly reduced.

Anisonyan (4) also studied the pyrolysis of methane in the temperature range 1023-1373 K. The reaction rate was accelerated by addition of ethylene, propylene and benzene. These observations agreed with Kodama's (3) earlier results.

More recent studies on the pyrolysis of pure methane have been made by Schneider (5) in both static and flow systems. He concluded that two parallel simultaneous processes occured: (a) initial formation of a methylene radical followed by disproportionation with another methylene radical with methane to produce acetylene or ethane and (b) a chain reaction propagated by reaction of a methyl

radical with methane to produce ethane. The ethane was further dehydrogenated through ethylene, acetylene and finally carbon and hydrogen.

III. Flow System

There is an abundance of literature on the methane pyrolysis using flow reactors (6). The results from earlier studies are generally unreliable because of difficulties in temperature control and product analysis. The first significant work on product analysis was done by Gordon (7) when he pyrolyzed methane in a clean porcelain tube over the temperature range 1280 to 1348 K. The products with a molecular weight lower than benzene were analyzed using a mass spectrometer. He identified naphthalene, anthracene, phenanthrene and pyrene by their ultraviolet absorption spectra. He observed that the reaction was approximately first-order, was accelerated with increasing extent of decomposition and was catalyzed by the addition of acetylene but not by ethylene. He also found that the reaction was slightly affected by a quartz surface but greatly affected by the porcelain surface. Even at the lowest temperature (1280 K), Gordon did not observe any induction period.

Germain and Vaniscotte (8) studied the reaction between 1273 and 1373 K in a silica reactor. They found that the reaction was not first-order but went through three different stages as the reaction proceeded. The effects of S/V ratio on the reaction were

distinctively different for each stage. In the first stage, the induction period decreased as the S/V ratio increased. In the second or rapid decomposition phase, the rate increased as the S/V ratio increased. In the final or slow decomposition stage, the rate decreased as the S/V ratio increased. They also found that the addition of ethane reduced the induction period, which totally disappeared when 0.5-3% of ethane was added. Added nitrogen was found to increase the reaction rate. They concluded that the pyrolysis of methane was a short-chain radical reaction, partly homogeneous and partly heterogeneous, with an activation energy of 87 kcal/mole. They suggested that the surface of the reactor acted as an initiator in the first stage and as an inhibitor in the final stage, and that ethane was an initiator.

Murgulescu and Schneider (9) studied the reaction in the temperature range 1233-1903 K. They observed that the acetylene yield increased at higher temperature and that low pressure favored acetylene formation at low temperature. They concluded that at 1145 K acetylene rapidly formed aromatic hydrocarbons.

A quite different and important technique was developed by Palmer (10) for the study of carbon film formation during the decomposition of various compounds. The electrical resistance of a carbon film on a glazed porcelain rod centrally located in an annular reactor was used as a measurement of the film thickness. In the methane pyrolysis, the deposition rate of the carbon film was

directly proportional to the rate of methane decomposition in the gas phase. Using this method, Palmer and Hirt (11) obtained a first-order rate constant with E = 101 kcal/mole and A = 10^{14}/sec.

Eisenberg and Bliss (12) made a careful study of the time-course of the methane pyrolysis in a quartz flow reactor at 1373-1473 K. They concluded that the reaction was not of a simple order because they observed an S-shaped growth curve. Together with their other observations that methane concentration affected the rate of reaction in a direct but nonlinear manner, that ethane greatly accelerated the reaction while hydrogen inhibited it, and that the S/V ratio did not affect the rate of decomposition for methane in a smooth fused-quartz reactor, they suggested the acceleration was the result of the following chain propagation

$$CH_3 + CH_4 \rightarrow C_2H_6 + H$$

Palmer, Lahaye and Hou (13) pyrolyzed methane in a porcelain tube at 1323-1523 K. They concluded that (a) the reaction began slowly, accelerated, then decelerated, (b) the rate was approximately first-order despite its complex behavior, (c) vitreous carbon deposited on the wall of the reaction tube and a small amount of soot and tar was collected at the exit, (d) the main gaseous products were acetylene and ethylene with lesser quantities of benzene, (e) hydrogen inhibited the decomposition and ethane accelerated it, (f) the rate was not appreciably affected by the S/V ratio. They explained the acceleration as caused by carbon nuclei in

the gas phase which were formed from light hydrocarbons.

IV. Shock Tube

One of the earliest studies of methane pyrolysis in a shock tube was by Greene, Taylor and Patterson (14) over the temperature 1900-2500 K. They confirmed that the reaction products were ethane, ethylene, acetylene, C-3 hydrocarbons, diacetylene, vinylacetylene, butadiene, butene, butane and minor amounts of carbon black. Glick (15) also studied the reaction in the temperature range 1500-2900 K and obtained first-order rate constants which were in good agreement with those obtained by Kassel at lower temperatures.

Skinner and Ruehrwein (16) pyrolyzed methane-argon mixtures (1-12%) over the temperature range 1200-1800 K and concluded that the reaction was first-order, that ethane was the primary pyrolysis product, and that the rate of the reaction was little affected by the presence of decomposition products. Their first-order rate constant was given by the equation

$$\log k = 14.71 - 101{,}000/2.3RT$$

The following scheme was suggested to account for their observations,

[1] $CH_4 \rightarrow CH_3 + H$

[2] $H + CH_4 \rightarrow CH_3 + H_2$

[3]. $2CH_3 \rightarrow C_2H_6$

in which reaction [1] is rate-determining.

On the other hand, Kevorkian, Heath and Boudart (17) and

Kozlov and Knorre (18) obtained an activation energy of 93 kcal/mole and an A factor of 1.32×10^{14} sec^{-1} for their first-order rate constant. In order to justify this measured activation energy, they proposed that the primary step was decomposition to methylene and molecular hydrogen. The endothermicity of this reaction was thought to be 85 kcal/mole and with an energy barrier of 9 kcal/mole for the reverse reaction, the activation energy for the decomposition would be 94 kcal/mole.

The method of adiabatic compression and expansion was first used by Volokhonovich, Markevich, Masterovoi and Azatyan (19) for the pyrolysis of methane between 1400 and 1673 K. Their first-order rate constant was given by the equation

$$\log k = 13.04 - 101{,}000/2.3RT$$

which was obtained from the initial rate of ethane production. Kontratiev (20), however, reinterpreted Volokhonovich's (19) data using an improved method and obtained the following expression for the rate constant

$$\log k = 15.0 - 103{,}000/2.3RT$$

He concluded that the initial step was decomposition to a methyl radical and a hydrogen atom followed by hydrogen abstraction from methane and combination of two methyl radicals.

Hartig, Troe and Wagner (21) studied the methane decomposition behind reflected shock waves from 1850 to 2500 K. The reaction was followed by measurement of infrared emission from methane

at 3.5 μm, by infrared emission of products at wavelengths between 2.9 and 3.0 μm, and ultraviolet absorption of methyl radicals at a wavelength of about 2160 Å. For the first time in shock tube experiments, an acceleration in the rate was observed below 2100 K. Their first-order rate constants were pressure-dependent and were given by the following equations,

$$\log k_1^{o} = 17.3 - (88{,}000 \pm 2{,}000)/2.3RT \qquad (k_1^{o} = 2k^{o})$$

$$\log k_1^{\infty} = 15.1 - (104{,}000 \pm 2{,}000)/2.3RT \qquad (k_1^{\infty} = 2k^{\infty})$$

respectively, for low and high pressure limits.

V. Studies Related to the initial dissociation

Rice and Dooley (22) studied the methane pyrolysis in a fast-flow system at temperatures from 1423 to 1473 K using tellurium mirrors. They were able to detect only methyl radicals rather than methylene radicals, and suggested that the initial step was

[1a] $CH_4 \rightarrow CH_3 + H$

Mass spectrometric identification of the initially formed radical by Eltenton (23), Robertson (24), and Nelson and Kuebler (25) confirmed the presence of methyl radicals rather than methylene radicals. In these three studies, however, pyrolysis was probably occurring on a hot surface rather than in the gas phase.

Belchetz and Rideal (26) brought about methane decomposition on a hot wire with a tellurium mirror placed within one mean free path. They concluded that methane dissociated to methylene and

hydrogen and that the methyl radical observed by Rice and Dooley (22) was a secondary product from the methylene radical, i.e.

[1b] $CH_4 \rightarrow CH_2 + H_2$, $CH_2 + CH_4 \rightarrow 2CH_3$

Vompe (27) studied the methane pyrolysis in a shock tube between 1760 and 2600 K by using a time-of-flight mass spectrometer operated at the ionizing voltage of 100-200 eV to monitor CH_4^+, CH_3^+, and CH_2^+ fragments. He observed that in the absence of a high temperature the intensity ratios of ions with m/e 14, 15 and 16 were approximately 1:4:5, and that during the reaction the intensity ratio of the lines at m/e 15 and 16 was 3:2 throughout the observation period indicating the presence of a significant concentration of CH_3 radicals during the decomposition of methane. He was not able to explain, however, that the peak at m/e 14 appeared only at the first time-interval (45 μsecond) and then virtually disappeared. Although he could not exclude the possibility of reaction [1b] he concluded that the predominant process was reaction [1a].

Yano and Kuratani (28) and Yano (29) investigated the pyrolysis of equimolar mixtures of CH_4 and CD_4 from 1500 to 1600 K, using a single pulse shock tube. From the hydrogen isotopic distribution of the reaction products in the initial stage, they concluded that the initial step was reaction [1a].

On the other hand, Fedoseeva, Chernyak, Gulyaev and Polak (30) pyrolyzed a 1:10 mixture of CH_4 and CD_4 in argon plasma at 1700-4000 K. They analyzed the isotopic composition of the ethane fraction

from the effluent of the gas chromatograph and concluded that CH_2 and H_2 were the primary products. They claimed this conclusion was in agreement with Vompe's (26) observation that the CH_2 peak appeared only at the first 45 μsec.

VI. Summary of previous studies

A. Order of reaction.

The methane pyrolysis is generally accepted as a radical reaction, but the over-all order of the reaction remains uncertain. Disagreements arose mainly because of differing extents of the reaction in different studies. Autocatalysis has not been explained and could influence the reaction differently under various conditions. This is particularly true in conventional static and flow systems. The pressure-dependence of the initial dissociation has not been established. The only shock tube study in which pressure dependence of the first-order rate constants was observed was that of Hartig et al (21). In general, the shock tube technique is not a sensitive test for reaction order.

B. Activation energy.

Over-all activation energies ranged between 75 and 104 kcal/mole. In general, shock tube studies predicted the higher values, from 100 to 104 kcal/mole, and the conventional flow and static system yielded lower values, from 75 to 90 kcal/mole, with Palmer's (11) result of 101 kcal/mole as an exception.

C. Initial step.

The initial step in the mechanisms proposed by most investigators was deduced mainly from the measured activation energy. The formation of methylene was thought to be consistent with a low value of the activation energy while the formation of a methyl radical was indicated by the higher value.

No conclusion about the initial step can be drawn from studies on mirror experiments due to the poor reproducibility, wide varieties of pyrolysis methods and the lack of understanding of the mechanism of mirror removal (31). Belchetz and Rideal (26), for example, did not observe the presence of methyl radicals in the ethane pyrolysis although the decomposition undoubtedly occurs through homogeneous C-C bond rupture.

Yano's (28, 29) results on the pyrolysis of equimolar mixtures of CH_4 and CD_4 appear to be more reliable than Fedoseeva's (30), since the conversions were always very low (less than 0.2%) and the extents of isotopic exchange reaction between CH_4 and CD_4 were less than 10%.

VII. Object of the Present Study

Although the pyrolysis of methane has been studied many times before, important details of the reaction mechanism have remained obscure. It has not been shown clearly whether methane dissociates initially into $CH_3 + H$ or $CH_2 + H_2$, and the pressure

dependence of the primary dissociation has not been established. In shock tube studies the first-order rate constants for the primary dissociation were generally assumed to be pressure independent. This has not been confirmed. In static and flow systems, induction-periods and autocatalysis have been observed. The measured activation energies were usually between 75 and 90 kcal/mole which are well below the bond dissociation energy of methane. Radical chain reactions and the formation of methylene radical have been suggested; these have never been proved. Secondary reactions of ethane leading to the formation of higher hydrocarbons and finally carbon deposition have not been elucidated. The present work was undertaken to resolve some of these uncertainties, particularly those of the low-temperature pyrolysis, by a careful study of the static pyrolysis in its very early stages.

CHAPTER TWO: EXPERIMENTAL

I. Apparatus.

The pyrolysis was performed in a conventional static system. The main features of the apparatus are shown schematically in Fig. 1. The analytical part of the equipment is shown separately in Fig. 2 and will be described in detail in the following section.

A Duo-Seal rotary pump model 1400 in series with a mercury diffusion pump was used to evacuate the main vacuum line. Hoke metal valves, model 4171M2B, were used for the portions in contact with methane and the reaction products. Two U-traps at dry-ice temperature, U1 and U2, were installed to reduce the pressure of mercury vapour which erodes the copper bellows of the metal valves. The entire system could be evacuated at about 10^{-6} Torr. After each experiment an independent pumping system was used to evacuate the reaction vessel through a three-way stopcock S7. A Duo-Seal single stage rotary pump with a displacement capacity of 120 liters per minute was used to produce solid nitrogen in traps, T1, T2 and T3, in less than two hours.

The reaction vessel, R, was a quartz cylinder of 477.6 ml, 20.4 cm long and 6.0 cm O.D.. A quartz tube 64.1 cm long, connected axially through the center of the reaction vessel, served as an outlet for nitrogen gas and as a thermocouple well. Capillary tubing connected the reaction vessel to a fused quartz spiral pressure gauge,

PG, and through valves to the vacuum line. The reaction vessel was enclosed in a quartz tube 90 cm long, 7.0 cm O.D.. Nitrogen gas was continuously passed through this annular space at 20 Torr above atmospheric pressure and flow rate of about 2 ml/min. to eliminate the possibility of oxygen diffusion through the wall of the reaction vessel at high temperature (32). Before installation, the reaction vessel was treated with hot concentrated nitric acid and was washed several times with distilled water.

An autoclave high temperature cylindrical furnace and a power controller manufactured by Autoclave Engineers Inc. was used for the present study. Three high temperature variable resistors were used to control the local temperature along the length of the furnace. The temperature in the reaction vessel was measured with an Alumel-Chromel thermocouple. For continuous observation, a potential offset device with stability better than 0.02 mv was used to balance the emf from the thermocouple and the resulting emf was monitored on a millivolt chart recorder. The thermocouple, TC, was calibrated four times against the freezing point of sodium chloride (99% purity, Canlab.).

The temperature gradient along the center of the reaction vessel was determined by measuring the temperature at 1 cm intervals. At each point the temperature was monitored for 20 to 30 minutes. An average deviation of less than $0.3^{o}C$ within 8 cm from the center and less than 1^{o} in the last 2 cm was achieved.

Figure 1

The Vacuum System

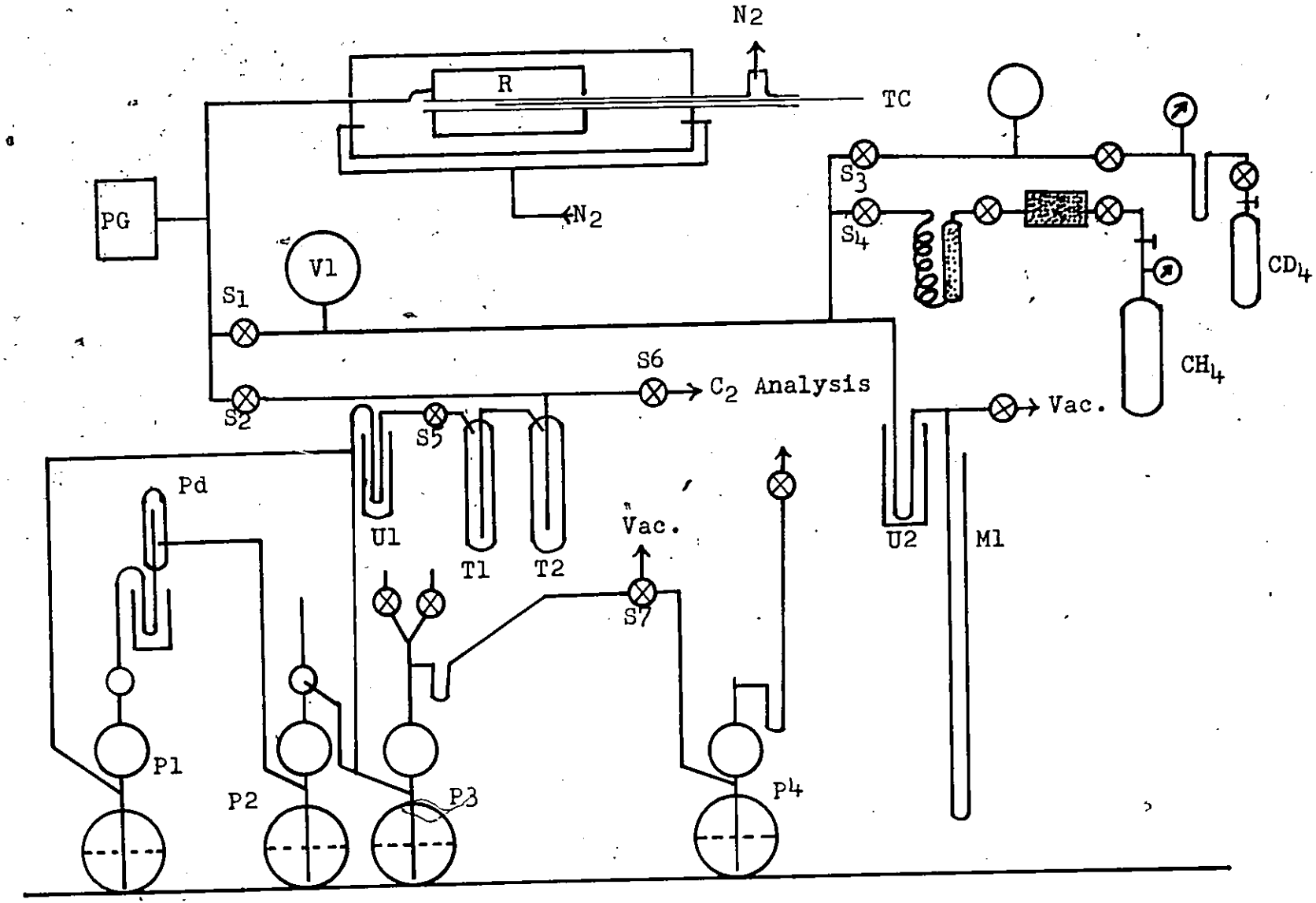
N2
R
TC
PG
N2
V1
S1
S3
S4
CD4
CH4
S6
C2 Analysis
S2
S5
Vac.
Pd
U1
T1
T2
Vac.
S7
U2
M1
P1
P2
P3
P4

II. Analytical System.

A Carle Standard Micro Detector and controller was used for the thermal conductivity detection. The detection elements were glass-coated thermistors. The detector was operated at 21.8 mA and helium was used as carrier gas. Helium was split into two streams and the inlet pressure in each column was regulated by using Edwards pressure controllers. Impurities present in the helium carrier gas interfered with the analysis of oxygen and caused a rapid de-activation of the molecular sieve column. To purify the carrier gas, a series of active charcoal and highly activated molecular sieve traps at liquid nitrogen temperature were used.

A complete separation of oxygen, argon, nitrogen and methane at room temperature was obtained with a 4 m x 6mm molecular sieve column activated by heating at 370 ^{o}C for twelve hours. The detection limit for oxygen was 1 ppm in methane with a sample size of 18 ml at 3 atmospheres pressure.

The product hydrogen was separated from methane on the molecular sieve column and was converted to water in a copper oxide furnace before entering the detector. At higher conversion, large amounts of hydrogen were collected through the solid nitrogen traps, T1 and T2 in series with a silica gel column at -196^{o}C, passed through a palladium thimble and measured in a gas burette, P2.

Hydrocarbon products were partially separated from the large quantity of methane on a 30 cm x 3 mm silica gel pre-column, C1, at

-78°C by continuous flushing of helium gas for 5 to 10 minutes. After most of the methane was removed, the pre-column C1 was warmed to room temperature and the effluent was injected into a second silica gel column, C2, composed of 30 cm x 3 mm plus 120 cm x 9 mm, maintained at room temperature. A separation of methane, ethane, ethylene and acetylene was completed in 40 minutes. In some of the later experiments, the pre-column was heated to about 90 °C with a hot water bath before the effluent was injected into a 4 m x 9 mm Durapak column at room temperature.

H_2, HD and D_2 were analyzed on a 2 m column of alumina treated with $MnCl_3$ and operated at the temperature of liquid nitrogen (33). Mixtures of methane and deuterated methanes were analyzed mass spectrometrically at an ionizing potential of 25 ev. The relative quantities of the species were estimated by comparing the spectrum with standard spectra of CH_4, CD_4 and a CH_4-CD_4(1:1) mixture.

III. Materials.

Research Grade methane, with a stated purity of 99.99%, was obtained from Matheson, Canada Ltd.. The impurities found were about 6 ppm of oxygen, 20 ppm of ethane and 100 ppm of nitrogen.

Oxygen was removed by passing the methane gas through a 30 cm pyrex cylinder containing 3 Kg of Ridox reagent (Fisher Scientific) activated at 230 °C. Ethane was removed by using a 3 m column of active charcoal at -78 °C. The charcoal column was activated by heating to

Figure 2

Sampling System for Gas Chromatography Analysis

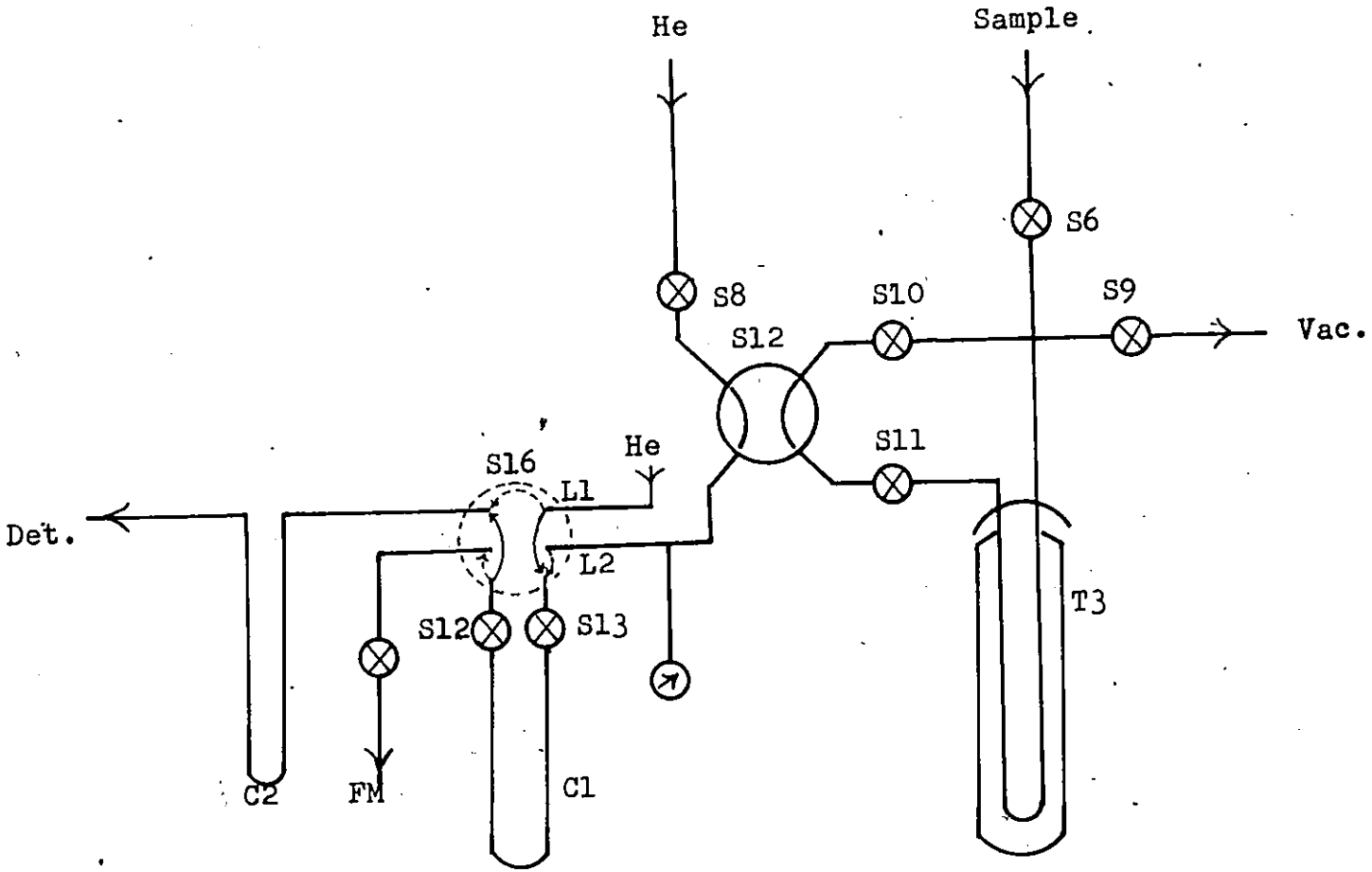
He
Sample
S6
S8
S10
S9
Vac.
S12
S11
He
S16
L1
Det.
L2
S12
S13
T3
C2
FM
C1

300° under vacuum for 24 hours with an additional hour of methane flushing. Two atmospheres pressure of methane was maintained in the purification line to avoid any contamination of oxygen from the atmosphere. The purified methane contained less than 1 ppm of oxygen and 0.1 ppm of ethane, the limits detectable by the present analytical method.

Matheson Research grade ethane, ethylene and acetylene were used for calibrations. Prior to use, the gases were distilled from bulb to bulb. No further purification was made. Hydrogen was purified by passing through a heated palladium thimble into a 3-liter storage flask.

Methane-d_4 with minimum isotopic purity of 99% in D atom was obtained from Merck Sharp and Dohme, Canada Ltd., and was passed through a pyrex cylinder containing Ridox reagent.

IV. Experimental Procedure.

The system was kept under continuous evacuation over night. Before the first experiment in a series was started, the reaction vessel was isolated from the main vacuum line for 30 to 50 minutes. The experiment was not begun if the system could not hold a vacuum of 10^{-5} Torr for this period. The entire system was re-evacuated to 10^{-6} Torr.

Methane was first expanded slowly into the balance volume V1 until a desired pressure was attained which was then measured on the

manometer M1. The methane was then introduced into the reaction vessel through S1. Initial methane pressures above 250 Torr were measured on the manometer, while lower pressures were measured with the pressure gauge PG. At the end of the reaction, the reaction mixture was expanded through S2 into the solid nitrogen traps, T1 and T2, which reduced the methane vapor pressure to about 10^{-2} Torr.

At low conversion (hydrogen less than 0.5 micromole), hydrogen was collected using Toepler pump P3 and transfered into the injection chamber for the gas chromatographic analysis. At higher conversions, hydrogen was collected with the Toepler pump P1 and measured in the gas burette P2.

Following the closing of valves S2 and S5, the solid nitrogen traps were removed from T1 and T2. The mixture of hydrocarbons and unreacted methane was transfered into the sampling loop T3 through S6 (Fig. 2). The following procedure was used for analysis of the hydrocarbon products. The carrier gas was directed through line L1 through the six-port valve S16 to the main column C2. With valves S8, S13 open and S6, S9, S10, S11, S15 closed, the pre-column C1 was immersed in a Dewar flask containing dry-ice acetone mixture ($-78^{\circ}C$). The analysis was started by closing S8. Following the removal of solid nitrogen trap T3, S10 and S11 were opened and the four-way valve S12 was immediately turned to the pick-up position. When the pressure inside L2 increased to 10 psi, S15 was opened. The pressure was maintained at this value by adjusting S8. Under this

pressure, helium passed through S8, S12, S10, T3, S11, L2, S13, S14 and S15 with a flow rate of 50 ml/min. Most of the methane could be flushed out in 5 minutes while the higher hydrocarbons were retained in C1. After the flushing was completed, S10, S11 and S15 were closed and S12 was turned back to the "out" position. The pressure in L2 was increased to 28 psi which was the pressure in the main column C2. By closing S13 and S14, the pre-column C1 was completely isolated and was warmed up to room temperature using a water bath. By switching S16 and opening S13, S14, the carrier gas was diverted from L1 through C1 to C2.

After the complete analysis, S16 was returned to the original position and sampling loop T3 was evacuated by opening S9.

V. Conditioning of the reaction vessel.

For the study of the pyrolysis of methane on a clean surface, air was admitted to the reaction vessel after each experiment to burn off any possible carbon deposit. The reaction vessel was then evacuated for more than 90 minutes, producing a vacuum of 10^{-5} Torr. To check the possibility of a trace of oxygen remaining in the reaction vessel after this procedure, a small pressure, 5 to 10 Torr, of methane was pyrolyzed for several seconds then pumped away. No difference in the results was observed with or without this pre-pyrolysis of small amount of methane before the experiment.

For the study of the decomposition on a carbon surface,

about 100 Torr of methane was pyrolyzed for more than six hours to produce the carbon surface.

CHAPTER THREE: RESULTS AND DISCUSSION

I. General description.

A. Primary, secondary and tertiary products.

The products hydrogen, ethane, ethylene, propylene and acetylene were analyzed as a function of time at the temperatures 995, 1038, 1068 and 1103 K over the pressure range 25 to 740 Torr. Typical yield-time plots are shown in Fig. 3 and Fig. 4. The results show clearly that in the initial stage of the reaction hydrogen and ethane are the only products. As the concentration of ethane builds up in the system, but while the conversion is still less than 0.01% ethane begins to be consumed in secondary reactions and its concentration gradually approaches a plateau value. Ethylene is clearly a secondary product. Propylene and acetylene are tertiary, and appear only after the concentration of ethylene has surpassed that of ethane. As the reaction proceeds still further a marked increase in the rate of formation of ethane and other products was observed. Exploration of possible mechanisms for this autocatalysis will be discussed in section IV., B.

Prolonged pyrolysis led to the deposition of carbon on the surface which enhanced the rate of decomposition. Fig. 5a and 5b show the yields of ethane and ethylene in carbon-coated and clean vessels respectively, for similar conditions of temperature and pressure. Fig. 5a shows that the ethane production on a carbon-coated vessel is

Figure 3

Yield-time plot for the formation of hydrogen, ethane, ethylene, acetylene and propylene. Curve Δ P represents the measurement of pressure change. 1038 K and 440 Torr.

□ Hydrogen

● Ethane

0 Ethylene

Δ Propylene

▲ Acetylene

◆ Pressure

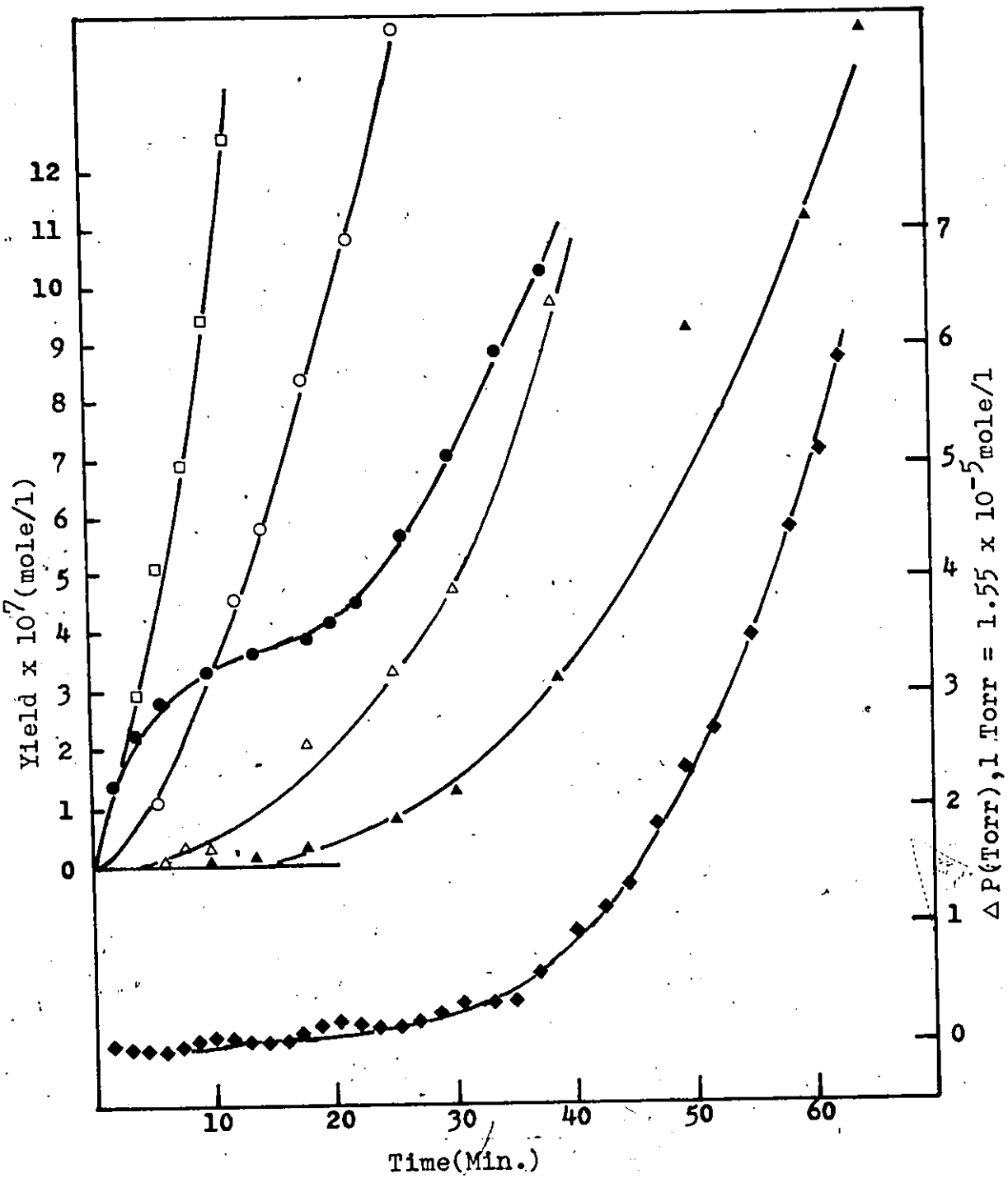
Yield x 10^7(mole/l)
Δ P(Torr), 1 Torr = 1.55 x 10^{-5}mole/l
Time(Min.)
0
1
2
3
4
5
6
7
8
9
10
11
12
10
20
30
40
50
60

Figure 4

Yield-time plot for the formation of hydrogen, ethane and ethylene at 154 Torr, 1068 K.

□, H_2

●, C_2H_6

○, C_2H_4

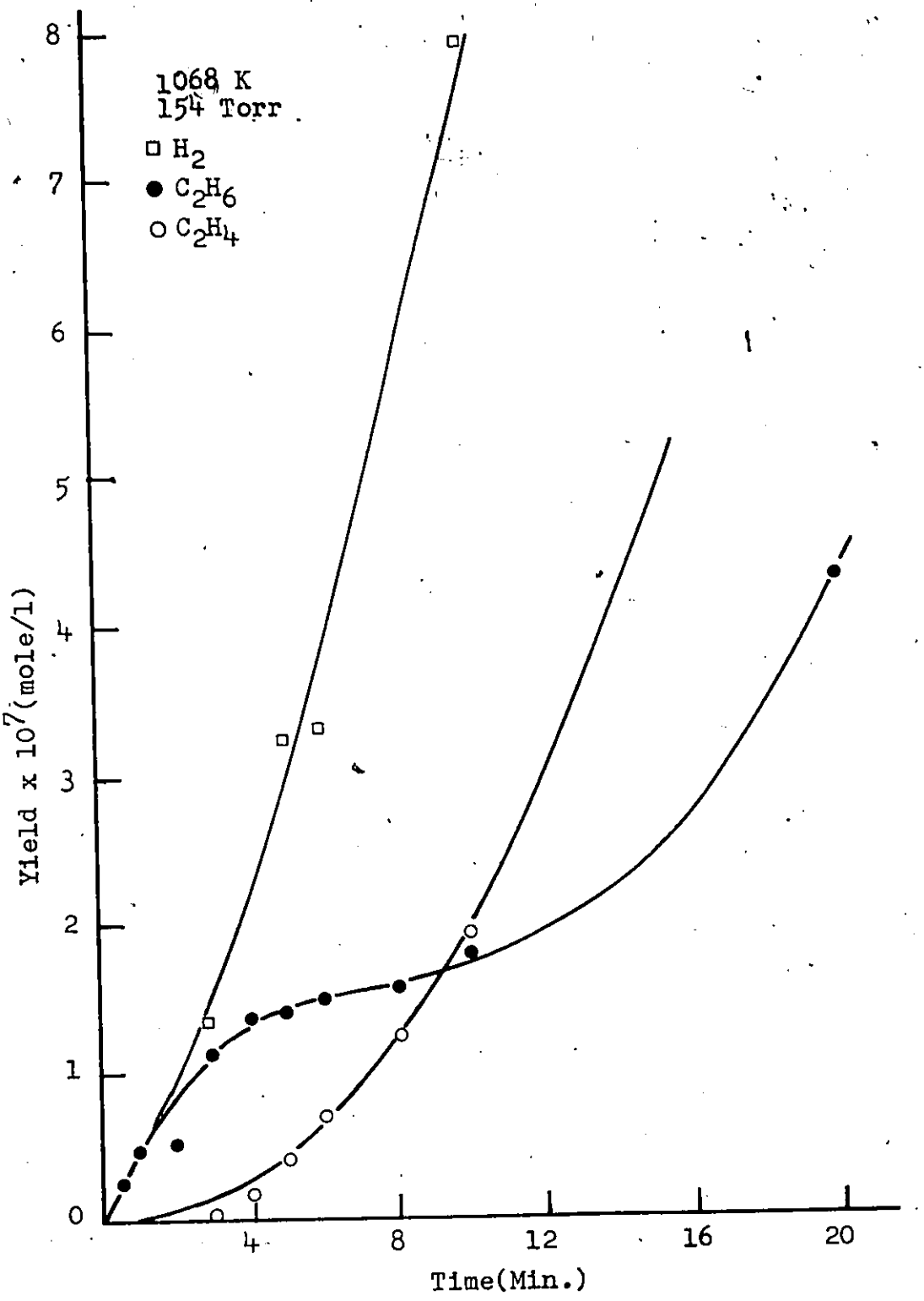
1068 K
154 Torr
□ H_2
● C_2H_6
○ C_2H_4
Yield x 10^7(mole/l)
0
1
2
3
4
5
6
7
8
4
8
12
16
20
Time(Min.)

Figure 5

Yield-time plots for the formation of ethane and ethylene at 100 Torr, 1038 K.

5a: Carbon coated vessel: ○, C_2H_6; ●, C_2H_4

5b: Clean vessel: ○, C_2H_6; ●, C_2H_4; -●-, $C_2H_6 + C_2H_4$

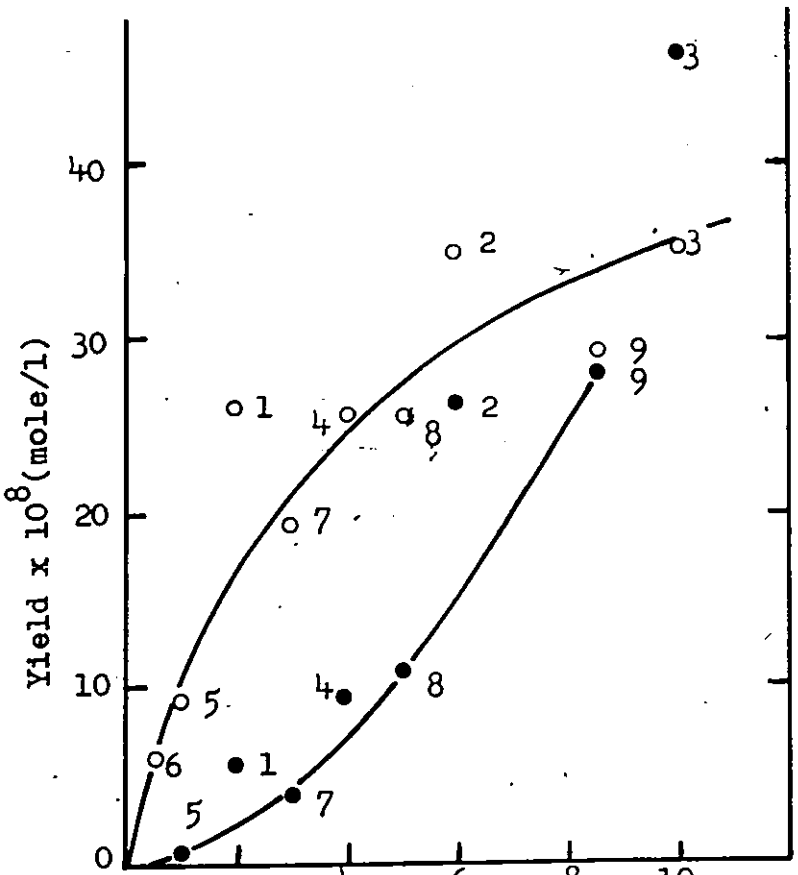
Yield x 10^8(mole/l)
0
10
20
30
40
2
4
6
8
10
Time(Min.)

Fig. 5a

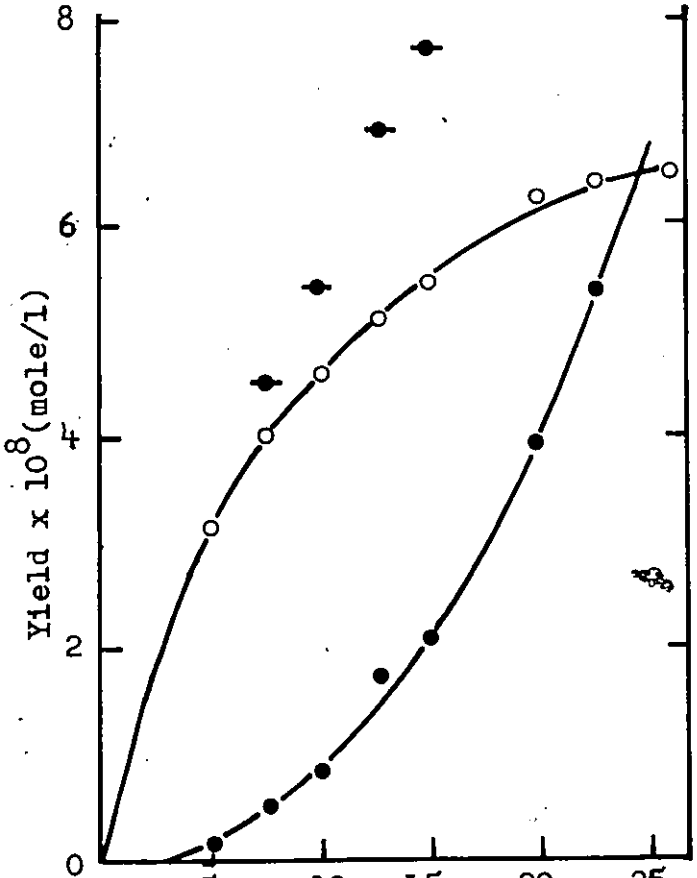
Yield x 10^8(mole/l)
0
2
4
6
8
5
10
15
20
25
Time(Min.)

Fig.5b

about 10 to 15 times faster than in a clean vessel (Fig. 5b). In Fig. 5a the experimental points show the sequence of the experiments and indicate a continuous de-activation of the surface. To check the extent of carbon deposition in the present experiments methane was pyrolyzed for a fixed time interval and the volatile products removed. A second pyrolysis was then performed for a short time of reaction and the rate of formation of ethane measured. This sequence was repeated several times. If any non volatile product accumulated on the surface of the vessel the rate of formation of ethane should show a gradual increase. Experiments were done with intervals of 6, 12, 24 and 36 minutes. The yields of ethane, ethylene, acetylene, propylene and allene from these experiments are listed in Appendix 2 (page 165). Fig. 6 shows the amounts of ethane and ethylene produced after two minutes decomposition of methane against the number of pyrolysis of 36-minute intervals at 440 Torr and 1038 K (compare Fig. 3). The yields of all these products were unaffected by allowing any non-volatile product to accumulate. It must be concluded that non-volatile deposition at this stage is not important. Nevertheless, to avoid accumulation of carbon from repeated experiments, air was admitted to the vessel after each experiment to burn off any carbon deposit as described in the experimental section.

With the present analytical technique, the rate of ethane and ethylene could be measured well before the autocatalysis became significant. In almost all previous studies in static and flow

Figure 6

Yields of ethane and ethylene after two minutes decomposition of methane against the number of pyrolysis of 36-minute intervals, at 1038 K, 440 Torr.

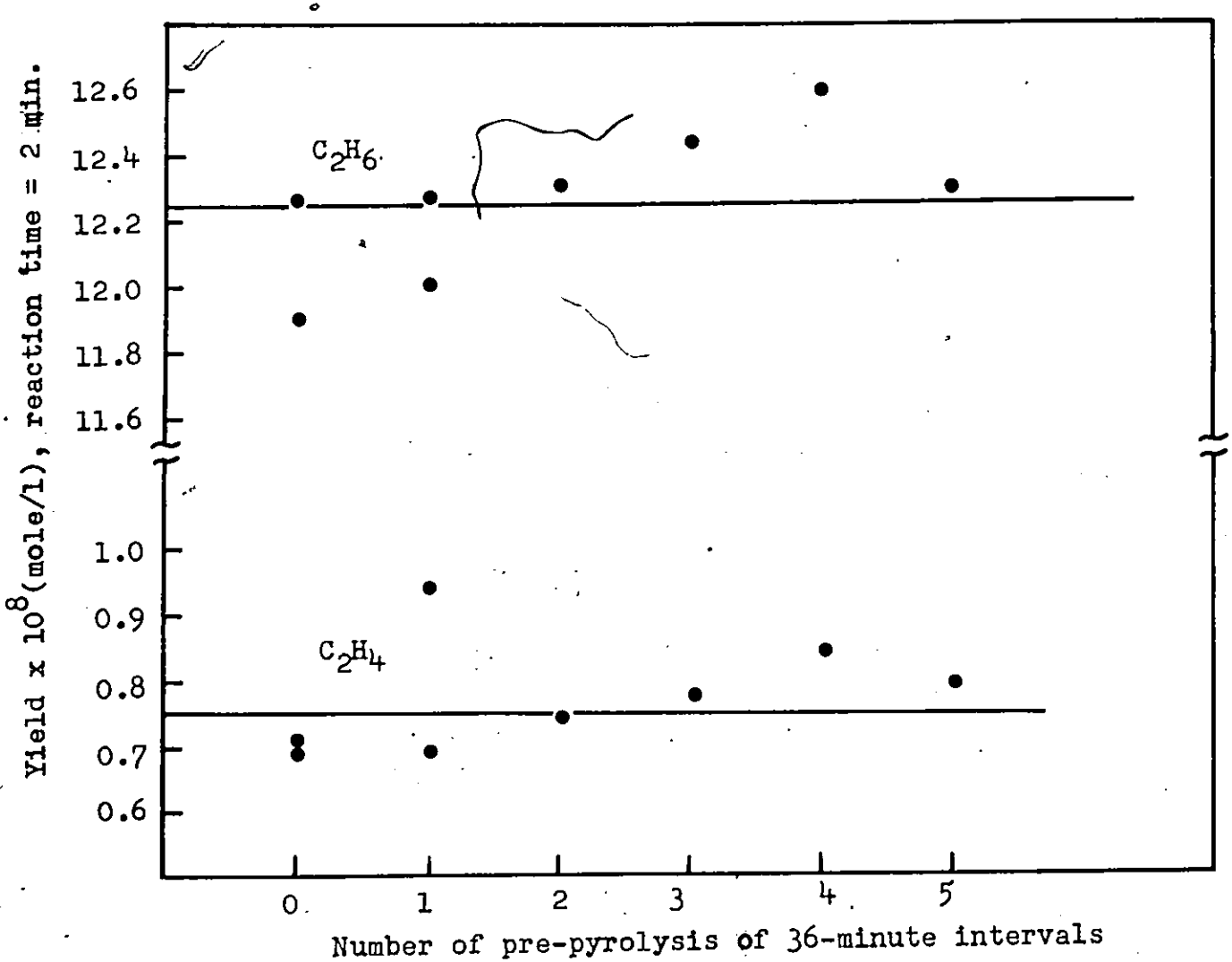
Yield x 10^8(mole/l), reaction time = 2 min.
12.6
12.4
12.2
12.0
11.8
11.6
C_2H_6
1.0
0.9
0.8
0.7
0.6
C_2H_4
0
1
2
3
4
5
Number of pre-pyrolysis of 36-minute intervals

systems the rates were measured at conversions where the autocatalysis was important. This is particularly true in the kinetic studies based on pressure measurement, since measurable pressure increase occurs only in the region of secondary acceleration. The measured pressure change is shown in Fig. 3.

B. Surface Effect.

The effect of surface/volume ratio on the rate of methane decomposition was studied by increasing the S/V ratio by a factor of 9.6. Experiments were done at 400 Torr and 1038 K. The results are presented in Fig. 7. The rates of ethane production are essentially the same. It may be concluded that the measurement of the initial rate of formation of ethane in the clean quartz vessel is a measure of the homogeneous dissociation of methane.

II. Kinetics and Mechanism of The Primary Decomposition.

A. The Initial Step.

Two initial dissociation reactions have been suggested in the methane pyrolysis,

[1a] $CH_4 \rightarrow CH_3 + H$

[1b] $CH_4 \rightarrow CH_2 + H_2$

The endothermicity of reaction [1a] has long been established as about 102-104 kcal/mole (11, 34, 35). The endothermicity of [1b] has been

Figure 7

Yield-time plot for the formation of ethane and ethylene at 440 Torr and 1038 K.

Unpacked vessel: ● ethane, ▲ ethylene.

Packed vessel: ○ ethane, △ ethylene.

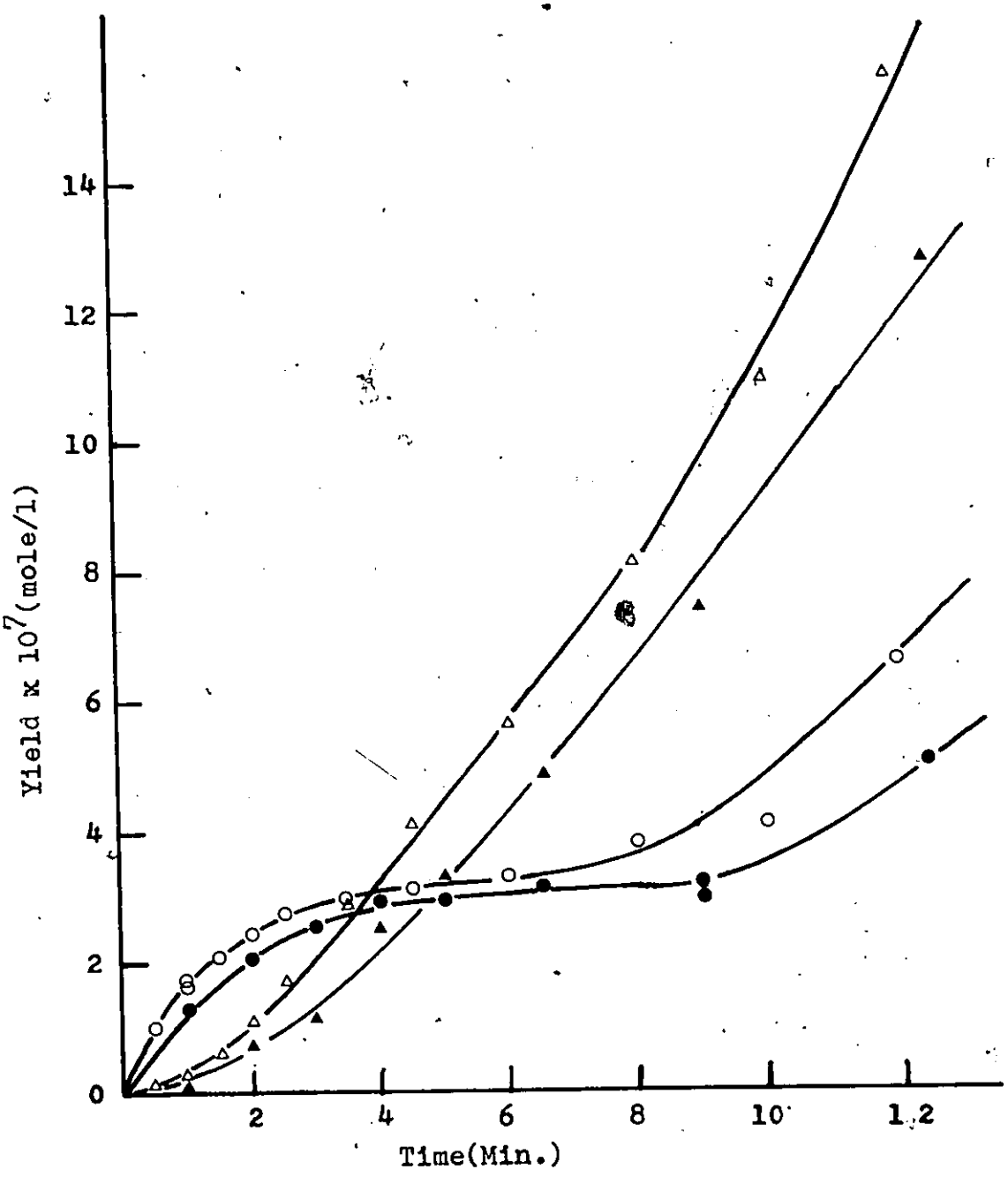
Yield x 10^7(mole/l)
0
2
4
6
8
10
12
14
2
4
6
8
10
12
Time(Min.)

much more uncertain; at one time it was thought to be substantially (10-20 kcal/mole) less than that of [1a], and in a number of studies of the methane pyrolysis where the activation energy was less than 103 kcal/mole, it was concluded that reaction [1b] must be predominant (15, 17, 36). Conversely, in other experiments, mostly in shock tubes, where the activation energy was about 103 kcal/mole, it was concluded that only reaction [1a] was important (16). Subsequently it became evident that the endothermicity of reaction [1b] was probably equal to orgreater than that of [1a], so that all the earlier conclusions about the initial dissociation process based on activation energy had to be discounted (11). There now appears to be convincing evidence (37) for a value of $\Delta H_f^o(CH_2)$ of about 93 kcal.mole, which makes reaction [1b] endothermic by about 111 kcal/mole at 298°K, or 113 kcal/mole at 1000°K. The rate constant for reaction of CH_2 with H_2, the reverse of reaction [1b], has been measured recently (38) and it thus becomes possible to calculate the rate constant for [1b]*. Thermochemical data used in these and later calculations are given in Table 1 together with the rate constant for reaction [1b] at 1000 K and the rate constant for the initial dissociation measured in the present study. It should be noted that both these values refer to the limiting high-pressure region. In the measurement by Braun et al (38), singlet CH_2 was consumed in the reaction with hydrogen irrespective of whether the resulting CH_4^* was stabilized, since the latter should have decomposed preferentially to CH_3 and H rather than reforming CH_2 and H_2.

* Details of the calculation are given in Appendix 4.

It is clear from Table 1 that reaction [1b] should be of negligible importance in the pyrolysis of methane. This conclusion is further strengthened by the fact that in several respects the calculations in Table 1 probably over-estimated the magnitude of k_{1b}, so that the values obtained should be regarded as upper limits. In particular, the rate constant measured by Braun et al (38) for the reverse reaction was for CH_2 in its excited singlet state; the corresponding reaction of the ground-state triplet is undoubtedly much slower. On the other hand, the heat of formation of 93 kcal/mole is presumably for ground-state CH_2 and there appear to be convincing arguments (39) that the singlet state lies from 6-10 kcal higher in energy than the triplet ground state. It is not clear whether singlet or triplet CH_2 would be produced in reaction [1b]; production of the former conserves spin, but if the energy barrier is much higher than for triplet formation, the latter may occur but with a reduced frequency factor associated with the spin violation. By using ΔH_f for the triplet in the present calculation, and the reverse rate constant for the singlet, the estimated value of k_{1b} is clearly an upper limit, and the true value may be much lower. It may also be noted that if there is an appreciable activation energy for the reaction of CH_2 with H_2 or if the CH_2 radicals in the experiments by Braun et al (38) were vibrationally excited, k_{1b} would be further over-estimated in the present calculation.

Experimentally it is not easy to distinguish between

TABLE 1[a]

Comparison of Measured Rate Constant and Calculated Value of k_{1b}

	ΔH_f^o (298) Kcal/mole	S^o cal/mole	Cp (298-1000 K) cal/deg mole
CH_4	-17.9	44.5	12.87
CH_3	34.0	46.1	11.7
CH_2	93	43.3	9.3
H_2	0	31.2	7.05
H	52.1	27.4	5.0

[a] All values are taken from ref (43) except ΔH_f (CH_2) which is from ref (37)

	log A ($l\ m^{-1}s^{-1}$ or s^{-1})	E Kcal/mole	log k (1000 K) (S^{-1})
Reaction [-1b]	9.62		
Reaction [1b]	14.8	113.3	-10.03
Measured rate	16.4	106.7	-6.9

reactions [1a] and [1b]. It will be seen later that the secondary reactions observed in the system point strongly to the presence of CH_3 radicals, but these could be generated from the reaction of CH_2 with CH_4 even if reaction [1a] did not occur. Analysis of the isotopic composition of hydrogen produced in the initial stage of the pyrolysis of a mixture of CH_4 and CD_4 should reveal the occurrence of reaction [1b]. Table 2 shows the results of the pyrolysis of equimolar mixtures of CH_4 and CD_4 at temperatures 1038, 1068 and 1103 K. The ratio of C_2H_6/C_2H_4 corresponds to the ratio of primary to secondary hydrogen, so that at the shortest times greater than 90% of the hydrogen should have come from the primary reactions. There are three possible reactions, however, which could cause exchange between the product hydrogen and deuterium:

(a) exchange catalyzed by CH_3 and CD_3 as follows,

[2a] $CH_3 + D_2 \rightarrow CH_3D + D$

[2b] $D + CH_4 \rightarrow HD + CH_3$

[2c] $CD_3 + H_2 \rightarrow CD_3H + H$

[2d] $H + CD_4 \rightarrow HD + CD_3$

A rapid deuterium exchange in methane was observed which occurred by the following alternating chain reactions,

$$CH_3 + CD_4 \rightarrow CH_3D + CD_3$$

$$CD_3 + CH_4 \rightarrow CD_3H + CH_3$$

TABLE 2

The Isotopic Composition of the Product Hydrogen from Pyrolysis of 1:1 Mixture of CH_4 and CD_4, Total Pressure, 443 Torr

T = 1038 K

t min	$\frac{[C_2H_6]}{[C_2H_4]}$	$\frac{[HD]}{[H_2]}$	$\frac{[HD]^2}{[H_2][D_2]}$	$\frac{[CH_3D]}{[CH_4]_o}$ %
0.61	30	0.98	-	-
1.01	30	0.53	1.6	-
1.01	-	0.59	3.31	-
3.02	-	1.06	4.75	-
4.00	3.47	1.15	6.21	-
4.00	-	1.19	5.26	3.93
6.00	2.75	1.36	3.93	-
8.00	1.12	1.10	3.69	8.00
12.00	0.51	1.32	4.22	-
16.00	-	1.43	4.87	13.8
24.00	-	1.48	4.40	27.2
		Average	4.5 ± 0.7	

T = 1068 K

t min	$\frac{[C_2H_6]}{[C_2H_4]}$	$\frac{[HD]}{[H_2]}$	$\frac{[HD]^2}{[H_2][D_2]}$	$\frac{[CH_3D]}{[CH_4]_o}$ %
0.50	23.2	1.15	5.02	6.07
1.01	20.3	1.19	5.36	3.54
2.00	3.00	1.72	3.84	6.25
3.51	1.25	1.26	4.51	10.2
5.01	0.81	1.41	4.95	13.9
		Average	4.7 ± .5	

TABLE 2 continued

T = 1103 K

t min	$\frac{[C_2H_6]}{[C_2H_4]}$	$\frac{[HD]}{[H_2]}$	$\frac{[HD]^2}{[H_2][D_2]}$	$\frac{[CH_3D]}{[CH_4]_o}$ %
0.26	14.7	1.22	5.24	2.42
0.40	6.4	1.25	5.13	3.51
0.51	4.3	1.34	4.48	4.44
0.77	1.95	1.16	3.63	7.20
1.01	1.36	1.35	4.59	9.94
1.51	0.84	1.32	4.15	15.1
		Average	4.5 ± .5	

These reactions will be discussed in detail in Section V of this chapter. The extent of this exchange is given by the ratio $\frac{CH_3D}{CH_4}$ shown in Table 2. If the rate constants for reactions [2a] and [2c] are similar to those for the abstraction reactions from methane, as written above, then the percentage of hydrogen reacting by these reactions will be the same as the percentage of methane reacting this way, since both are first order. Actually, the percentage of hydrogen reacting will be approximately half the value for methane since hydrogen is a product and initially its concentration is zero. Thus if 10% of the methane has been converted to CH_3D, then 5% of the hydrogen has reacted by reaction [2c].

(b) A molecular reaction between CH_4 and D_2 (CD_4 and H_2 as well) was postulated by Watt, Borrell, Lewis and Bauer (40). The rate of this process in the present system may be calculated from the empirical rate law given by Watt et al (40),

$$d[HD]/dt = k_p[D_2]^{1.1}[CH_4]^{0.3}[Ar]^{0.6}$$

where $k_p = 1.1 \times 10^9 (T)^{\frac{1}{2}} e^{-52,000/RT}$ 1/(mole sec) $\simeq 0.82$.

If the collision efficiency of CH_4 is similar to that of Ar, the equation becomes

$$d[HD]/dt = k_p[D_2]^{1.1}[CH_4]^{0.9}$$

At 1068 K, 440 Torr, $[CH_4 + CD_4]$ is about 6.6×10^{-3} mole/l and D_2 concentration is 2.1×10^{-7} mole/l,

$$d[HD]/dt = 0.8\ (2.1 \times 10^{-7})^{1.1}(6.6 \times 10^{-3})^{0.9}$$
$$= 3.9 \times 10^{-10}\ \text{mole/(l sec)}$$

This rate is about 0.2% of the rate of formation of HD and may be ignored.

(c) A four center exchange reaction between H_2 and D_2 has been proposed by Bauer (41). The empirical rate low for this reaction was given by

$$d[HD]/dt = k_p[Ar][D_2]^{0.66}[H_2]^{0.38}$$

where $k_p = 10^{12.84}(T)^{\frac{1}{2}}e^{-42,260/RT}$

Burcat and Lifshitz (42) re-investigated this reaction and found that the sum of the order of H_2 and D_2 was 1.3 rather than 1.04 and the order with respect to Ar was 0.65. Yano (29) also studied the reaction at much lower concentrations of H_2 and D_2 (0:1%) rather than 1-5% used by Bauer (40) and Burcat et al (42). He observed that the sum of the order (H_2 and D_2) increased to 1.8. Although there are large discrepancies in these three studies with respect to the order of the reaction, the rate measurements are in good agreement, yielding an activation energy within 40 ± 2 kcal/mole.

By examining Bauer's proposed mechanism

$$H_2 + M_i \underset{k_{-i}}{\overset{k_i}{\rightleftharpoons}} H_2^{(v)} + M_i$$

$$D_2 + M_i \underset{k'_{-i}}{\overset{k'_i}{\rightleftharpoons}} D_2^{(v)} + M_i$$

$$H_2^{(v)} + D_2 \xrightarrow{kp} 2HD$$

$$D_2^{(v)} + H_2 \xrightarrow{k'p} 2HD$$

where M_1 = Ar, $M_2 = H_2$, and $M_3 = D_2$, $H_2^{(v)}$ represents vibrationally excited hydrogen, the rate of HD formation can be estimated. Application of the steady-state approximation to this vibrationally excited species in the mechanism gives

$$H_2^{(v)} = \frac{k_i[H_2][M_i]}{k_{-i}[M_i] + kp[D_2]}$$

$$\frac{d[HD]}{dt} = 2\, kp[H_2^{(v)}][D_2]$$

$$\frac{d[HD]}{dt} = \frac{2\, k_p\, k_i\, [H_2][D_2][M_i]}{k_{-i}[M_i] + k_p[D_2]}$$

k_{-i} and k_p are essentially equal to the collision rate constant. Therefore $k_{-i}[M_i] >> k_p[D_2]$ and

$$\frac{d[HD]}{dt} = 2k_p\, K_i[H_2][D_2]$$

since ΔH_i = 42 kcal/mole

$$\frac{d[HD]}{dt} = 2\, k_p\, e^{-42,000/RT}[H_2][D_2]$$

Taking $k_p \simeq$ collision number (7.0×10^{10} 1/mole), the yield of HD at the shortest reaction time of 30 seconds at 1068 K is about 4.5×10^{-10} mole/1. The yield observed experimentally was 2.3×10^{-7} mole/1. It

is therefore concluded that molecular hydrogen should not have been exchanged appreciably after its formation under the experimental conditions.

The data in Table 2 are scattered because the amounts of hydrogen, and particularly deuterium, analyzed were necessarily small, but within this scatter there is no significant deviation from a value of about four expected for hydrogen formed by an atomic mechanism. Reaction [1b] should of course yield a $[HD]^2/[H_2][D_2]$ ratio of zero. From these experiments and from the calculations in Table 1, it can be concluded that reaction [1b] is the only initial dissociation of importance.

B. Secondary Reactions.

The initial stages of the reaction before propylene and acetylene are formed may be explained by a very simple mechanism

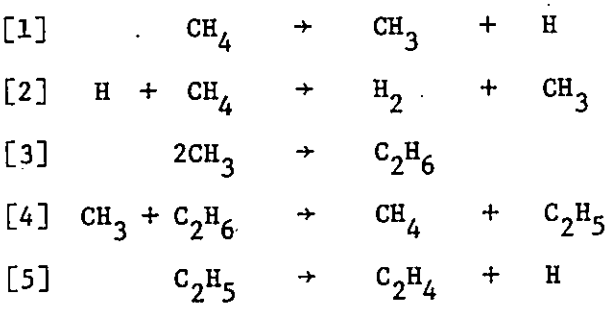

[1] $CH_4 \rightarrow CH_3 + H$

[2] $H + CH_4 \rightarrow H_2 + CH_3$

[3] $2CH_3 \rightarrow C_2H_6$

[4] $CH_3 + C_2H_6 \rightarrow CH_4 + C_2H_5$

[5] $C_2H_5 \rightarrow C_2H_4 + H$

In the earliest stages where only reactions [1], [2], and [3] are important the yield of hydrogen was equal to the yield of ethane and no pressure increase was observed. As reactions [4] and [5] became important ethane was converted to ethylene and hydrogen. During this

Figure 8

Yield-time plot for sum of the formation of hydrogen and ethane at 109 Torr, 1038 K.

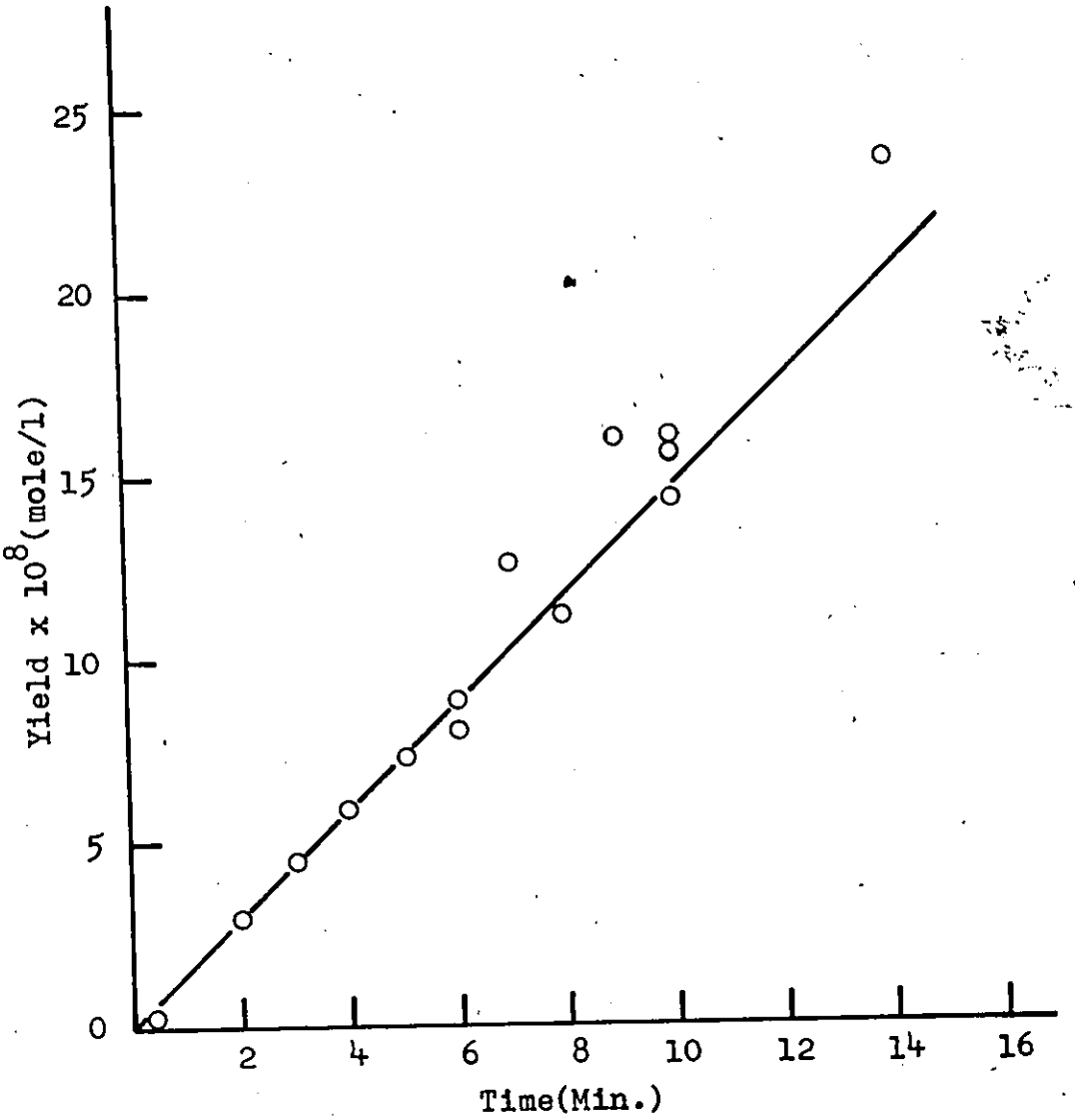
25
20
15
10
5
0
Yield x 10^8(mole/l)
2
4
6
8
10
12
14
16
Time(Min.)

Figure 9

Yield-time plot for the formation of ethane, ethylene and the sum of ethane and ethylene at 1038 K, 100 Torr.

○ , C_2H_6

● , C_2H_4

■ , $C_2H_6 + C_2H_4$

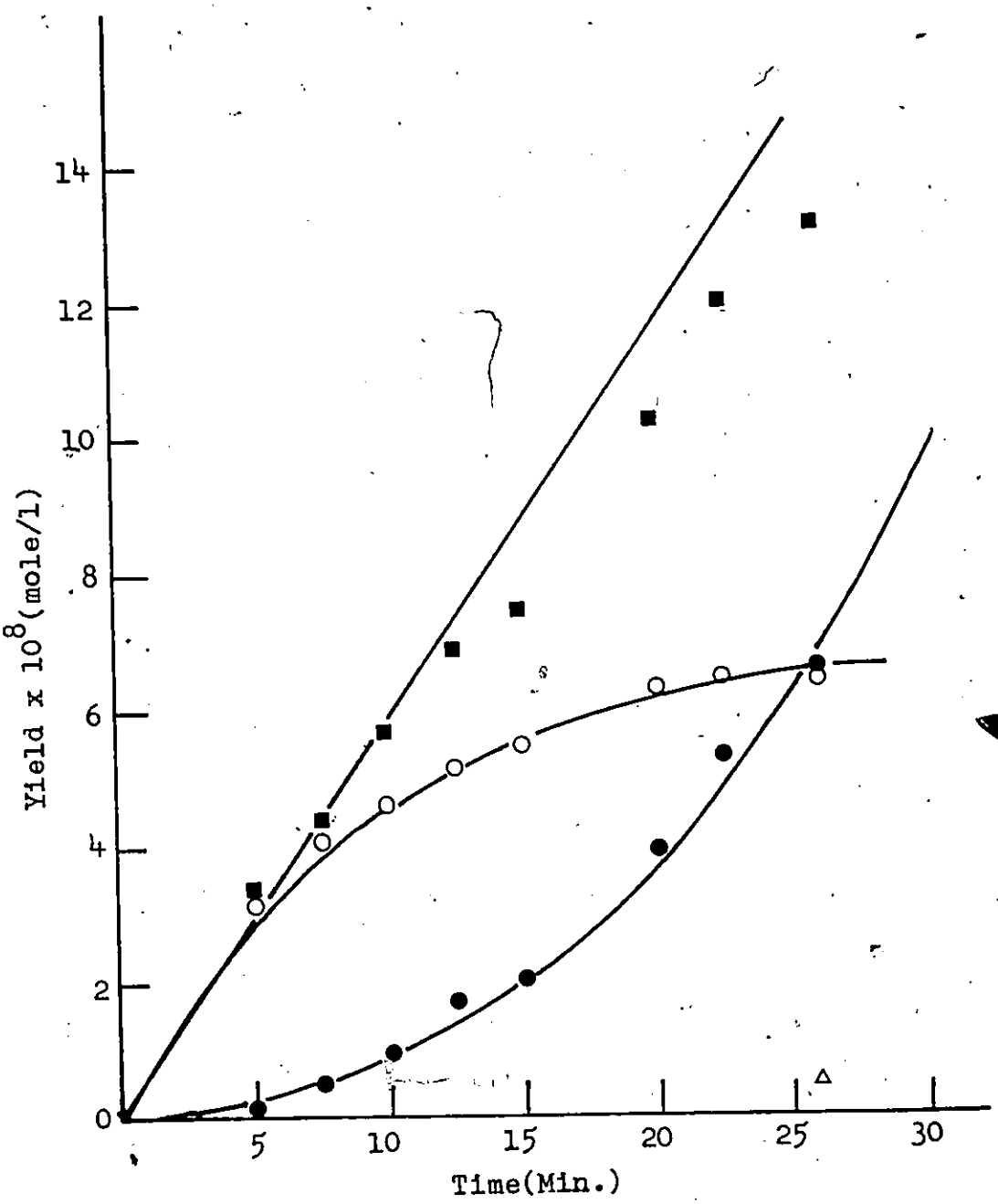
Yield x 10^8(mole/l)
0
2
4
6
8
10
12
14
5
10
15
20
25
30
Time(Min.)
Δ

period the quantities $(C_2H_4 + C_2H_6)$ and $(H_2 + C_2H_6)/2$ were both linear functions of time, showing that these were the only products at this stage of the reaction. The yield of ethane as it approaches its steady-state value can in fact be quantitatively accounted for by reactions [4] and [5]. Typical plots are shown in Fig. 8 and Fig. 9.

C. Measurement of k_1.

From the proposed mechanism it follows that

$$[6] \quad k_1[CH_4] = R^o_{C_2H_6} = R^o_{H_2}$$

where R^o signifies an initial rate of formation.* Values of R^o for ethane and hydrogen can be obtained directly from yield-time plots, but because reactions [4] and [5] become important at very low conversion, accurate initial rates could not always be measured. $R^o_{C_2H_6}$ may be equated to $R(C_2H_6 + C_2H_4)$ or $\frac{1}{2}R(H_2 + C_2H_6)$, which corrects for loss of ethane in reaction [4], and k_1 was obtained from linear plots of these functions. The values of $R^o(C_2H_6)$ were also evaluated by using a computer to obtain the 4th degree least square curve fit. These various measurements of initial rates were in substantial agreement and the final values given in Table 3 represent an average of the values obtained by the different methods. Error limits based on the values obtained by the various methods are indicated in Fig. 10 by vertical bars.

D. The Pressure Dependence of k_1.

Log k_1 is shown in Fig. 10 as a function of log (methane

* A similar expression applies if the initiation step is reaction [1b]. See Appendix 5 for a derivation.

TABLE 3

Measured Values of k_1 and Calculated Values for $k_1^{\infty} s^{-1}$, k_1^{o} & mole^{-1} s^{-1}, E^{∞} and A^{∞}

$T^{o}K$	P, Torr	k_1 sec^{-1} x 10^{8}
995	741	2.82
	640	2.95
	540	2.34
	440	2.40
	333	1.32
	230	1.58
	162	1.07
	108	1.07
	51	.74

$k_1^{\infty} = 6.66 \times 10^{-8}$; $k_1^{o} = 1.23 \times 10^{-5}$

$T^{o}K$	P, Torr	k_1 sec^{-1} x 10^{7}
1038	741	2.57
	642	2.29
	542	1.95
	441	1.86
	338	1.38
	236	1.26
	188	1.12
	109	.81
	96	.74
	66	.71
	43	.51
	32	.39

$k_1^{\infty} = 6.50 \times 10^{-7}$; $k_1^{o} = 1.12 \times 10^{-4}$

		x 10^{7}
1068	742	8.71
	440	7.08
	233	4.90
	154	3.72
	104	3.58
	75.5	2.34
	48.6	1.70
	25.2	.98

$k_1^{\infty} = 2.74 \times 10^{-6}$; $k_1^{o} = 4.53 \times 10^{-4}$

		x 10^{6}
1103	743	3.86
	602	4.06
	440	3.02
	233	2.06
	121	1.27
	49	.69

$k_1^{\infty} = 1.37 \times 10^{-5}$; $k_1^{o} = 2.14 \times 10^{-3}$

$E^{\infty} = 107.6$ kcal/mole; $A^{\infty} = 2.8 \times 10^{16}$ sec^{-1}

Figure 10

The variation of k_1 with pressure. The experimental results are shown as vertical bars, indicating the error limits, while the solid lines are the calculated values. The temperatures are: 995, 1038, 1068 and 1103 K.

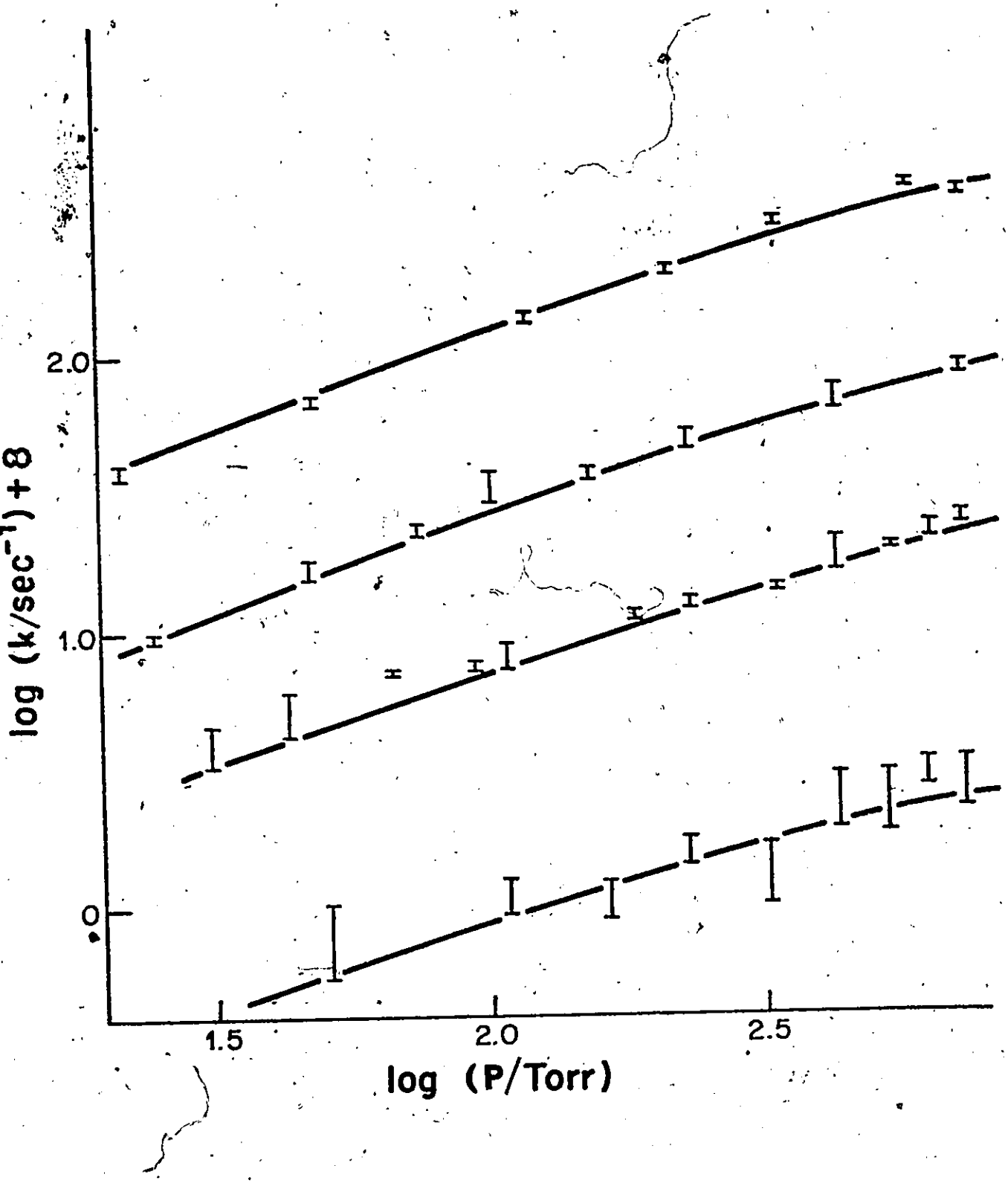
log (k/sec^{-1})+8
2.0
1.0
0
1.5
2.0
2.5
log (P/Torr)

pressure). It is clear that k_1 depends markedly on the pressure of methane under the conditions of the present experiments. The simplest explanation of this behaviour is that reaction [1] is a unimolecular reaction in its pressure-dependent region. Such a pressure-dependence is indeed expected for a molecule as small as methane (34), although it has not been clearly demonstrated before at these temperatures. Alternatively, it might be suggested that the dependence of k_1 on methane pressure could arise from a complex radical-chain mechanism. The only possible propagation step in pure methane appears to be

[7] $CH_3 + CH_4 \rightarrow C_2H_6 + H$

This has frequently been suggested in the past (12, 36), and together with reaction [2] constitutes a chain yielding C_2H_6 and H_2. There are several arguments against such a chain in the methane pyrolysis. First, reaction [7], an inversion reaction at a simple saturated carbon atom, is without precedent in gas-phase radical reactions and would have a high activation energy (43) and probably a low A-factor. The chain mechanism in fact would require E_7 to be about 50 kcal/mole to give the overall observed activation energy, and therefore reaction [7] although unlikely, probably cannot be ruled out a priori. Secondly, if reaction [7] occurred, the rate of reaction would be given by the expression

[8] $$R^o_{C_2H_6} = R^o_H$$
$$= k_1[CH_4] + k_7[CH_4]\,(k_1[CH_4]/k_3)^{\frac{1}{2}}$$

with the right-hand side consisting of two terms, the first for the non-chain process, the second for the chain reaction. Recognizing that both k_1 and k_3 may be pressure dependent, it can be seen that their dependence on methane pressure will cancel at low pressure and disappear at high pressure, leaving a simple overall dependence of the chain process on $[CH_4]^{3/2}$ in the high and low pressure limits. At intermediate pressure when both k_1 and k_3 are pressure dependent, the order will rise above 3/2 because k_3 would reach its high-pressure limit well before k_1. The result on a log-log plot of k_1 against CH_4 pressure would be two parallel lines at high and low pressure with slope 1/2, displaced laterally and joined by a sigmoid curve at intermediate pressure. This prediction may be compared with Fig. 10 in which the slope in fact decreases monotonically from about 0.6 at the lowest pressure to 0.4 at the highest. The contribution of ethane formation from reaction [7] can also be estimated by using $E_7 \sim 50$ kcal/mole, $A_7 \sim 10^9$ 1/mole sec, $[CH_4] = 1 \times 10^{-2}$ mole/l and $[CH_3] \sim (R^o_{C_2H_6}/k_3)^{\frac{1}{2}} \sim 1 \times 10^{-10}$ mole/l at 1000 K and 760 Torr; with these values the rate of reaction [7], R_7, is only 0.01% of $R^o_{C_2H_6}$ (10^{-10} mole/l sec). Since these values probably represent an upper limit for k_7 the contribution from this process is probably not significant. Finally, and most convincingly, it will be seen that the measured values of k_1 over the whole range of pressure and temperature are quantitatively in accord with theoretical calculations for the simple unimolecular dissociation of methane in its pressure-dependent region. Thus while the occurrence of reaction [7] cannot be ruled out completely, the present evidence weighs heavily against it, and it seems most unlikely that it is of any importance in the methane pyrolysis.

E. Theoretical Calculations of k_1 and Its Pressure-dependence.

Calculations of k_1 were based on the RRKM theory, well described by Forst (44) and Robinson and Holbrook (45). The general expression for the unimolecular rate constant is

$$[9] \quad k_{uni} = \frac{L^{\ddagger} Q_1^{+}}{h\, Q_1 Q_2} \exp(-E_o/RT) \int_0^{\infty} \frac{\sum_{E_{V=0}^{+}}^{E^{+}} P(E_v^{+}) \exp(-E^{+}/RT)\, dE^{+}}{1 + k_a (E^{*} + \langle \Delta E_J \rangle) / k_2[M]}$$

$$[10] \quad \text{where } k_a (E^{*} + \langle \Delta E_J \rangle) = \frac{L^{\ddagger} \sum_{E_{V=0}^{+}}^{E^{+}} P(E_v^{+})}{h\, F\, N^{*}(E^{*})}$$

The sum of states, $\Sigma P(E_v^{+})$, was evaluated by the direct count method. The density of states, $N^{*}(E^{*})$, was calculated using the approximation described by Tardy, Rabinovitch and Whitten (46). The centrifugal correction factor, F, was given by Marcus (47) and by Waage and Rabinovitch (48) as follows

$$[11] \quad N^{*}(E^{*} + \langle \Delta E_J \rangle) = F.N.^{*}(E^{*})$$

$$[12] \quad \text{where } F = \frac{[E^{*} + aE_z - (\frac{I^{+}}{I} - 1)\, RT]^{s-1}}{(E^{*} + aE_z)^{s-1}}$$

A constant energy increment of 0.5 kcal/mole was used in the computations. The symbols follow the nomenclature used by Robinson and Holbrook:

ΣP = sum of states of the transition state for energy = E^+;

$N^*(E^*)$ = density of states of molecules of energy E^*;

Q_1^+ = partition function of adiabatic modes of the activated complex;

Q_1, Q_2 = partition functions of rotation and vibrational modes of the molecule;

E^+ = total non-fixed energy in the active degrees of freedom of the activated complex;

E_o = critical energy;

E^* = non-fixed energy in the energized molecule;

E_z = total zero-point energy;

$L^{\ddagger}$ = reaction path degenracy.

Values for k_1^{∞} were not obtained in the present study but are not necessary for the calculation since the critical energy, E_o, for methane is well established. A value of E_o of 103 kcal/mole gave agreement with the magnitude of the measured value of k_1 while the dependence on pressure was matched by adjustment of the bending frequencies and of the moment of inertia of the activated complex. The methyl radical was assumed to be planar in the complex. All rotations were taken as abiabatic and centrifugal corrections were applied to the two external rotations. The complex is similar to the Model 4 described by Placzek et al (49). The values used in the calculations are shown in Table 4. The vibrational frequencies of the molecule and of the methyl radical were taken from JANAF (50).

The results of the calculations are listed in Table 5 and

TABLE 4

Values used in the Calculations

Molecule		Activated Complex	
designation	frequency cm^{-1}	designation	frequency[a] cm^{-1}
ν_1	2914	ν_1	3002
ν_2	1526 (2)	ν_2	580
ν_3	3020 (3)	ν_3	3184 (2)
ν_4	1306	ν_4	1380 (2)
		bending modes of dissociating bond	280 (2)

Moment of inertia

$I_a = I_b = I_c = 5.33 \times 10^{-40}$ gm cm^2

$I_a = 5.84 \times 10^{-40}$ gm cm^2

$I_b = I_c = 17.0 \times 10^{-40}$ gm cm^2

Collision diameter = $3.8A^o$

E_o = 103.0 kcal/mole

Number of rotations for centrifugal correction = 2

Collision efficiency, $\lambda = 1$

Statistical factor, $L^{\ddagger} = 4$

---

[a] For purposes of calculation ν_1 and ν_3 were combined as 3122 cm^{-1}.

TABLE 5

Calculated Values of k_1 based on the model described in Table 4.

T(K)	log(P/Torr)	$\log(k_1/sec)$	$\log(k_1/k_\infty)$
995	-1	-10.7903	-3.6140
	0	- 9.7978	-2.6214
	1	- 8.8574	-1.6811
	2	- 8.0956	-0.9193
	3	- 7.5754	-0.3991
	4	- 7.2983	-0.1219
	5	- 7.2011	-0.0247
	6	- 7.1816	-0.0052
1038	-1	- 9.8704	-3.6829
	0	- 8.8773	-2.6898
	1	- 7.9335	-1.7460
	2	- 7.1605	-0.9730
	3	- 6.6234	-0.4349
	4	- 6.3260	-0.1385
	5	- 6.2163	-0.0288
	6	- 6.1930	-0.0055
1068	-1	- 9.2911	-3.7289
	0	- 8.2977	-2.7356
	1	- 7.3516	-1.7895
	2	- 6.5715	-1.0093
	3	- 6.0218	-0.4596
	4	- 5.7125	-0.1503
	5	- 5.5941	-0.0320
	6	- 5.5679	-0.0058

TABLE 5 continued

T(K)	log(P/Torr)	$\log(k_1/sec)$	$\log(k_1/k_\infty)$
1103	-1	- 8.6459	-3.7829
	0	- 7.6522	-2.7892
	1	- 6.7037	-1.8406
	2	- 5.9154	-1.0524
	3	- 5.3524	-0.4894
	4	- 5.0281	-0.1650
	5	- 4.8991	-0.0361
	6	- 4.8692	-0.0062

are shown in Figure 10 as the solid lines. The calculated values for k_1 are seen to represent both the pressure-dependence and the absolute values for k_1 found experimentally. This provides strong confirmation of the interpretation of the present results in terms of the simple mechanism described by reactions [1] - [5].

Values of k_1^∞ obtained from equation [9] are listed in Table 3 together with the corresponding values of A^∞ and E^∞ calculated at each temperature. The striking feature of these results is the large difference (4.6 kcal/mole) between E^∞ and E_o. For a dissociation reaction in the high-pressure region, the experimental activation energy is always larger than E_o, which is defined as the difference in zero-point energies of the reactants and the activated complex, because the population of excited vibrational levels will always be larger in the activated complex than in the reactant. The difference between E^∞ and E_o has commonly been found to be about 2 kcal/mole. For example for the isomerization of 1,1-dichlorocyclopropane, E^∞ = 57.7 and E_o = 55.5 kcal/mole (45). Most of the unimolecular decompositions which have been studied have activation energies in this range. The critical energy for decomposition of methane is much larger and the temperature at which decomposition occurs is correspondingly higher. Taking into account as well the very low vibrational frequencies of three of the normal modes of the complex as compared to the reactant, a relatively large population of excited vibrational levels in the activated molecule will be expected. The

result is a large difference between E^{∞} and E_o, larger than has previously been reported. Unfortunately, a theoretical interpretation is still not available; Slater's formulation leads to $E_o = E^{\infty}$ whereas RRKM theory does not give a simple relation between E_o and E^{∞}.

F. Comparison of k_1 Measured in Static, Flow and Shock Tube Pyrolysis.

Using the parameters for the unimolecular dissociation of methane determined in the preceeding section, the rate constant may be calculated for a wide range of temperature and pressure. These values are shown as solid lines in Fig. 11. The values of k_1 obtained at the highest temperature in the present work are shown together with recent values of k_1 obtained from shock tube pyrolysis and studies in a flow system. In most of these studies Argon was used as diluent. To compute a total equivalent pressure of methane, Ar was assumed to be 1/3 as efficient as methane as a collision partner (45). The same efficiency was assumed for other inert diluents. For comparison purposes only representative data were chosen from the range of values reported by most authors.

The data of Palmer and Hirt (11) obtained in a flow system at 1200 and 1400 K are in good agreement with the calculated values. From shock tube studies, the results of Skinner and Ruehrwein at 1200 and 1400 K (16), Kozlov and Knorre at 1800 and 2000 K (18), and Glick at 2000 K (15) are in very close agreement; those of Kevorkian,

Heath and Boudart at 1670 K (17) and Glick at 2200 K (15) are slightly higher, and those of Napier and Subrahmanyam at 2000 K (51) slightly lower, than the calculated values. In all of these studies the authors assumed that the rate constant was not pressure-dependent. However, the scatter in the rate constants obtained by Glick at 2200 K and by Kozlov and Knorre at 1800 K would encompass the variation with pressure which we predict, and their data are therefore compatible with the present results. In only one shock-tube study, that of Hartig, Troe and Wagner (21), was the rate constant shown to be pressure-dependent. This dependence is also close to that predicted by the present model but the measured value of k_1 is about six times lower than the calculated value; the reason for this discrepancy is not obvious. Agreement between observed and calculated rate constants is on the whole very good, especially as it is well known that the uncertainty in the measurement of temperature in a shock tube may easily be fifty degrees. All the results except those of Hartig et al fall within this range of the calculated values.

The most interesting aspect of these comparisons is the demonstration that all the measurements of the rate constant for dissociation of methane reported so far have been made in the pressure-dependent region. This fact was recognized in only one study, that of Hartig et al. An Arrhenius plot of rate constants in the pressure-dependent region is not very meaningful because the activation energy in this region is not simply related to the bond

Figure 11

The variation of k_1 with pressure for temperatures up to 2200 K. The solid lines are calculated from [9] and the experimental results were obtained in shock-tube studies or flow-system pyrolysis. 0, ref. 16; ×, ref. 11; ●, ref. 17; □ ref. 18; I, ref. 51; ■, ref. 15; ▲, ref. 21.

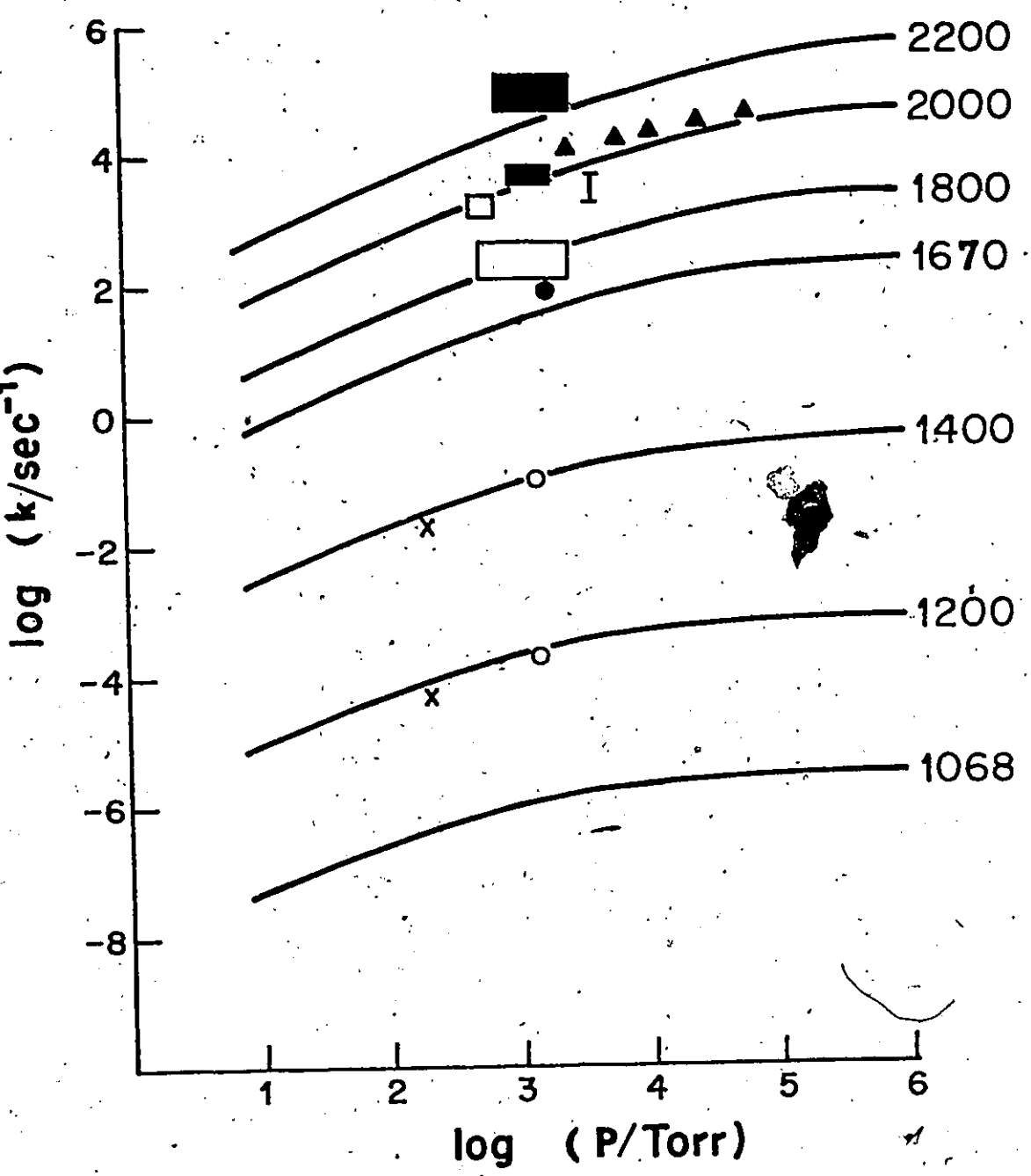
2200
2000
1800
1670
1400
1200
1068
6
4
2
0
-2
-4
-6
-8
1
2
3
4
5
6
log (k/sec⁻¹)
log (P/Torr)

dissociation energy and because the ratio k/k^{∞} is itself a function of temperature. Indeed a wide range of values for the activation energy of k_1 has been reported (85 - 103 kcal/mole) and the reason for the disagreement may be traced to the pressure-dependence of k_1. Fortuitously, however, the measured activation energy from several studies of about 103 kcal/mole appeared close to the bond dissociation energy and the authors were led to believe that a high-pressure value for k_1 had been measured. The present calculations show that the activation energy of k_1 in the pressure-independent region, E^{∞}, of 107 kcal/mole, is in fact several kcal/mole higher than $D^{o}(CH_3\text{-}H)$, which was taken as 103 kcal/mole. The observed activation energy of k_1 in its pressure-dependent region is therefore lower than the value of E^{∞} as predicted by unimolecular theory.

G. Calculations of k_{-1} and Comparison With Measured Values.

Using the value of the equilibrium constant for reaction [1] and the expression obtained for k_1, values of k_{-1}, the rate constant for the combination of a methyl radical and a hydrogen atom, were calculated over a range of pressures at 500, 700 and 1038 K. The results are shown in Fig. 12 and are listed in Table 6 together with the thermodynamic values used in the calculation. The results of three recent measurements of k_{-1} are also included. These measurements were made in an Ar or He carrier and the total pressure has therefore been reduced by a factor of three to correct for the

TABLE 6

Equilibrium Constant and Rate Constants for the reaction[a]

$$CH_4 \underset{-1}{\overset{1}{\rightleftarrows}} CH_3 + H$$

T^oK	ΔH kcal/mole	ΔS_p[b] cal/mole.deg.	log K_c[c]	log k_1	log k_{-1}	log P (Torr)
500	105.0	31.5	-40.62	-31.76	8.86	0
				-30.89	9.73	1
				-30.34	10.28	2
				-30.10	10.52	3
700	105.8	32.76	-27.64	-19.19	8.45	0
				-18.29	9.35	1
				-17.63	10.01	2
				-17.25	10.39	3
1038	106.6	33.53	-16.96	-8.88	8.08	0
				-7.93	9.03	1
				-7.16	9.80	2
				-6.62	10.34	3

[a] Units mole l^{-1} where applicable. Data are taken from ref (43)

[b] standard state 1 atm. of ideal gas.

[c] $K_p = K_c (RT)^{\Delta n}$.

Figure 12

The variation of log k_{-1} with pressure. The solid lines are calculated as described in the text and the experimental points are recent measurements of k_{-1}. O, ref. 52; Δ, ref. 54; ●, ref. 55; □, ref. 53.

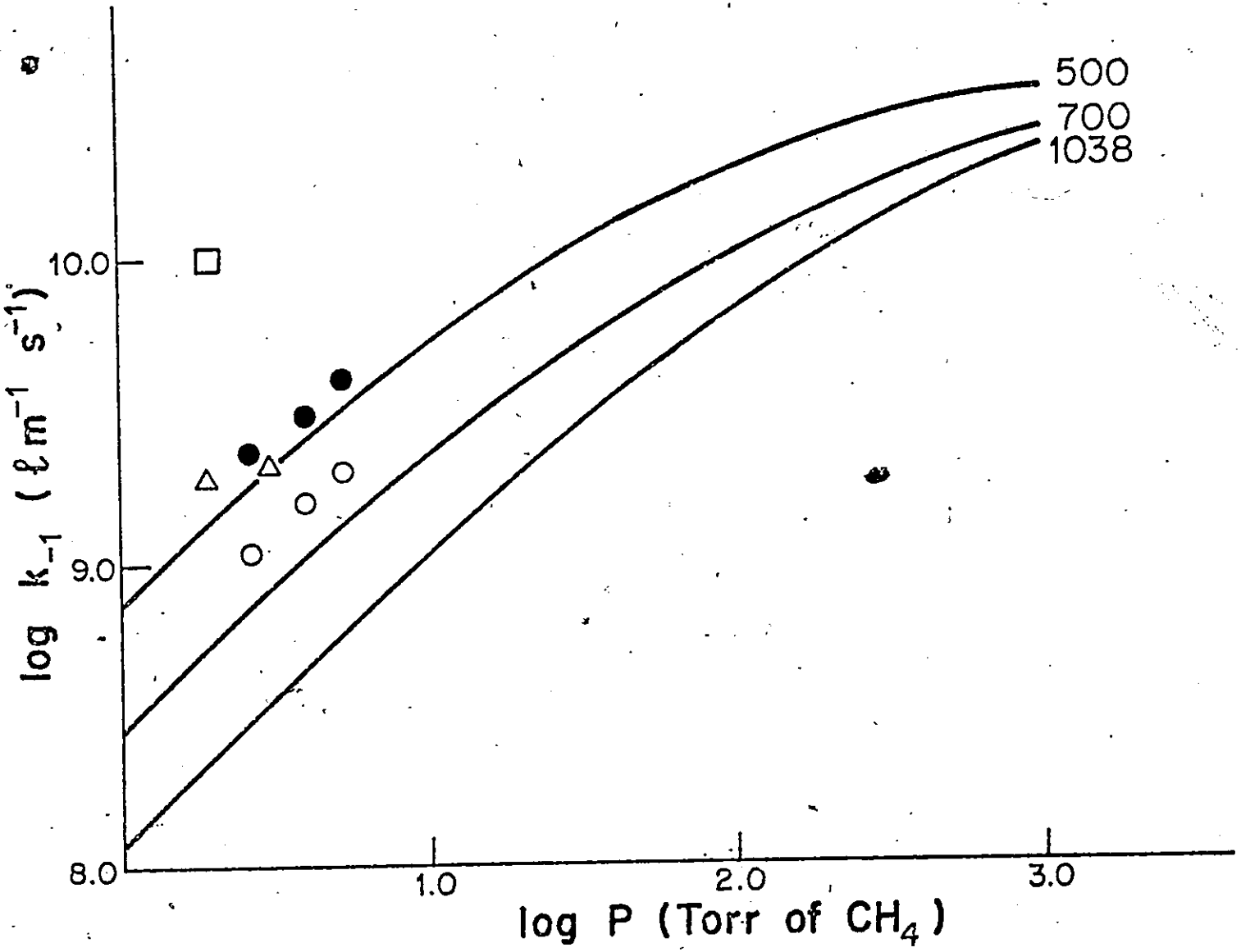
500
700
1038
10.0
9.0
8.0
log k_{-1} ($\ell m^{-1} s^{-1}$)
1.0
2.0
3.0
log P (Torr of CH_4)

efficiency of these gases as third bodies relative to methane (45). The measurements of Camilleri, Marshall and Purnell in the range 500 - 700 K (52) are in good agreement with the present calculations. Comparison with the data of Dodonov et al (53), Pratt and Veltman (54) and Halstead et al (55) all at about 295 - 300 K is less certain because extension of equation [9] to this temperature presented some computational difficulties and was not pursued. If the trend at the three higher temperatures continues, the value of Dodonov et al appears rather high; the other data are somewhat lower than predicted, but in reasonable agreement. The value of k_{-1}^{∞} obtained in these calculations is 2.5×10^{11} 1 $mole^{-1}s^{-1}$, which is about 1/4 of the collision number for these radicals.

The extension of equation [9], with the model of the activated complex for methane described herein, down to 500 K and up to 2200 K provides a stringent test for the theory: The agreement with other measurements at both ends of the temperature range is strong support for the validity of this method. There are several approximations in these calculations which might be expected to limit the range of applicability of any particular model. For example, in the calculation of the density of states the harmonic oscillator approximation has been used. The limitations of this assumption have been discussed by Forst (44) and Forst and Prasil (56) have investigated the dependence on energy of the density of states and of the unimolecular rate constant k_a, equation [10], for a small molecule, hydrogen peroxide.

Their results showed that the unimolecular rate constant calculated using Morse oscillators is lower by about a factor of two than the rate constant calculated using purely harmonic oscillators, in the "low energy" region applicable to thermal systems. The ratio of the two rate constants, however, did not change appreciably with an increase in the excitation energy in the low energy region. The excitation energy of the activated complex for the thermal dissociation of methane lies well within this low energy region considered by Forst and Prasil (56) and it may be concluded that inclusion of anharmonic effects in the present calculations will not change the relative values of the rate constants over the temperature range considered here.

The model of the activated complex is itself an approximation and modifications to it could be explored for better agreement over the whole temperature range. For example, Forst and Prasil (56) have calculated the effect on k_a of a complex in which one oscillator is coupled with a two-dimensional rotor, taking hydrogen peroxide as the dissociating molecule. Some lowering of k_a was observed as the excitation energy and the rotational quantum number was increased. The effect, however, was not large in the low range of excitation energy encountered in thermal systems, and taking into account the large uncertainties in the values of k_1 in the region of 2000 K and of k_{-1} at the low temperature end it was not considered profitable to pursue such calculations. It may be concluded that the model chosen

for the activated complex provides a reasonable agreement with other measurements in the temperature range 500 - 2000 K.

III. Kinetics and Mechanism of the Formation of Ethane.

A. Mechanism.

The series of reactions [1] to [5] accounts quantitatively for the yield of ethane up to about the attainment of its plateau value. Within this region, the autocatalysis is not important and the amounts of tertiary products, acetylene and propylene, are generally less than that of ethane and ethylene. It also accounts quantitatively for the formation of hydrogen and ethylene when the amounts of acetylene, propylene and allene formed are small.

[1] $CH_4 \rightarrow CH_3 + H$

[2] $H + CH_4 \rightarrow CH_3 + H_2$

[3] $2CH_3 \rightleftarrows C_2H_6$

[4] $CH_3 + C_2H_6 \rightarrow CH_4 + C_2H_5$

[5] $C_2H_5 \rightarrow C_2H_4 + H$

B. Evaluation of the Rate Constant, k_4.

From the proposed mechanism it can be seen that initially reactions [1], [2] and [3] describe the course of the decomposition but as ethane accumulates it begins to disappear in the dehydrogenation sequence, reactions [4], [5] and [2], and should reach

a plateau value if no other processes intervene.

At the plateau region, the rate of disappearance of ethane is equal to its rate of formation or the rate of methane dissociation, R_o,

$$[13] \qquad R_o = \alpha\, k_4[CH_3][C_2H_6]_{ss}$$

where $\alpha = k_5/(k_5 + k_{-4}[CH_4])$, the fraction of ethyl radicals formed in reaction [4] which decompose via reaction [5], and $[C_2H_6]_{ss}$ is the concentration of ethane at the steady state. The steady state approximation for methyl radicals gives

$$[14] \qquad CH_3 = \{(R_o + k_{-3}[C_2H_6]_{ss})/k_3\}^{\frac{1}{2}}$$

Note that while reaction [-3], the reverse of reaction [3], must be taken into account in calculating the radical concentration, and in fact becomes the dominant source of methyl radicals, it does not enter directly into the steady-state equation for ethane, because it does not lead to a net consumption of methyl radicals, since these ultimately can only recombine to reform ethane in the present system. Combination of equations [13] and [14] gives

$$[15] \qquad R_o = \alpha\, k_4(R_o + k_{-3}[C_2H_6]_{ss}/k_3)^{\frac{1}{2}}[C_2H_6]$$

Experimentally, ethane is observed to reach a more or less well-defined steady-state plateau before the reaction begins to accelerate (Fig. 3), and from such plateau values, k_4 has been

calculated from the steady-state equation [15]. R_o is the initial rate of the formation of ethane. Values of k_{-3} were derived from RRKM calculations based on model I described by Lin and Laidler (57) for the ethane decomposition. A value of 4.0×10^{10} 1/(mole sec) was used for k_3^∞ in the present calculation. This value is calculated from the value of 2.4×10^{10} 1/(mole sec) at 300 K assuming a square root dependence of the rate constant on temperature. The discrepancy between this value of k_3 and the measured values for k_{-3} has been discussed by Waage and Rabinovitch (58). For the present calculation of k_4, the accepted value of k_3 was used because other measurements of k_4 were made relative to this value of k_3. All measurements of k_4 may therefore be compared in a consistent manner.

Values of k_4 and the data from which they were derived are shown in Table 7. No variation of αk_4 with methane pressure was observed, and it may be concluded that reaction [-4] was negligible under these experimental conditions, i.e., $\alpha = 1$. This conclusion was supported by the fact that propane was not detected in the products before the autocatalysis region (less than 1×10^{-9} mole/1). Average values of k_4 are given in the final column of Table 7.

In a series of experiments at 880 K a small amount of ethane was added to the reactant methane and its consumption with time was measured. Dissociation of methane (reaction [1]) can be neglected compared to reaction [-3], and the rate of disappearance of ethane may be expressed as

TABLE 7

Values of k_4

PCH_4 Torr	$[C_2H_6]_{ss}$ $\frac{mole}{\ell} \times 10^8$	R_o $\frac{mole}{\ell sec} \times 10^{10}$	k_{-3} $sec^{-1} \times 10^3$	k_4 $\frac{\ell}{mole\ sec} \times 10^{-6}$
T = 995 K				
51	2.09	.044	0.84	6.85
108	3.98	.152	1.01	8.62
440	23.03	1.33	1.32	5.31
540	24.08	1.79	1.36	6.46
640	33.50	2.29	1.39	5.13
741	28.26	2.83	1.42	7.60
			average	6 ± 1
T = 1038 K				
31.9	1.675	.166	4.64	14.5
108	5.49	1.31	6.66	18.2
188	10.99	3.15	7.60	15.1
236	15.08	4.50	7.98	13.6
338	21.99	7.79	8.57	13.2
441	37.69	11.6	9.00	9.90
543	31.41	15.8	9.32	15.0
642	46.06	20.2	9.57	10.1
741	50.25	24.8	9.77	10.1
			average	13 ± 3

TABLE 7 continued

P_{CH_4} Torr	$[C_2H_6]_{ss}$ $\frac{mole}{\ell} \times 10^8$	R_o $\frac{mole}{\ell sec} \times 10^{10}$	k_{-3} $sec^{-1} \times 10^3$	k_4 $\frac{\ell}{mole\ sec.} \times 10^{-6}$
T = 1068 K				
25.2	2.09	0.422	12.7	14.6
48.6	4.18	1.324	15.9	15.9
75.5	7.12	2.79	18.2	15.1
104	8.38	4.74	19.9	19.5
154	15.3	8.99	22.0	15.1
233	20.9	17.20	24.3	17.6
339	36.9	30.61	26.2	13.5
440	44.0	45.29	27.6	15.1
600	67.0	71.63	29.1	13.7
742	73.3	97.43	30.1	14.6
			average	15 ± 2

$$d[C_2H_6]/dt = k_4(k_{-3}/k_3)^{\frac{1}{2}}[C_2H_6]^{3/2}$$

Integrating from $[C_2H_6]_o$ to $[C_2H_6]_t$ gives

$$[16] \quad \frac{[C_2H_6]_o^{\frac{1}{2}} - [C_2H_6]_t^{\frac{1}{2}}}{[C_2H_6]_o^{\frac{1}{2}}\,[C_2H_6]_t^{\frac{1}{2}}} = \tfrac{1}{2}\, k_4(k_{-3}/k_3)^{\frac{1}{2}}\, t$$

A plot of the left-hand side of this equation against t is shown in Fig. 13. Using values for k_{-3} and k_3 obtained as before, a value of $k_4 = 4.6 \times 10^6$ 1/(mole sec) may be calculated from the slope of this line.

This value of k_4 together with the average values of k_4 from Table 7 are shown in an Arrhenius plot in Fig. 14, which also includes previous measurements of k_4 (59, 60, 61, 62, 63, 64). In recent years there has been growing evidence that Arrhenius plots for some simple hydrogen abstraction reactions show marked upward curvature in the region 700 - 1500 K, so that the rate constants measured at these temperatures are considerably higher than predicted from simple Arrhenius equations measured at lower temperatures. This behaviour has been discussed by Clark and Dove (65) who have shown that the observed increase in activation energy for reactions such as [2] and [4] may be accounted for within the framework of activated complex theory. The present results provide confirmation of a "high" value of k_4 around 1000 K first reported by Pacey and Purnell (60) from a study of the pyrolysis of butane, and support the suggestion that the Arrhenius A factor is temperature dependent.

Figure 13

Plot of $\frac{[C_2H_6]_o^{\frac{1}{2}} - [C_2H_6]_t^{\frac{1}{2}}}{[C_2H_6]_o^{\frac{1}{2}}[C_2H_6']_t^{\frac{1}{2}}}$ against t at 880 K

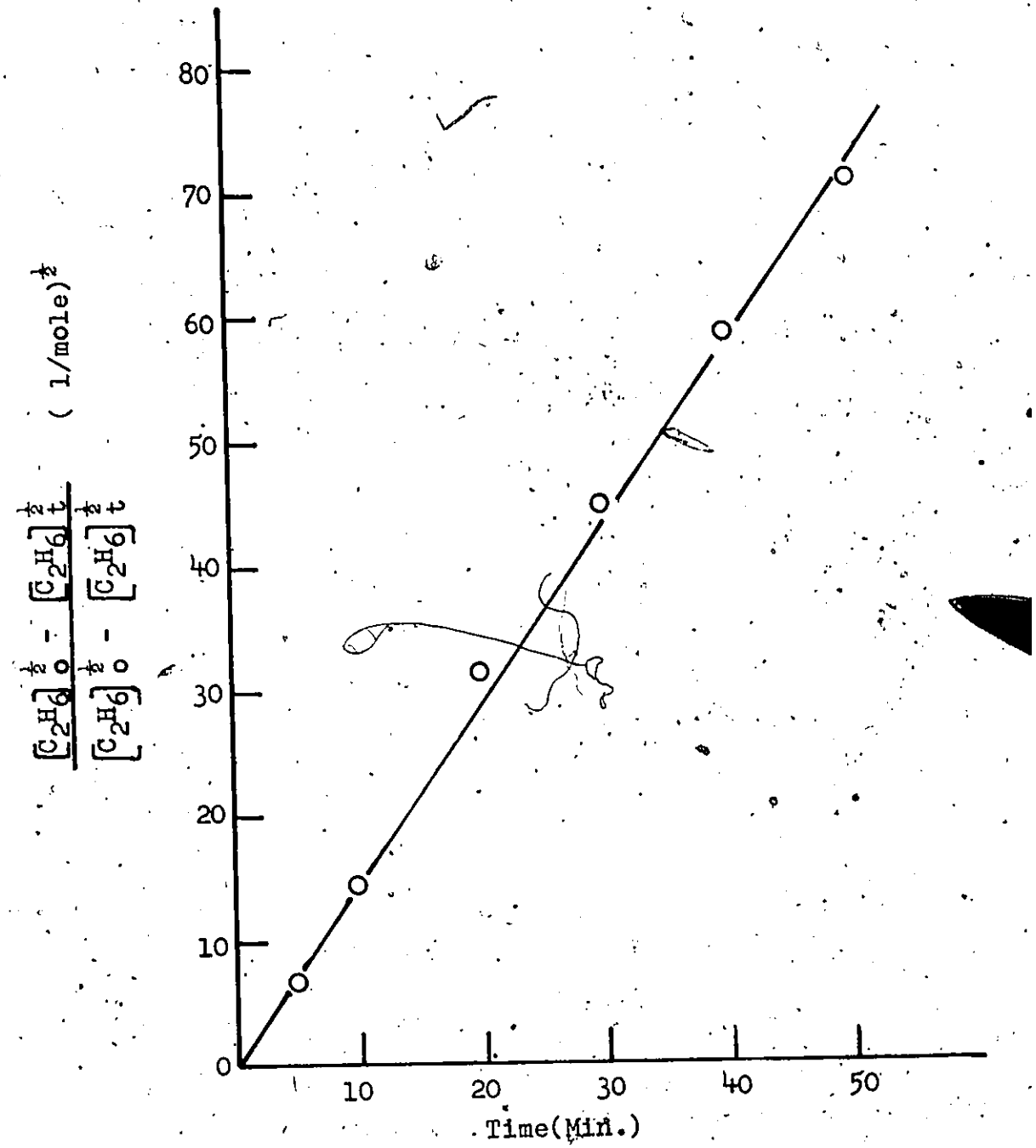
$\frac{[C_2H_6]_o^{\frac{1}{2}} - [C_2H_6]_t^{\frac{1}{2}}}{[C_2H_6]_o^{\frac{1}{2}} - [C_2H_6]_t^{\frac{1}{2}}}$ (1/mole)$^{\frac{1}{2}}$
0
10
20
30
40
50
60
70
80
10
20
30
40
50
Time(Min.)

Figure 14

Arrhenius plot of k_4

X : reference (59)

0 : reference (60)

+ : reference (61)

▲ : reference (62)

□ : reference (63)

■ : reference (64)

● : this work

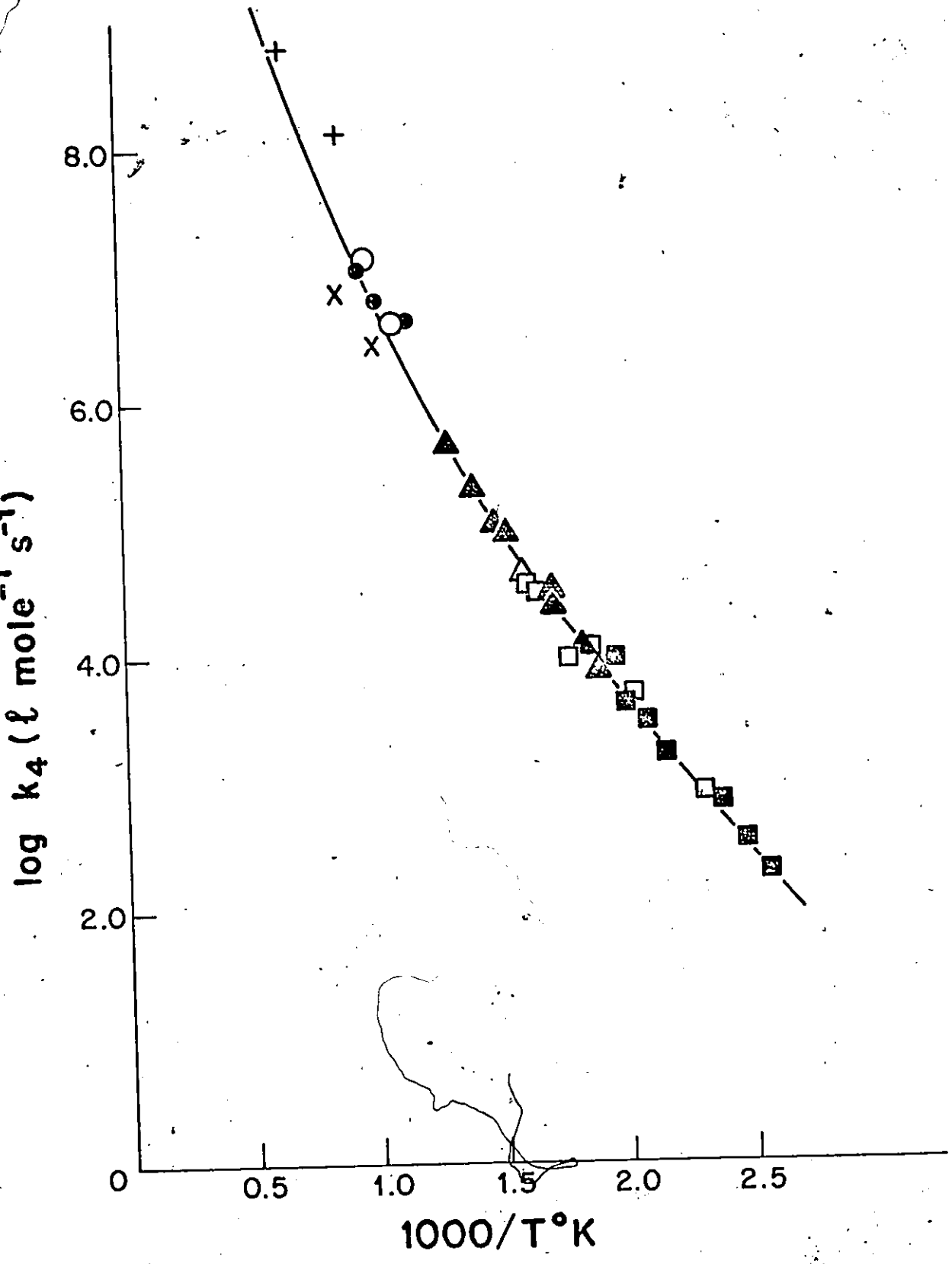
8.0
6.0
4.0
2.0
0
log k_4 (ℓ mole^{-1} s^{-1})
0.5
1.0
1.5
2.0
2.5
1000/T°K

IV. The Mechanism of the Pyrolysis.

A. The following mechanism represents a summary of the reactions occurring prior to the autocatalysis region.

Primary formation of ethane and hydrogen

[1] $CH_4 \rightarrow CH_3 + H$

[2] $H + CH_4 \rightarrow CH_3 + H_2$

[3] $2CH_3 \rightarrow C_2H_6$

net reaction: $2CH_4 \rightarrow C_2H_6 + H_2$

Reaction [1] is rate controlling, and always followed by reaction [2] which is much faster. In the initial stages of the pyrolysis reaction [1] is the only primary radical source. Both reaction [1] and [3] are pressure dependent.

Secondary reaction of ethane

[4] $CH_3 + C_2H_6 \rightarrow CH_4 + C_2H_5$

[5] $C_2H_5 \rightarrow C_2H_4 + H$

[2] $H + CH_4 \rightarrow CH_3 + H_2$

net reaction: $C_2H_6 \rightarrow C_2H_4 + H_2$

Reactions [4], [5] and [2] constitute a chain reaction converting ethane to ethylene and hydrogen. Reaction [4] is rate controlling and

reaction [-4], the reverse of [4], is largely negligible so that every C_2H_5 formed in [4] decomposes.

Unimolecular decomposition

[-3] $C_2H_6 \rightarrow 2\ CH_3$

Reaction [-3], the reverse of [3], can become an important secondary source of radicals under some conditions.

Secondary reactions of ethylene

Radical chain dehydrogenation

[17] $CH_3 + C_2H_4 \rightarrow CH_4 + C_2H_3$

[18] $C_2H_3 \rightarrow C_2H_2 + H$

[2] $H + CH_4 \rightarrow CH_3 + H_2$

net reaction: $C_2H_4 \rightarrow C_2H_2 + H_2$

Reaction sequences [17], [18] and [2], and [19], [20] and [2] constitute two parallel chain decompositions of ethylene, propagated by methyl radicals, and initiated by abstraction and addition respectively. Reaction [17] is rate controlling in the first sequence, and its reverse, [-17], is probably negligible. In the addition sequence on the other hand, reaction [-19] is probably much faster than reaction [20], making the latter rate controlling.

Radical chain methylation

[19] $CH_3 + C_2H_4 \rightleftarrows n\text{-}C_3H_7$

[20] $n\text{-}C_3H_7 \rightarrow C_3H_6 + H$

[2] $H + CH_4 \rightarrow CH_3 + H_2$

net reaction: $C_2H_4 + CH_4 \rightarrow C_3H_6 + H_2$

Secondary reactions of acetylene

Radical chain dehydrogenation

[21] $CH_3 + C_2H_2 \rightleftarrows CH_4 + C_2H$

[22] $C_2H \rightarrow C_2 + H$

This dehydrogenation sequence does not occur because reaction [21] is much too endothermic (~ 139 kcal/mole) to be of any importance at the present temperatures; this cannot therefore be a source of carbon in the methane decomposition.

Radical chain methylation

[23] $CH_3 + C_2H_2 \rightarrow CH_3CHCH$

[24] $CH_3CHCH \rightarrow CH_3CCH + H$

[2] $H + CH_4 \rightarrow CH_3 + H_2$

net reaction: $C_2H_2 + CH_4 \rightarrow CH_3CCH + H_2$

As with ethylene, the reverse of the addition reaction, [-12], is probably much faster than reaction [24], so that the latter is rate controlling.

Secondary reactions of propylene

Radical chain dehydrogenation

[25] $CH_3 + C_3H_6 \rightarrow CH_4 + C_3H_5$

[26] $C_3H_5 \rightarrow CH_2CCH_2 + H$

[2] $H + CH_4 \rightarrow CH_3 + H_2$

---

stoichiometry: $C_3H_6 \rightarrow CH_2CCH_2 + H_2$

Both addition and abstraction sequences can occur with propylene. Abstraction appears to predominate, as yields of allene were much higher than those of butene.

Radical chain methylation

[27] $CH_3 + C_3H_6 \rightarrow CH_3CH_2CHCH_3$

[28] $CH_3CH_2CHCH_3 \rightarrow CH_3CH_2CH{=}CH_2 + H$

[2] $H + CH_4 \rightarrow CH_3 + H_2$

---

stoichiometry: $C_3H_6 + CH_4 \rightarrow CH_3CH_2CH{=}CH_2 + H_2$

Unimolecular decomposition

[29] $C_3H_6 \rightarrow H + C_3H_5$ or

$CH_3 + C_2H_3$

This can become a significant source of radicals when the propylene concentration becomes high enough.

The mechanism outlined above is in essence very simple, and depends on the following premises:

(1) The CH_3 radical is the only radical present in significant concentrations.

(2) Hydrocarbon products disappear solely through reaction with methyl radicals in chain sequences with no net consumption of radicals. A minor exception is dissociation reactions [-3] and [29].

(3) Other hydrocarbon radicals dissociate so rapidly that they take part in no other reactions. An exception is C_2H which instead is maintained at a negligibly low concentration by back reaction with methane [-21].

(4) Hydrogen atoms always react by reaction 2 to form hydrogen.

These premises are made tenable by the large excess of methane always present, so that even at the highest conversions products were always less than 3% of the methane, and by the relatively high temperature, which renders the higher radicals very shortlived with respect to decomposition.

The several chain reaction sequences propagated by methyl

radicals follow a common pattern, with initiation by abstraction or addition, and propagation by radical decomposition, but there are notable differences. Thus with ethane, only abstraction is possible, but with ethylene both abstraction and addition sequences occur; with acetylene the abstraction sequence is blocked by the stability of the C_2H radical so that only addition is important, while with propylene, abstraction of the allylic hydrogen is apparently much faster than addition, and the former predominates. Finally, it should be noted that initially there is no radical-chain decomposition of methane; further, that the chain sequences initiated by abstraction do not consume methane, and only with the addition sequences, beginning with ethylene, is methane consumed; even then it is a short chain, limited by the amount of olefin present.

B. Autocatalysis, carbon formation and surface effects.

The third or autocatalytic stage in the methane pyrolysis, in which the yield of ethane begins to rise sharply again after the steady-state plateau (Fig. 3) is not predicted or explained by the reaction mechanism postulated above. The autocatalysis is most evident in the yield of ethane, but almost certainly affects the other products as well, although it is less obvious because their yields are already rising sharply. Autocatalysis has frequently been reported in the decomposition of methane, and under various conditions of pressure, temperature, conversion or surface, may have a variety of

causes. It is most commonly associated with the formation of carbon, and attributed to reactions occurring at a carbon surface.

The effect of carbon deposits in the present system was investigated in several ways. Ordinarily, oxygen was admitted to the reaction vessel after each experiment to oxidize any carbon that might be present, and the vessel was thoroughly pumped out; this procedure yielded highly reproducible results over long periods of time. In some experiments a carbon deposit was first laid down in the vessel by pyrolyzing methane for a few hours; subsequent pyrolyses in the presence of this carbon surface showed faster than normal and somewhat erratic rates of reaction. In further series of experiments begun with the usual clean surface, methane and volatile products were removed at intervals, but any carbon deposit was retained; a new sample of methane was then admitted and the reaction continued (see Section 1 A). If the accumulation of a nonvolatile carbon deposit were responsible for the autocatalysis, this should not be affected by periodic removal of volatile products, and autocatalysis should set in at the usual <u>total</u> time of reaction. This was not observed; experiments with products removed at intervals showed no acceleration in rate even though carried on far past the usual time for autocatalysis. Even experiments in which each <u>interval</u> was well into the autocatalytic stage showed no increase in rate over many intervals. It can only be concluded that carbon deposits play no part in autocatalysis in the present system.

Surface effects were also investigated by experiments in a reaction vessel filled with quartz tubes which increased the surface/volume ratio by a factor of 10. Initial rates of ethane formation were quite unaffected, and the early stages of the decomposition were undoubtedly homogeneous. Formation of seconcary products and of ethane in the autocatalytic stage showed some surface enhancement, suggesting a small surface component in the secondary reactions, probably less than 10% of the whole. This relative lack of sensitivity to surface/volume ratio again indicates that surface deposits of carbon are not very important in the reaction mechanism.

Two plausible alternatives may be suggested to account for the observed autocatalysis. The first of these is that carbon is indeed responsible, but a fine smoke-like suspension of carbon particles rather than a surface deposit (13). These would have an enormous surface area and therefore be much more effective than a surface deposit of carbon; the particles would also be swept out of the reaction vessel with the methane and volatile products, so that no cumulative effects would be observed in the "interval" experiments. Experiments described in Chapter 4 show that this hypothesis is not tenable.

The second alternative is that homogeneous reactions can cause the autocatalysis. A new source of radicals must become important in the autocatalysis region, and the rate of this new initiation process must rise very sharply with time. Simple computer

simulation of the reaction system shows which type of reactions might have the right properties. Disproportionation reactions between olefins and methane such as $C_2H_4 + CH_4 \rightarrow C_2H_5 + CH_3$ are kinetically wrong, as they cannot cause a sharp enough rise in the reaction rate, as well as being too slow. Bimolecular reactions of olefins or acetylene such as $2\ C_2H_2 \rightarrow C_2H + C_2H_3$ are more promising in as much as they yield autocatalysis curves of the proper shape, but again the reaction rates are probably too slow. A bimolecular reaction of acetylene yielding a diradical which can initiate radical chains would also have the right kinetic properties. This type of reaction would have a lower activation energy than the bimolecular reaction giving two radicals (66) and could be fast enough to give the observed yields of products. Diradical formation has been postulated in the pyrolysis of acetylene itself (67) and seems to offer the most plausible mechanism for homogeneous autocatalysis in the present system, but these suggestions must be regarded as speculative. The lack of a complete yield-time study of hydrocarbon products with carbon number higher than 3 has impaired a successful simulation.

V. Isotope exchange reaction between CH_4 and CD_4 in the pyrolysis of methane.

A. Mechanism of the exchange reaction.

As mentioned earlier (Section II) CH_3D and CD_3H were major products of the pyrolysis of CH_4/CD_4 mixtures (Table 2, page 36). This same exchange reaction was studied previously at higher temperatures (1340 - 1745 K) in a shock tube by Burcat and Lifshitz (68), who concluded that it proceeded by a radical chain mechanism. There seems little doubt that the same mechanism is operative in the present system.

Initially, dissociation of CH_4 and CD_4 is the only important source of radicals.

[1a] $CH_4 \rightarrow H + CH_3$

[1b] $CD_4 \rightarrow D + CD_3$

These will be followed by the abstraction reactions

[2a] $H + CH_4 \rightarrow H_2 + CH_3$

[2b] $H + CD_4 \rightarrow HD + CD_3$

[2c] $D + CH_4 \rightarrow HD + CH_3$

[2d] $D + CD_4 \rightarrow D_2 + CD_3$

The isotopic exchange leading to formation of CH_3D and CD_3H will proceed by an alternating chain propagated by the reactions,

[30] $CH_3 + CD_4 \rightarrow CH_3D + CD_3$

[31] $CD_3 + CH_4 \rightarrow CD_3H + CH_3$

Three termination steps involving CH_3 and CD_3 may be written as follows,

[3a] $CH_3 + CH_3 \rightarrow C_2H_6$

[3b] $CH_3 + CD_3 \rightarrow C_2H_3D_3$

[3c] $CD_3 + CD_3 \rightarrow C_2D_6$

The rates of the formation of CH_3D and CD_3H in the chain are given by,

[32] $$d[CH_3D]/dt = k_{30}[CH_3][CD_4]$$
$$d[CH_3H]/dt = k_{31}[CD_3][CH_4]$$

These rates are equal, hence

$$[CD_3] = \frac{k_{30}[CH_3][CD_4]}{k_{31}[CH_4]}$$

Addition of CH_3 on both sides of the equation gives,

$$[CH_3] + [CD_3] = [CH_3]\frac{k_{31}[CH_4] + k_{30}[CD_4]}{k_{31}[CH_4]}$$

or

[33] $$[CH_3] = \frac{k_{31}[CH_4]}{k_{31}[CH_4] + k_{30}[CD_4]} ([CH_3] + [CD_3])$$

Substitution of [33] into [32] leads to the following expression,

$$[34] \qquad d[CH_3D]/dt = \frac{k_{30}k_{31}[CH_4][CD_4]}{k_{30}[CD_4] + k_{31}[CH_4]} ([CH_3] + [CD_3])$$

The total radical concentration, $([CH_3] + [CD_3])$, can be evaluated by using the steady-state equations

for CH_3:

$$2k_{1a}[CH_4] - 2k_{3a}[CH_3] - 2k_{3b}[CH_3][CD_3] + 2k_{-3a}[C_2H_6] + 2k_{-3b}[C_2H_3D_3] = 0$$

and for CD_3:

$$2k_{1b}[CD_4] - 2k_{3c}[CD_3] - 2k_{3b}[CH_3][CD_3] + 2k_{-3c}[C_2D_6] + 2k_{-3b}[C_2H_3D_3] = 0$$

Therefore,

$$[CH_3] + [CD_3] = \left\{ \sum_{i=a}^{b} \frac{k_{1i}[M_i]}{k_3} + \sum_{i=a}^{c} \frac{k_{-3i}[E_i]}{k_3} \right\}^{\frac{1}{2}}$$

in which $k_{3a} = k_{3b} = k_{3c} = k_3$

$M_a = CH_4$ $M_b = CD_4$

and $E_a = C_2H_6$, $E_b = C_2H_3D_3$, $E_c = C_2D_6$

and equation [34] becomes

$$[35] \qquad d[CH_3D]/dt = \frac{k_{30}k_{31}[CH_4][CD_4]}{k_{30}[CD_4] + k_{31}[CH_4]} \left\{ \sum_{i=a}^{b} \frac{k_{1i}[M_i]}{k_3} + \sum_{i=a}^{c} \frac{k_{-3i}[E_i]}{k_3} \right\}^{\frac{1}{2}}$$

In the present study, equimolar mixtures of CH_4-CD_4 were used. Hence,

[36] $$d[CH_3D]/dt = k_s[CD_4][CH_3]$$

where

$$k_s = \frac{2k_{30}k_{31}}{k_{30} + k_{31}}$$

Because of the lack of information on the relative values of k_{1a} and k_{1b} as well as those of the termination constants the following approximations were made.

$$CH_3 = \frac{1}{2}\left\{\frac{\sum_{i=a}^{b} k_{1i}[CH_4] + \sum_{i=a}^{c} k_{-3i}[E_i]}{k_3}\right\}^{\frac{1}{2}}$$

which may be further simplified as

$$CH_3 = \frac{1}{2}\left\{\frac{2k_1[CH_4] + k_{-3a}\sum_{a}^{c}[E_i]}{k_3}\right\}^{\frac{1}{2}}$$

k_s may be regarded as an average rate constant for abstraction of a methyl radical from methane. Equation [36] was used to obtain k_s.

B. Measurement of the relative concentrations of CD_4, CD_3H, CH_3D, and CH_4 from mass spectra.

Mass spectra for pure CH_4, CD_4 and a 1:1 mixture of CH_4-CD_4 were obtained before and after each series of mass spectrometric analyses of product mixtures. Usually four spectra were used to obtain the average mass peaks for each sample at an ionizing potential of 25 eV. The simple subtraction method to compute the relative concentration of CD_4, CD_3H, CH_3D and CH_4 is illustrated in Table 8.

TABLE 8

Calculation of relative concentrations of CD_4, CD_3H, CH_3D and CH_4

Material	m/e						
	20	19	18	17	16	15	14
CD_4	100	3.034	71.30	1.165	2.378	0	0
CH_4				1.1	100	67.24	2.497
Mixture spectrum	90.5	14.1	59.4	21.4	129.4	81.2	2.9
Step 1: CD_4	-)90.5	2.8	64.5	1.05	2.15		
		11.3	-5.1	20.35	127.25	81.2	2.9
Step 2: CD_3H		-) 11.3	0.2	6.03	0.09	0.2	
		-)	7.6	0	0.06		
			-12.9	14.32	127.10	81.0	2.9
Step 3: CH_3D			-) 0.1	13.02	8.75	0.3	0
			-13.0	1.30	118.37	80.7	2.9
Step 4: CH_4				-) 1.30	118.37	79.6	2.9
Residue			-13.0			1.1	

In Table 8, only step 3 and step 4 involved the use of simultaneous equations for mass 17 and 16. In step 2, two possible fragmentations of CD_3H were taken into account. The resulting relative peak heights were normalized to 54.8. Thus the relative concentration CD_4:CD_3H:CH_3D:CH_4 in this example becomes 21.3:2.66:3.10:27.7. The sensitivity coefficient for each component was ignored as these factors cancel in the determination of rate constants.

C. Measurement of the experimental rate constant k_s.

From the rate law given by [32] and [36], k_s can be evaluated as

$$[37] \qquad -\frac{d[CH_4]}{dt} = -\frac{d[CD_4]}{dt} = \frac{d[CH_3D]}{dt} = \frac{d[CD_3H]}{dt} = k_s[\text{methyl}][\text{methane}],$$

where $[\text{methyl}] = \frac{1}{2}[CH_3 + CD_3]$

and $[\text{methane}] = [CD_4]$ or $[CH_4]$,

Hence

$$[38] \qquad \log [CH_4] = \log [CH_4]_o - \frac{1}{2.303} k't$$

$$[39] \qquad \log [CD_4] = \log [CD_4]_o - \frac{1}{2.303} k't$$

$$[40] \qquad \log \left(1 - \frac{[CH_3D]}{[CH_4]_o}\right) = -\frac{1}{2.303} k't$$

$$[41] \qquad \log \left(1 - \frac{[CD_3H]}{[CD_4]_o}\right) = -\frac{1}{2.303} k't$$

where $k' = k_s [\text{methyl}]$.

These expressions are valid only when no CH_2D_2 is formed. Secondary attack of methyl radicals on CH_4 and CD_4 can lead to the formation of CH_2D_2.

$$\begin{matrix} CH_3 \\ CD_3 \end{matrix} + CH_3D \rightarrow \begin{matrix} CH_4 \\ CD_3H \end{matrix} + CH_2D$$

$$CH_2D + \begin{matrix} CH_4 \\ CD_4 \end{matrix} \rightarrow \begin{matrix} CH_3D \\ CH_2D_2 \end{matrix} + \begin{matrix} CH_3 \\ CD_3 \end{matrix}$$

The four possible net reactions are

[42]
$$CH_3 + CH_3D + CH_4 \rightarrow CH_4 + CH_3D + CH_3$$
$$CH_3 + CH_3D + CD_4 \rightarrow CH_4 + CH_2D_2 + CD_3$$
$$CD_3 + CH_3D + CH_4 \rightarrow CD_3H + CH_3D + CH_3$$
$$CD_3 + CH_3D + CD_4 \rightarrow CD_3H + CH_2D_2 + CD_3$$

total net reaction: $2CH_3D + 2CD_4 \rightarrow 2CH_2D_2 + 2CD_3H$

Four similar reactions convert CD_3H and CH_4 into CH_3D and CH_2D_2. The concentrations of CH_3D and CD_3H remain unaffected by these reactions which merely convert CH_4 and CD_4 into CH_2D_2.

The abstraction of a D atom from CH_3D by a methyl radical has no effect on the product distribution. Radical combination involving CH_2D and CD_2H will be small as these radicals are removed rapidly by the excess CH_4 and CD_4. The rates of formation of CH_2D_2 and CH_3D may be written as follows (assuming all methyl + methane abstraction reactions have the same rate constant, k_s).

[43] $\Delta[CH_2D_2] = k_s[CH_3 + CD_3](3/4)(2/4)(1/2)[CH_3D]\Delta t$

[44] $\Delta[CH_3D] - k_s[CH_3][CD_4]\Delta t$

where the factors 3/4, 2/4, 1/2 are to account statistically for the number of H atoms in CH_3D, the number of effective reactions and the average concentration of CH_3D, respectively. Dividing equation [43] by [44], assuming $[CH_3] = [CD_3]$, yields:

$$[CH_2D_2] = (3/8)([CH_3D]/[CD_4])^2 \times 100\%$$

The maximum conversion of CD_4 or CH_4 was 20%. Hence the amount of CH_2D_2 formed may be calculated as follows:

$$[CH_2D_2] = (3/8)(0.2)^2 100\%$$
$$= 1.5\%$$

Therefore it may be concluded that the radical attack on CH_3D or CD_3H does not affect the concentrations of CH_3D and CD_3H, and provides only minor routes for the disappearance of CH_4 and CD_4.

The re-dissociation of ethane in the system creates some difficulty in the accurate calculation of methyl radical concentrations. From the yield-time plot for ethane formation in Fig. 3, it can be seen that the methyl radical concentration increases with time, satisfying the relationship:

[45] $CD_3 = CH_3 = \{R_o/k_3 + k_{-3}[C_2H_6](t)/k_3\}^{\frac{1}{2}}$

Substituting this radical concentration into equation [37] for the

rate of disappearance of methane gives

$$d[CH_4]/[CH_4] = k_s \{R_o/k_3 + k_{-3}[C_2H_6](t)/k_3\}^{\frac{1}{2}} dt$$

Integration of this equation requires a polynomial curve-fitting of the ethane concentration and is only feasible using a computer. For simplicity the methyl radical concentration was taken as the average of its concentration at time zero ($[\dot{C}_2H_6] = 0$) and its concentration when the ethane concentration reached a constant value, $[C_2H_6]_{ss}$. The calculated values of the methyl radical concentration at these two limits are listed in Table 9. The maximum deviation of these two extreme concentrations from the ayeraged concentration is about 35%.

Rate constants, k', were evaluated from the data shown in Fig. 15 to Fig. 20 using equations [38] to [41], and the averages of the four values are listed in Table 10. The fundamental data are listed in Appendix 3. In the experiments at the lowest temperature, 880°K, ethane was added to increase the rate of initiation, which was then calculated from equation [45].

TABLE 9

T (K)	Total methyl concentration ($[CH_3] + [CD_3]$), mole/l		
	at initial stage	at $[C_2H_6]_{ss}$	Average
	$(R_o/k_3)^{\frac{1}{2}}$	$\{R_o/k_3 + k_{-3}[C_2H_6]_{ss}/k_3\}^{\frac{1}{2}}$	
880*	2.04×10^{-12}	4.32×10^{-11}	4.32×10^{-11}
957	2.13×10^{-11}	2.56×10^{-11}	2.34×10^{-11}
995	6.02×10^{-11}	1.09×10^{-10}	8.46×10^{-10}
1038	1.73×10^{-10}	3.43×10^{-10}	2.58×10^{-10}
1068	3.58×10^{-10}	6.87×10^{-10}	5.22×10^{-10}
1103	8.04×10^{-10}	17.6×10^{-10}	12.8×10^{-10}

* 0.237% of ethane was added.

Figure 15

Plot of log β and log $(1 - \gamma)$ against time at 880 K, 440 Torr of 1:1 mixture of CH_4-CD_4.

15 a: O, $\beta = [CH_4]$; ●, $\beta = [CD_4]$

15 b: O, $\gamma = [CH_3D]/[CH_4]_o$; ●, $\gamma = [CD_3H]/[CD_4]_o$

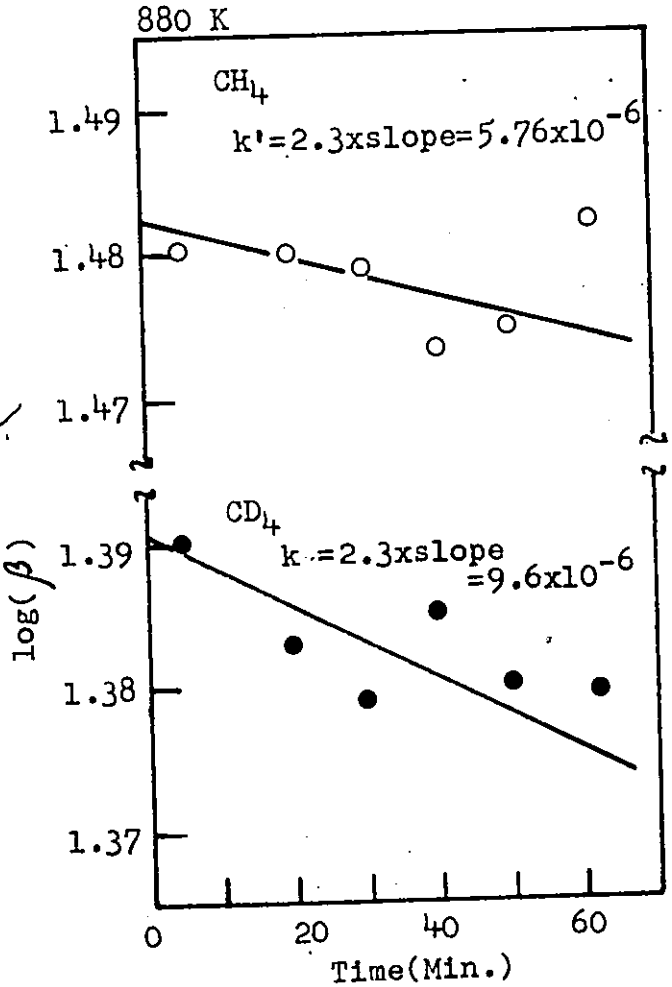

Fig. 15a

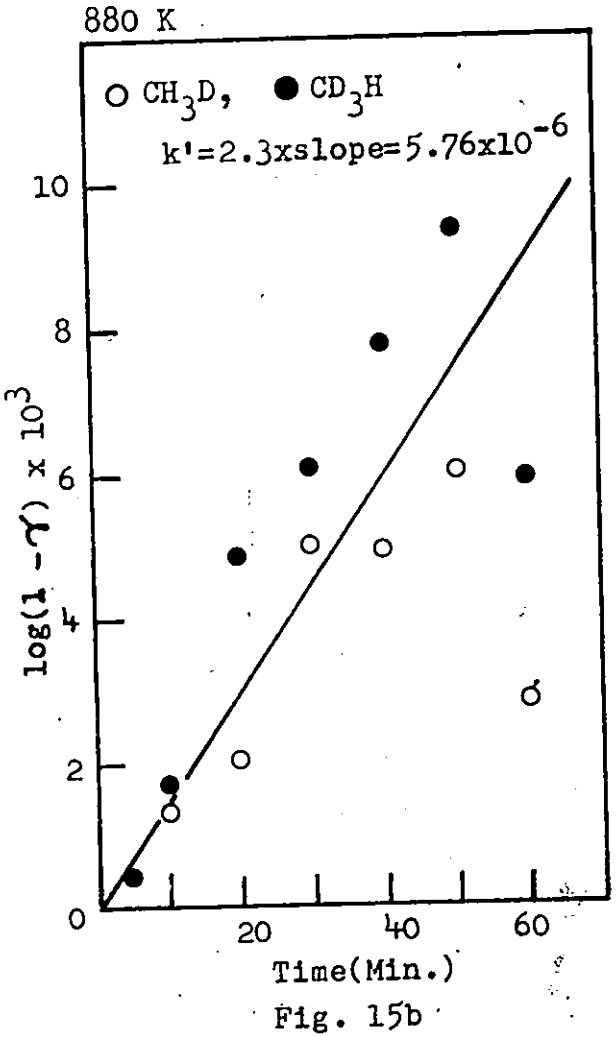

Fig. 15b

Figure 16

Plot of log β and log $(1 - \gamma)$ against time at 957 K, 440 Torr of 1:1 mixture of CH_4-CD_4

16 a: O, $\beta = [CH_4]$; ●, $\beta = [CD_4]$

16 b: O, $\gamma = [CH_3D]/[CH_4]_o$; ●, $\gamma = [CD_3H]/[CD_4]_o$

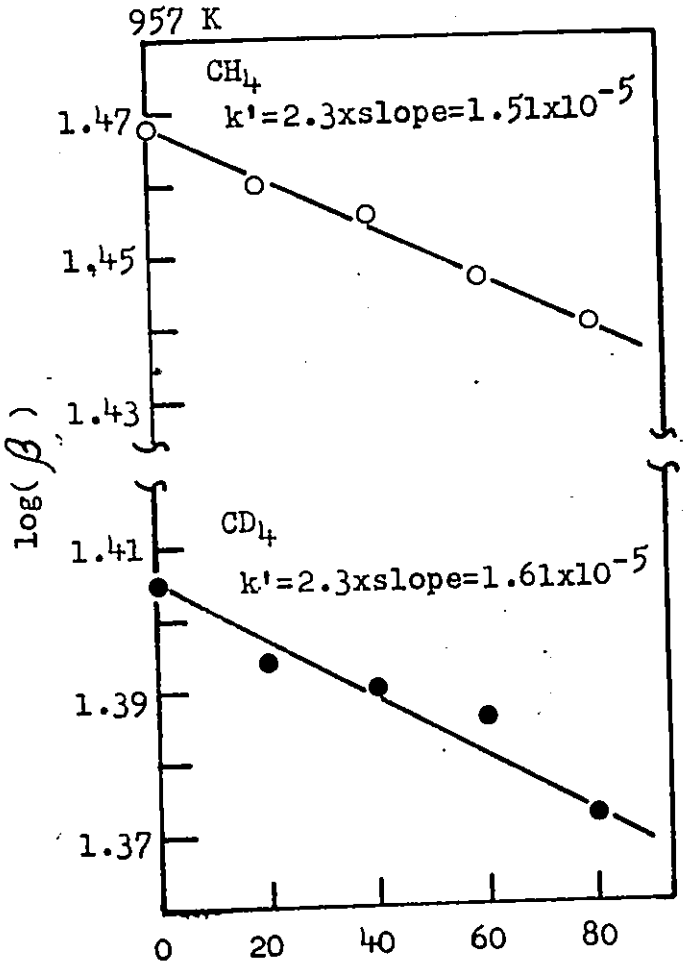

Fig. 16a

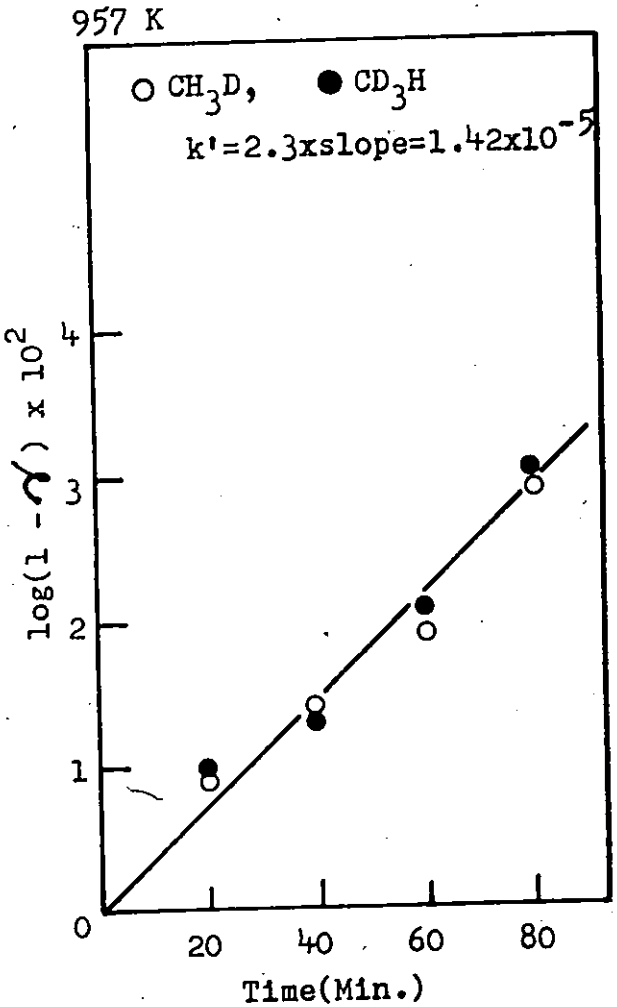

Fig. 16b

Figure 17

Plot of log β and log (1 - γ) against time at 995 K, 440 Torr of 1:1 mixture of CH_4-CD_4.

17 a: ○, $\beta = [CH_4]$; ●, $\beta = [CD_4]$

17 b: ○, $\gamma = [CH_3D]/[CH_4]_o$; ●, $\gamma = [CD_3H]/[CD_4]_o$

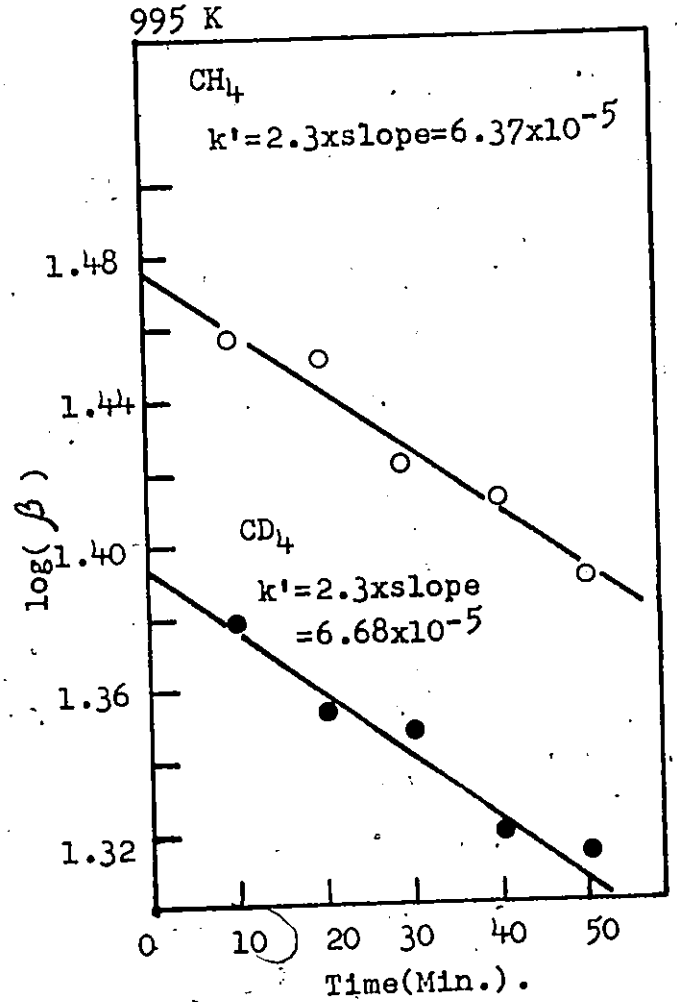

Fig. 17a

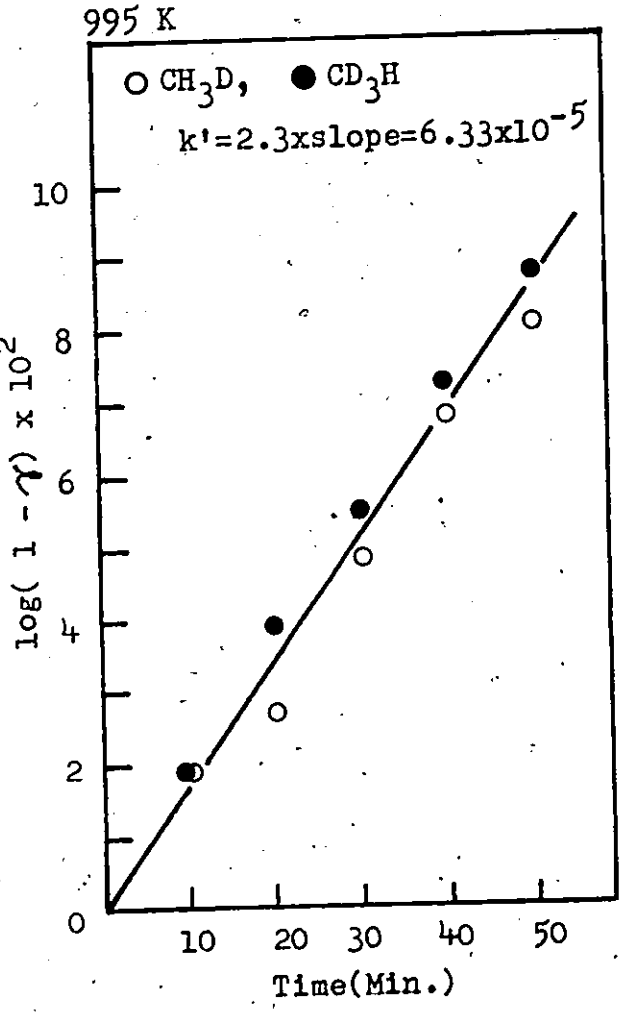

Fig. 17b

Figure 18

Plot of log β and log (1 − γ) against time at 1038 K, 440 Torr of 1:1 mixture of CH_4-CD_4

18 a: ○, $\beta = [CH_4]$; ●, $\beta = [CD_4]$

18 b: ○, $\gamma = [CH_3D]/[CH_4]_o$; ●, $\gamma = [CD_3H]/[CD_4]_o$

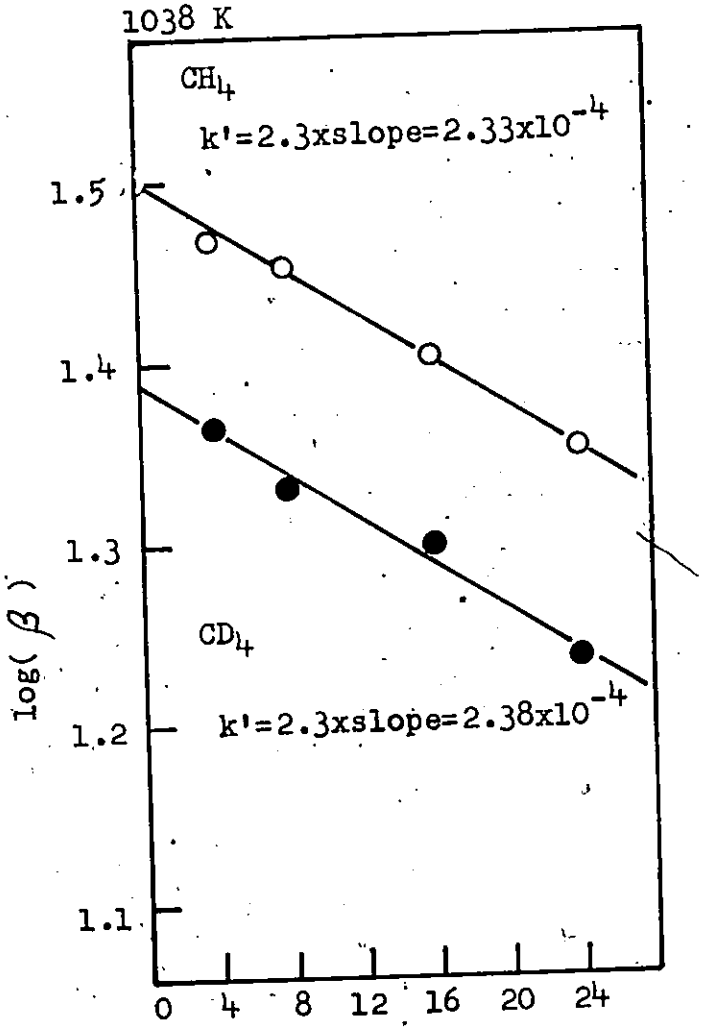

Fig. 18a

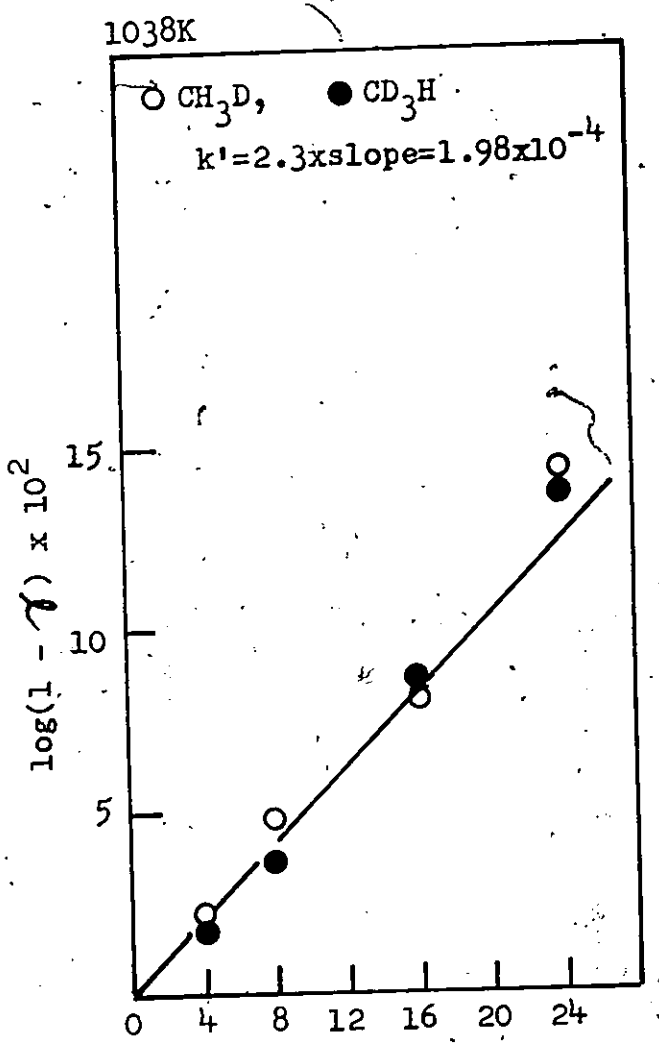

Fig. 18b

Figure 19

Plot of log β and log (1 − γ) against time at 1068 K, 440 Torr of 1:1 mixture of CH_4-CD_4

19 a: ○, $\beta = [CH_4]$; ●, $\beta = [CD_4]$

19 b: ○, $\gamma = [CH_3D]/[CH_4]_o$; ●, $\gamma = [CD_3H]/[CD_4]_o$

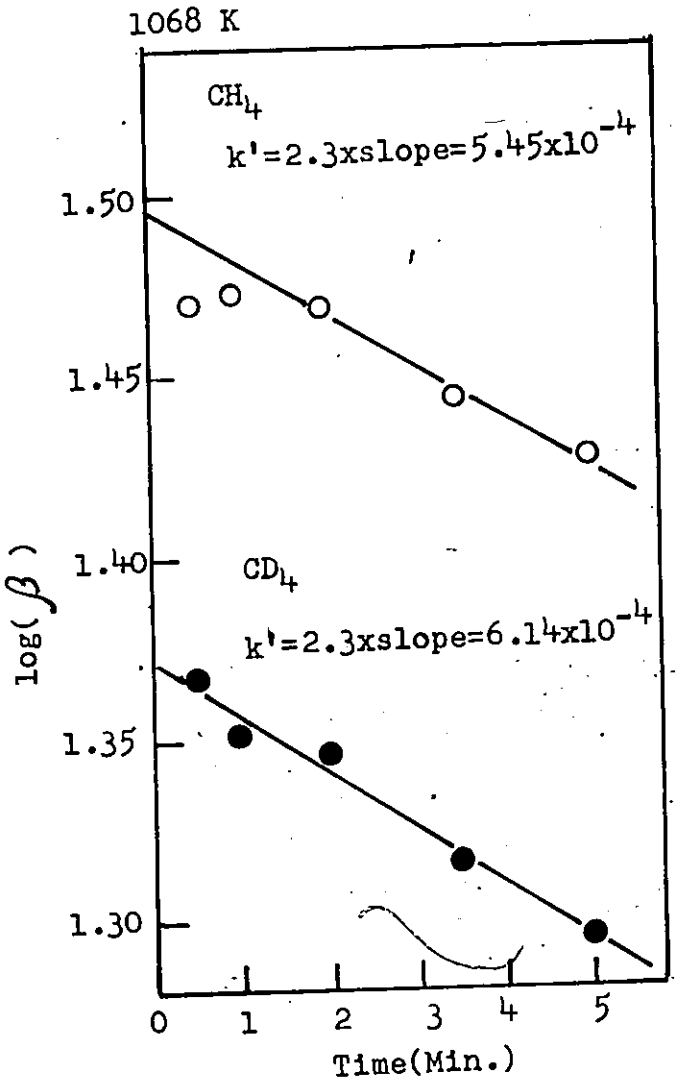

Fig. 19a

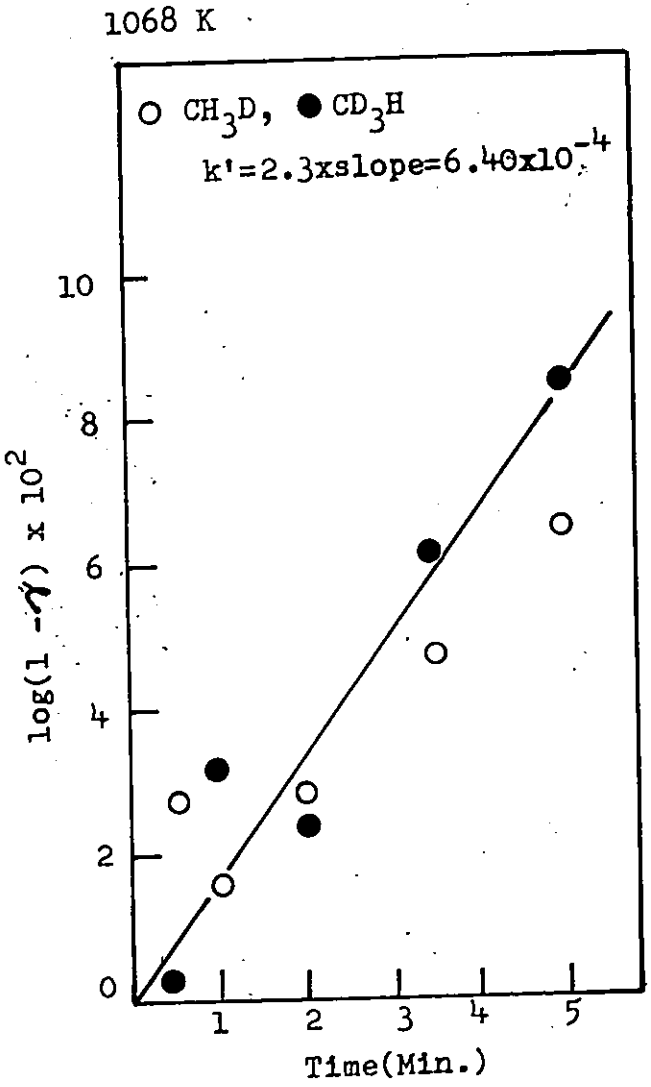

Fig. 19b

Figure 20

Plot of log β and log (1 - γ) against time at 1103 K, 440 Torr of 1:1 mixture of CH_4-CD_4

20 a: ○, $\beta = [CH_4]$; ●, $\beta = [CD_4]$

20 b: ○, $\gamma = [CH_3D]/[CH_4]_o$; ●, $\gamma = [CD_3H]/[CD_4]_o$

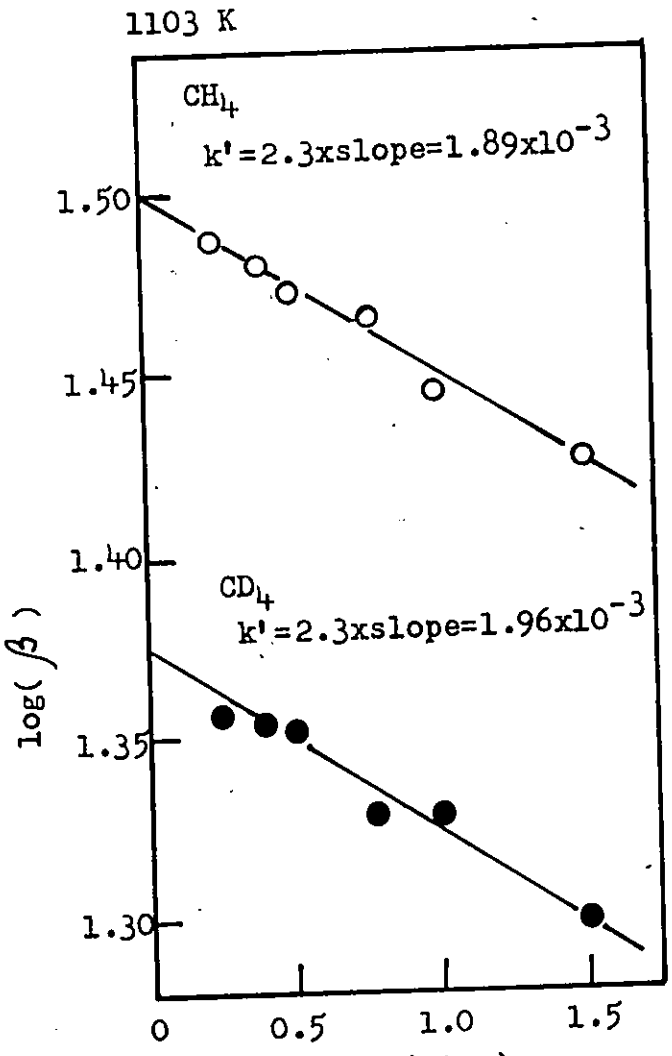

Fig. 20a

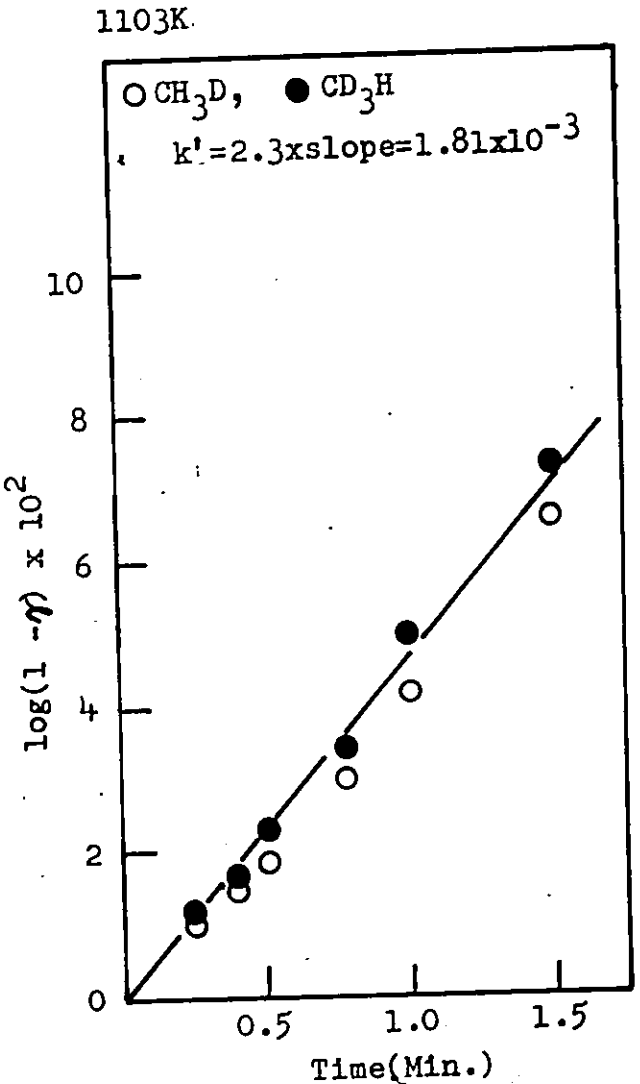

Fig. 20b

TABLE 10

Experimental rate constant, k_s measured from pyrolysis of equimolar mixture of CD_4-CH_4 at total pressure 440 Torr and temperature 880-1103 K

T(°K)	$k_s[CH_3]$, sec^{-1}	$[CH_3]$, mole/l	k_s, 1/(mole sec)
880*	6.72×10^{-6}	2.16×10^{-11} †	3.11×10^{5}
957	1.49×10^{-5}	1.67×10^{-11}	8.92×10^{5}
995	6.42×10^{-5}	4.23×10^{-11}	1.52×10^{6}
1038	2.16×10^{-4}	1.29×10^{-10}	1.67×10^{6}
1068	6.09×10^{-4}	2.61×10^{-10}	2.33×10^{6}
1103	1.88×10^{-3}	6.47×10^{-10}	2.93×10^{6}

* 0.237% of ethane was added to produce methyl radical.

† Concentration of $CH_3 = CD_3 = \frac{1}{2}$ methyl radicals generated from ethane.

D. Comparison with low temperature data.

It can be shown that the maximum deviation of k_{30} from the measured k_s is small. Since

$$k_s = \frac{2k_{30}k_{31}}{k_{30} + k_{31}}$$

(i) $k_s = k_{30} = k_{31}$ if $k_{30} = k_{31}$

(ii) $k_s = 2k_{30}$ if $k_{31} >> k_{30}$

(iii) $k_s = 2k_{31}$ if $k_{30} >> k_{31}$

Case (iii) is less likely than case (ii) since reactions [30] and [31] involve similar transition states and reaction [30] requires the breaking of a C-D bond. The Arrhenius plot for k_s is shown in Fig. 21 together with data for k_{30} obtained by Dainton and McElcheran (69). A shaded area was drawn in the figure to cover the extremes, (i) and (ii), of the possible values of k_{30} in the temperature range 880 - 1103 K. Due to the isotope effect, k_{30} is probably about 2-3 times smaller than k_{31} at 1000 K, and k_{30} will be about 0.7 k_s rather than 0.5 k_s. Therefore the actual values of k_{30} must fall within this shaded area. As can be seen from Fig. 21, even the lowest values of k_{30} are considerably higher than the values given by a linear Arrhenius extrapolation from the low temperature data. Although this finding strongly indicates a non-Arrhenius behaviour of reaction [30], it must be regarded as speculative. It may be concluded, however, that the isotope exchange reaction in the mixture of CH_4 and CD_4 occurs by

the chain propagation reactions [30] + [31]. This conclusion is clearly demonstrated in the experiments with the addition of ethane at 880 K in which the main source of methyl radicals is the dissociation of ethane.

E. Comparison with high temperature data.

The measurements of Burcat and Lifshitz (68) at 1340-1745 K are not shown in Fig. 21 but are in good agreement with an extrapolation of the present results. Burcat and Lifshitz did not take into account the redissociation of ethane in determining the methyl radical concentration. Recalculating their data to allow for this, and using the more reliable values of k_1 obtained in Section II, made relatively small changes in their values of k_s, which remain well above those expected from an extrapolation of the low temperature data.

Figure 21

Arrhenius plot for k_s and k_{30}

●, k_s

0 ——— 0, k_{30} (reference 69)

-●- ----- -●-, -●-; k_{31} (reference 69)

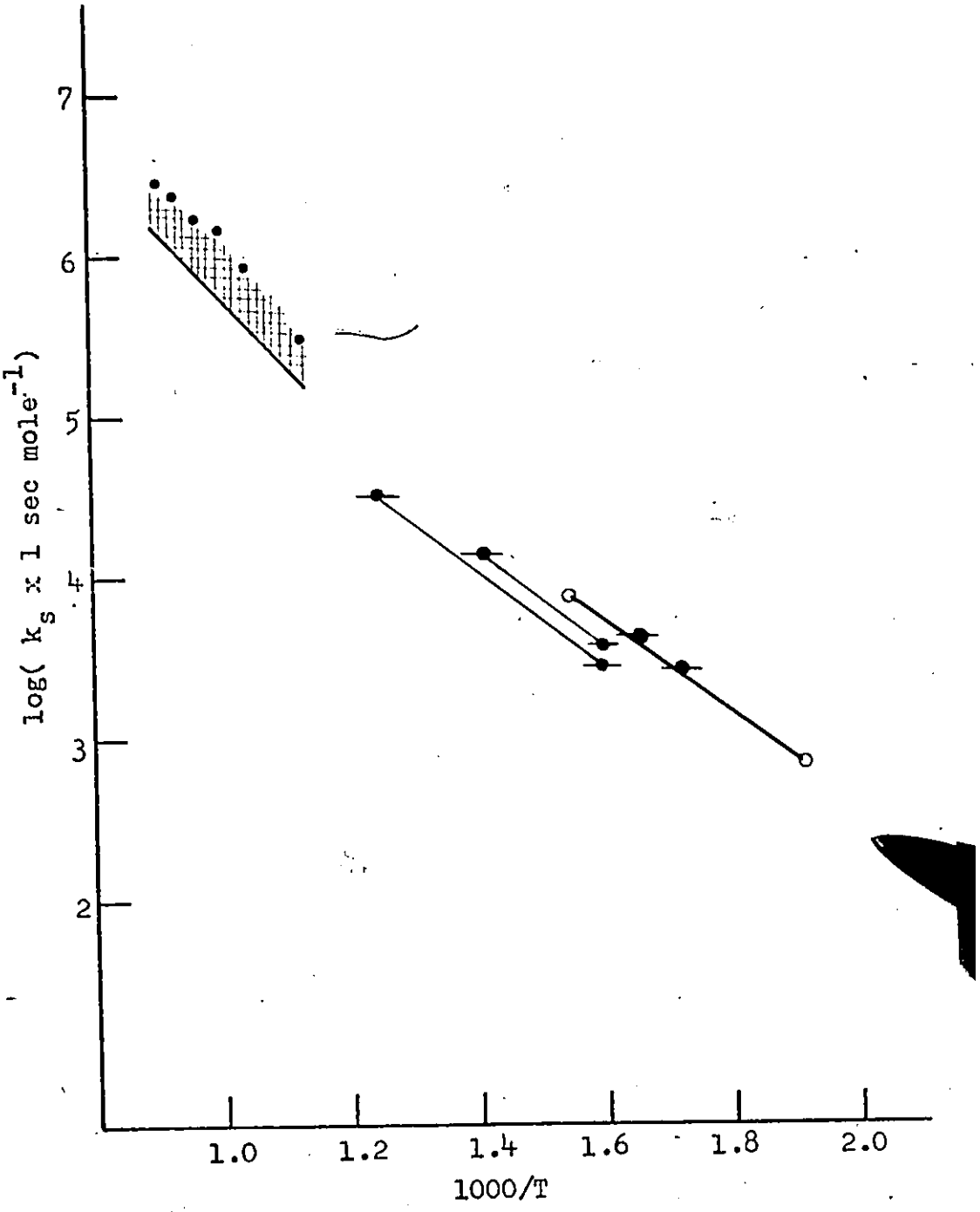
7
6
5
4
3
2
log(k_s x 1 sec mole^{-1})
1.0
1.2
1.4
1.6
1.8
2.0
1000/T

CHAPTER FOUR: CARBON FORMATION

I. Introduction.

The reaction in which carbon is formed during the pyrolysis of hydrocarbons has interested chemists for years. Although some progress has been made (10 a, 10 b, 70), the mechanism of its formation remains virtually unknown. Many theories have been suggested based on studies of flame and combustion, but it is not known whether they apply to the pyrolysis of pure hydrocarbons. Nevertheless, some of these theories are summarized below:

A. Formation of atomic carbon and C_2 molecules and their polymerization with acetylene.

In 1954, Gaydon (71) suggested that carbon atoms or C_2 molecules acted as nuclei for the decomposition of acetylene in flames and that reactions

$$C + C_2H_2 \rightarrow C_3 + H_2$$

$$C_2 + C_2H_2 \rightarrow C_4 + H_2$$

were energetically possible. The main objection to this theory is related to the heat of reaction required for the formation of C atoms and C_2 molecules.

B. Formation and polymerization of C_2 molecules.

A direct polymerization between C_2 molecules to form solid carbon was discussed by Smith (72) in 1940. Gaydon and Wolfhard (73), however, showed that the concentration of C_2 molecules was probably

too low. Although flames of C_2N_2 showed very strong C_2 bands, they did not give carbon and in diffusion flames, C_2 appeared only after solid carbon.

C. Rapid chain polymerization to large hydrocarbon molecules which cracked to carbon.

Gaydon (74) postulated that in the presence of an excess of fuel molecules, free radicals initiated chain polymerization processes leading to the formation of higher hydrocarbons which decomposed thermally to solid carbon and hydrogen.

Porter (75 a) disputed this theory, arguing that the time available in a pre-mixed flame is not long enough to produce high polymers.

Rummel and Veh (76) suggested that the soot particles were precipitated as residual skeletons of big aromatic or polycyclic molecules.

D. Formation of C_2H_2 followed by polymerization and dehydrogenation.

This theory was first proposed by Porter (75), who argued that the low endothermicity of the formation of C_2H_2 from graphite and hydrogen (54 kcal/mole) indicated a very low activation energy for the reverse reaction (hydrogen elimination).

E. Formation of liquid droplets.

Parker and Wolfhard (77) suggested that higher hydrocarbons of low vapor pressure condensed to form liquid droplets in the gas

phase which in turn dehydrogenated to carbon.

Johnson and Anderson (78), on the other hand, considered that formation of liquid droplets was a secondary process occurring after cooling of reaction products, and that they were not precursors of carbon formation. They suggested that a chemical condensation process proce ded nucleation of solid particles.

It should be emphasized that the present study on the formation of carbon films is preliminary. The purpose of this work is to determine the effect of carbon on the pyrolysis of methane, or more specifically, to establish the time at which the carbon begins to accumulate on the walls of the reaction vessel and find the relation, if any, of its formation with that of the other products. From the time interval experiments discussed in Chapter 3, Section 1, it was concluded that at the early stage of the autocatalysis the decomposition of hydrocarbon products rather than carbon is responsible for the acceleration observed. A direct measurement of the formation of carbon film is therefore necessary to verify this conclusion.

II. Experimental.

Experiments were first performed in a quartz vessel, 2.2 cm I.D. and 50 cm long, fitted with plane windows and mounted at the center of a tubular furnace, 50 cm long. Each end of the furnace was plugged with a similar cylindrical evacuated cell, 30 cm long, to minimize heat loss, so that the reaction vessel, including its plane windows, was virtually free of temperature gradients. The vessel was

Figure 22

Apparatus for the Study of Carbon Formation

L, He-Ne laser

V1, reaction vessel

V2, V3, empty vessels

F, corning #4308 filter

PD, photodiode

EM, Electrometer

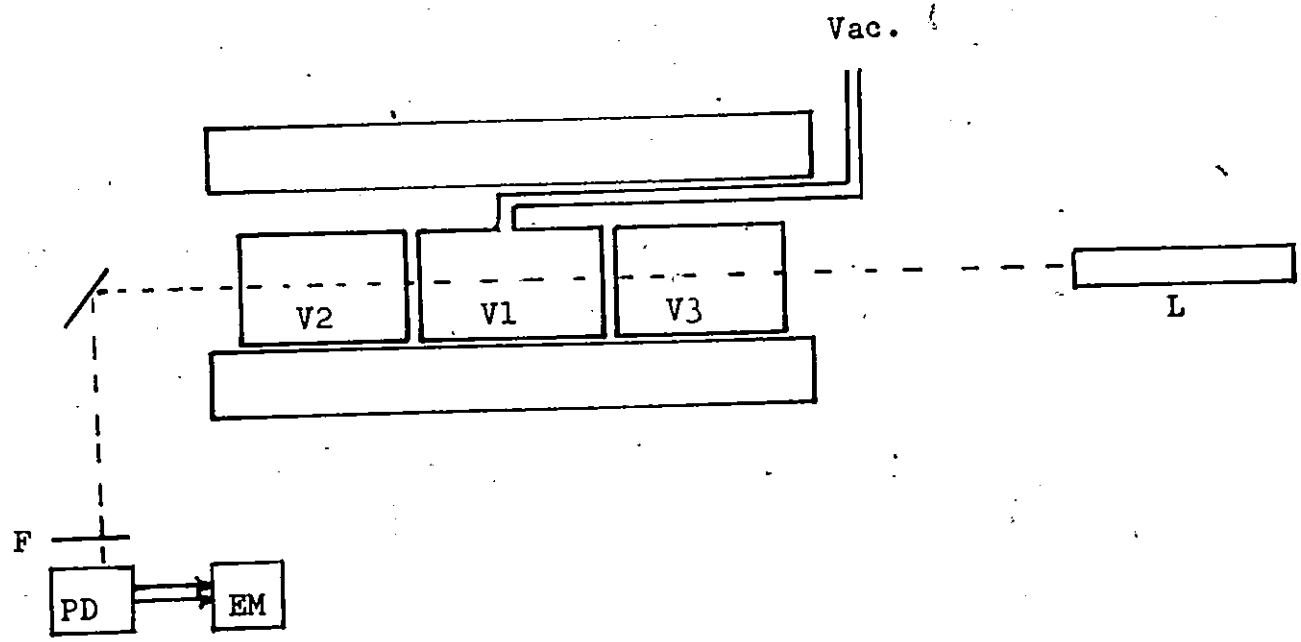
Vac.
V2
V1
V3
L
F
PD
EM

connected to the vacuum line by small-bore tubing to reduce the diffusion of particles and reaction products into the cold zone. The carbon formation observed should thus be characteristic of the isothermal pyrolysis of methane at the vessel temperature. Deposition of carbon on the vessel windows during the course of the pyrolysis was measured by the absorption of light (632.8 nm) from a 2 mW He-Ne laser, using several traverses, and measuring the transmitted light with a photodiode. In some experiments four additional quartz discs were mounted in the light path within the vessel to enhance the sensitivity. In other experiments the laser beam was passed transversely through the reaction vessel through two small holes drilled in the tubular furnace and viewed through the end windows in an attempt to observe particle formation in the gas phase by scattering of the beam.

Fig. 22 shows the arrangement of the experiment; V1, reaction vessel; V2 and V3, empty vessels used as insulators; PD, photodiode; EM, electrometer; L, He-Ne laser; F, corning #4308 filter. The filter was installed to reduce the infrared emission from the furnace and to attenuate the laser beam to avoid light saturation of the photodiode.

III. Results and Discussion.

The calibration of the light transmission of the carbon film was performed at about 1200 K by introducing methane into the reaction vessel and pyrolyzing it for two hours, when approximate equilibrium between methane, carbon and hydrogen was attained.

The equilibrium constant K_p at this temperature between methane and hydrogen is 63 Atm. Therefore, for an initial pressure of methane of 100 Torr, 99.2% of the methane will be decomposed at equilibrium. It was assumed that the carbon film formed at 1200 K had the same properties as the film formed in the pyrolysis experiments at 1103 K.

To calculate the surface area of the carbon, the structure of the pyrolytic carbon was assumed to be similar to that of graphite. The area, A, occupied by a carbon atom is half of the hexagon,

$$A = \tfrac{1}{2}\ 5.24 \times 10^{-16}\ cm^2$$
$$= 2.62 \times 10^{-16}\ cm^2$$

Thus, a mono-layer of carbon film deposited on the walls of the vessel corresponds to 1.77×10^{-5} mole/l of carbon in the gas phase.

Table 11 and Fig. 23 show the calibration of the optical density of the carbon film as a function of methane pressure under conditions of the equilibrium dissociation of the methane. If the limit of detection is four times the noise ($I_o/I = 1.005$), an amount of carbon corresponding to 3.4×10^{-6} mole/l in the gas phase can be detected with the present method. The time-yield plot of carbon formation at 1104 K and 443 Torr is shown in Fig. 24. Fig. 25 shows the plot of the logarithm of the concentration of carbon against the reaction time; there appears to be an autocatalytic reaction, first order with respect to the amount of carbon formed. This is quite

TABLE 11

Optical Density of Carbon Films

T: 1200 K, Volume: 24.3 cm^3, Surface Area: 67.9 cm^2 (with four discs inside the reaction vessel)

P_{CH_4} (Torr)	$\log(I_o/I)$	Calc. num of C layer	CH_4 converted into C(mole/l)
5.0	0.253	3.76	6.67×10^{-5}
8.2	0.260	6.19	11.0×10^{-5}
11.5	0.405	8.65	15.4×10^{-5}
17.9	0.628	13.5	23.9×10^{-5}
23.5	0.760	17.7	31.4×10^{-5}
29.0	1.01	21.9	38.8×10^{-5}

Figure 23

Calibration of the Optical Density of Carbon Films

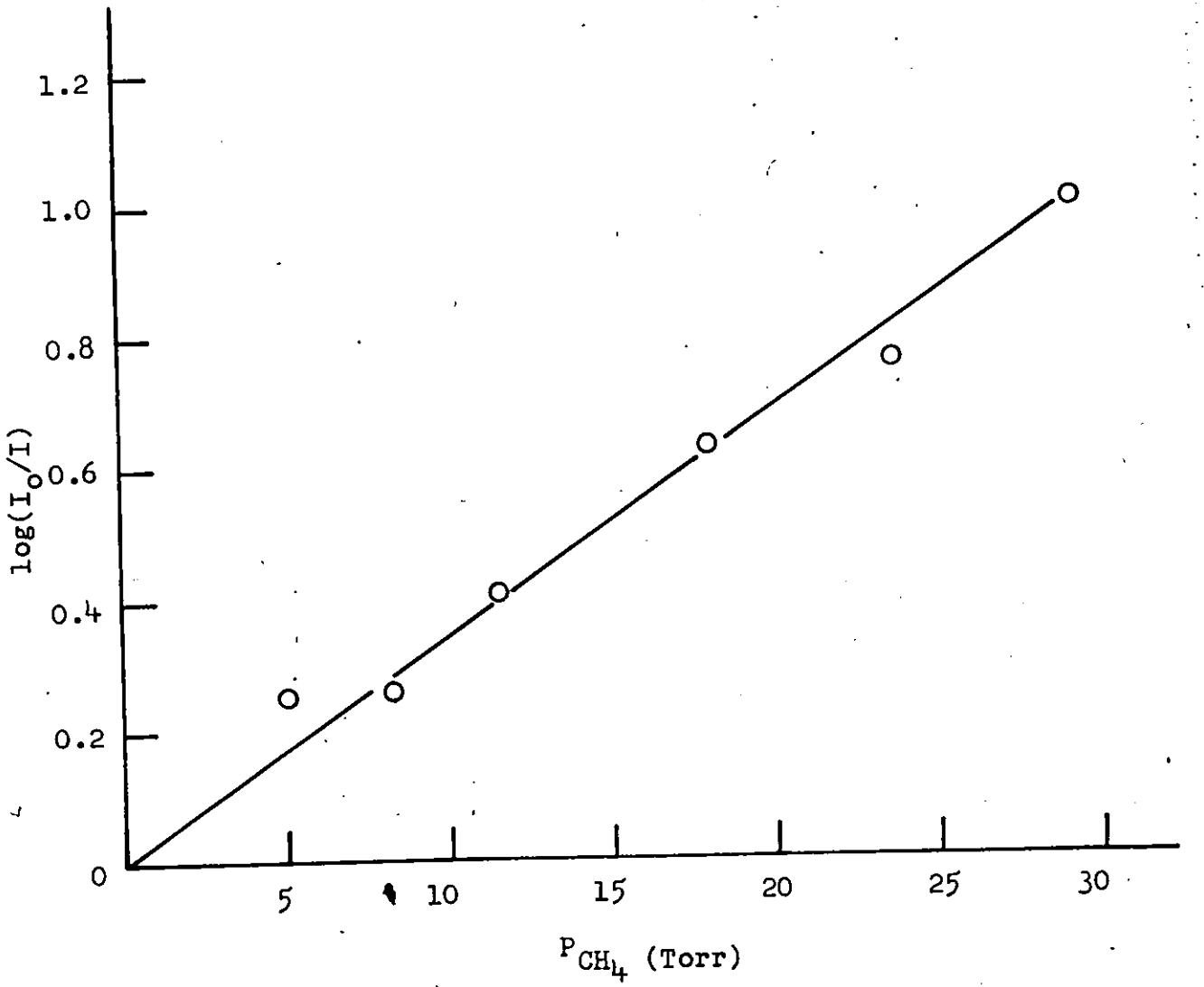
1.2
1.0
0.8
0.6
0.4
0.2
0
log(I_o/I)
5
10
15
20
25
30
P_CH4 (Torr)

Figure 24

Yield-time plot for carbon formation at 443 Torr, 1103 K

Figure 25

Plot of log [Carbon] vs time at 443 Torr, 1103 K

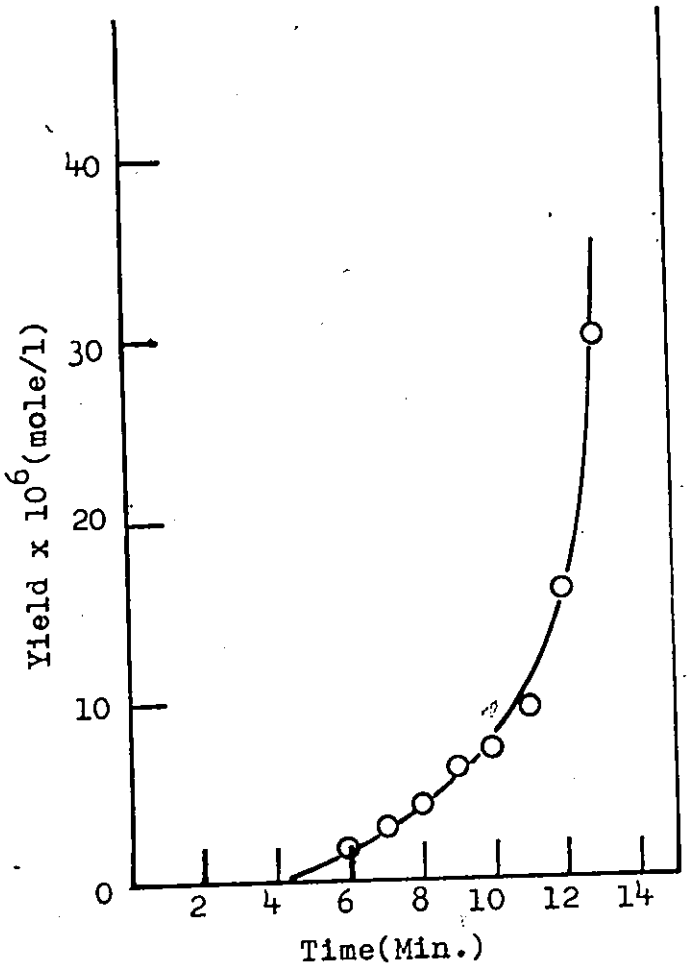
Yield x 10^6(mole/l)
40
30
20
10
0
2
4
6
8
10
12
14
Time(Min.)

Fig 24

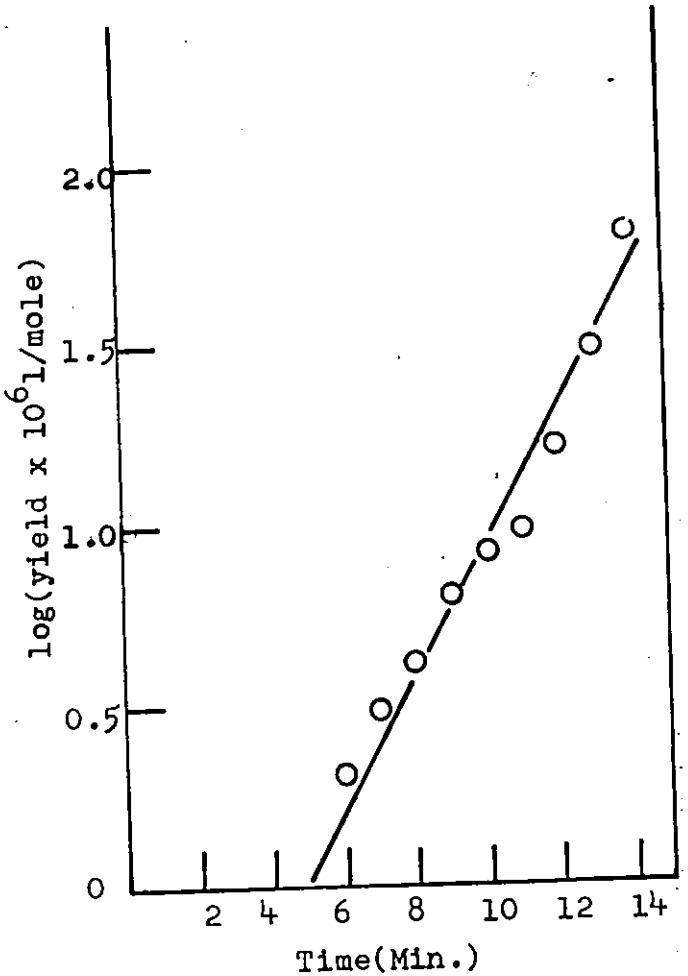
log(yield x 10^6l/mole)
2.0
1.5
1.0
0.5
0
2
4
6
8
10
12
14
Time(Min.)

Fig. 25

Figure 26

Yield-time plot for carbon and volatile products at 440 Torr, 1103 K

○, C_2H_6

□, C_2H_4

▲, C_2H_2

—, Carbon (equivalent to atomic carbon in the gas phase)

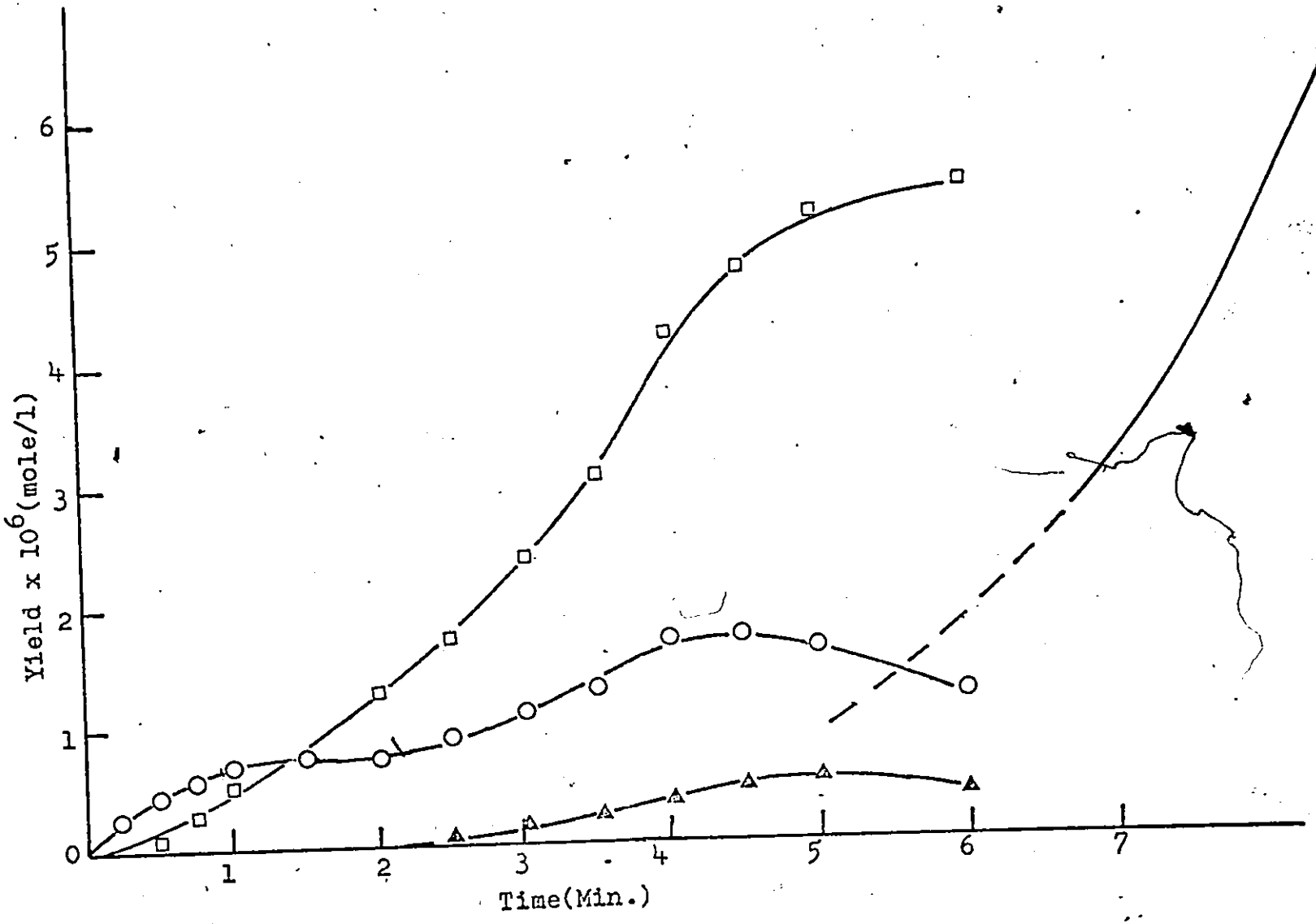
Yield x 10^6(mole/l)
0
1
2
3
4
5
6
7
Time(Min.)

interesting since after the first layer of carbon is deposited on the surface, the rate should become zero-order unless the acceleration is caused by some gas-phase precursors of the carbon deposit or by a small number of active sites on the carbon surface.

However, with these limited results, it is not fruitful to discuss further the mechanism of the formation of carbon.

Extrapolation of the curve shown in Fig. 24 to zero carbon concentration (Figs. 25 and 26) shows that carbon is not formed until after the secondary acceleration of ethane and the other products. It appears that carbon deposition is not responsible for the autocatalysis at least in the early stages. This was also concluded from the results of the time interval experiments discussed in Chapter 3. The carbon film on the walls of the reaction vessel undoubtedly affects the rate of the decomposition (see Figs. 5a, 5b) but becomes important only in the later stages of the reaction. Attempts to observe the presence of fine carbon particles in the gas phase by viewing the passage of the laser beam through the hot reacting gas were entirely negative. A suspension of carbon particles would be expected to scatter the light beam so that it would be visible to the eye. Nevertheless the beam could not be observed in the hot zone. It may be concluded that carbon particles of a size large enough to scatter the light from the He-Ne laser are not present in large concentrations. Further studies are, however, necessary to resolve this complex problem of the role of the carbon deposit.

CLAIMS TO ORIGINAL RESEARCH

1. An analytical method was developed to measure very low concentrations of C_2 products, C_3 products and butane in the presence of excess methane.
2. The initial decomposition of methane was found to be a homogeneous gas phase dissociation of the C-H bond rather than the formation of hydrogen and methylene radical.
3. The first-order rate constant of the reaction was measured and its pressure-dependence was determined.
4. A model of the unimolecular decomposition of methane was proposed. Theoretical RRKM calculations led to good agreement between shock tube data and the present work. The rate constant for the combination of a methyl radical and a hydrogen atom was calculated over a range of pressure at 500, 700 and 1038 K; the values were in good agreement with data from low temperature studies.
5. The present study confirmed that all previous studies in conventional static and flow systems except that of Palmer et al (11) were in the region where the autocatalytic acceleration is important.
6. The rate of hydrogen abstraction from ethane by a methyl radical was measured at 880, 995, 1038 and 1068 K. This provided additional evidence for the temperature dependence of the Arrhenius activation energy of this reaction.

7. A new mechanism was proposed to account quantitatively for the formation of all C_2 and C_3 hydrocarbons.

8. The combined rate constant $k_s = \frac{2k_{30}k_{31}}{k_{30}+k_{31}}$ for reactions

[30] $CH_3 + CD_4 \rightarrow CH_3D + CD_3$

[31] $CD_3 + CH_4 \rightarrow CD_3H + CD_3$

was measured over the temperature range 880 to 1103 K. These measurements indicated that the isotope exchange reaction between CH_4 and CD_4 occurs through a radical chain.

9. A method was developed for the measurement of carbon deposit which forms during the pyrolysis of methane.

10. From the yield-time plot of the carbon formation, it was found that the vitreous carbon on the walls of the reaction vessel did not form in the early stages of the autocatalysis but at later stages of the reaction.

REFERENCES

1. a. M. Berthelot, Ann.Chim.Phys., 9, 471(1866).

   b. W.A. Bone and H.F. Conward, J.Chem.Soc., 93, 1197(1908).

   c. G.C. Holliday and H.C. Exell, J.Chem.Soc., 1066(1929).

   d. G.C. Holliday and W.J. Gooderham, J.Chem.Soc., 1594(1931).

2. L.S. Kassel, J.Am.Chem.Soc., 54, 3949(1932).

3. S. Kodama, K. Tarama, K. Matsukawa, T. Yano, H. Nakano, Y. Fujimori, S. Kato, A. Mori and S. Hayakawa, J.Chem.Soc. Japan, Pure Chem.Sect., 70, 421(1949).

4. A.A. Anisonyan, Dokl.Akad.Nauk.Arm.SSR, 50, 278(1970): C.A., 74, 24028u.

5. I.A. Schneider, Acad.rep.populare Romine, Studii Cercetari Chim., 8, 97(1960).

6. L. Kramer and J. Happel, "The Chemistry of Petroleum Hydrocarbon", B.T. Brooks et al.ed., Vol. II, chap. 25, p. 71, Reinhold, New York (1955).

7. A.S. Gordon, J.Am.Chem.Soc., 70, 395(1948).

8. a. J.E. Germain and C. Vaniscotte, Bull.Soc.Chim., France, 692(1957).

   b. J.E. Germain and C. Vaniscotte, Ibid., 319(1958).

8. c. J.E. Germain and C. Vaniscotte, Ibid., 7, 964(1958).

9. I.G. Murgulescu and I.A. Schneider, Acad.rep.populare Romine, Studii cercetari Chim., 8, 367(1960).

10. a. H.B. Palmer, Carbon, 1, 55(1963).

b. T.J. Hirt and H.B. Palmer, Carbon, 1, 65(1963).

c. T.J. Hirt and H.B. Palmer, Proceeding of the fifth carbon conference, 1. pp. 406, 639. Pergamon Press, Oxford, New York (1962).

11. H.B. Palmer and T.J. Hirt, J.Phys.Chem., 67, 709(1963).

12. B. Eisenberg and H. Bliss, Chem.Eng.Progr., Symp.Ser., 72, 3(1967).

13. H.B. Palmer, J. Lahaye and K.C. Hou, J.Phys.Chem., 72, 348(1968).

14. E.F. Greene, R.L. Taylor and W.L. Patterson, Jr., J.Phys.Chem., 62, 238(1958).

15. H.S. Glick, 7th Combustion Symposium, Butterworth, London. p. 98 (1959).

16. G.B. Skinner and R.A. Ruehrwein, J.Phys.Chem., 63, 1736(1959).

17. V. Kevorkian, C.E. Heath and M. Boudart, J.Phys.Chem., 64, 964(1960).

18. G.I. Kozlov and V.G. Knorre, Combust.Flame, 6, 253(1962).

19. I.E. Volokhonovich, A.M. Markevich, I.F. Masterovoi and V.V. Azatyan, Dokl.Akad.Nauk.USSR, 146, 387(1962); C.A., 58 2307e.

20. V.N. Kontratiev, 10th Combustion Symposium, Combustion Institute, p. 319(1965).

21. R. Hartig, J. Troe and H.G. Wagner, 13th Combustion Symposium, Combustion Institute, Pittsburgh, p. 147(1971).

22. F.O. Rice and M.D. Dooley, J.Am.Chem.Soc., 56, 2747(1934).

23. G.C. Eltenton, J.Chem.Phys., 15, 455(1947).

24. A.J.B. Robertson, Proc.Roy.Soc. London, A 199, 394(1949).

25. L.S. Nelson and N.A. Kuebler, J.Chem.Phys., 37, 47(1962).

26. L. Belchetz and E.K. Rideal, J.Am.Chem.Soc., 57, 1168(1935).

27. G.A. Vompe, Khim.Vys.Energ., 2, 274(1968). C.A., 69, 76392.

28. T. Yano and K. Kuratani, Bull.Chem.Soc., Japan, 41, 799(1968).

29. T. Yano, Bull.Chem.Soc., Japan, 46, 1619(1973).

30. T.V. Fedoseeva, N.Ya. Chernyak, G.V. Gulyaev and L.S. Polak, Khim.Vys.Energ., 4, 268(1970).

31. a. H.M. Frey, "Progress Reaction Kinetics", G. Porter ed., Vol. 2, chap. 3, p. 142, Pergamon Press, England (1964).

31. b. W.B. DeMore and S.W. Benson, "Adv.Photochem.". W.A. Noyes, Jr. ed., Vol. 2, p. 223, John Wiley and Sons, New York (1964).

32. G. Boato, G. Careri, A. Cimino, E. Molineri and G.G. Volpi, J.Chem.Phys., 24, 783(1956).

33. T. Terao and R.A. Back, J.Phys.Chem., 73, 3884(1969).

34. S.W. Benson and H.E. O'Neal, Kinetic data on gas phase unimolecular reactions. NSRDS-NBS 21, Washington, D.C. (1970).

35. J.A. Kerr, Chem.Rev., 66, 465(1966).

36. E.W.R. Steacie, "Atomic and Free Radical Reactions", Reinhold, New York (1954).

37. a. P. Warneck, Z.Naturforsch, Teil A, 26, 2047(1971).

b. W.A. Chupka and C. Lifshitz, J.Chem.Phys., 48, 1109(1968).

c. J.W. Simons and R. Curry, Chem.Phys.Lett., 38, 171(1976).

38. W. Braun, A.M. Bass and M. Pilling, J.Chem.Phys., 52, 5131(1970).

39. H.M. Frey, J.Chem.Soc.Commum., 1024(1972).

40. W.S. Watt, P. Borrell, D. Lewis and S.H. Bauer, J.Chem.Phys., 45, 444(1966).

41. S.H. Bauer and E. Ossa, J.Chem.Phys., 45, 434(1966).

42. A. Burcat and A. Lifshitz, J.Chem.Phys., 47, 3079(1967).

43. S.W. Benson, Thermochemical Kinetics, Wiley and Sons, New York (1968).

44. W. Forst, Theory of Unimolecular Reactions, Academic Press, New York (1973).

45. P.J. Robinson and K.A. Holbrook, Unimolecular Reactions, Wiley Interscience, New York (1972).

46. D.C. Tardy, B.S. Rabinovitch and G.Z. Witten, J.Chem.Phys., 48, 1427(1968).

47. R.A. Marcus, J.Chem.Phys., 43, 2658(1965).

48. E.V. Waage and B.S. Rabinovitch, Chem.Rev., 70, 377(1970).

49. D.W. Placzek, B.S. Rabinovitch and G.Z. Whitten, J.Chem.Phys., 43, 4071(1965).

50. JANAF Thermochemical Tables, 2nd ed., NSRDS-NBS 37, Washington, D.C. (1970).

51. D.H. Napier and N. Subrahmanyam, J.Appl.Chem.Biotechnol., 22, 303(1972).

52. P. Camilleri, R.M. Marshall and J.H. Purnell, J.Chem.Soc. Faraday Trans. 1, 70, 1434(1974).

53. A.F. Dodonov, G.K. Lavrovskaya and V.L. Tal'Roze, Kinet.Katal., 10, 477(1969).

54. G. Pratt and I. Veltman, J.Chem.Soc. Faraday Trans. 1, 70, 1840 (1974).

55. M.P. Halstead, D.A. Leathard, R.M. Marshall and J.P. Purnell, Proc.Roy.Soc., London, Ser.A, 316, 575(1970).

56. W. Forst and Z. Prasil, J.Chem.Phys., 53, 3065(1970).

57. M.C. Lin and K.J. Laidler, Trans.Faraday Soc., 64, 79(1968).

58. E.V. Waage and B.S. Rabinovitch, Int.J.Chem.Kinetics, 3, 105(1971).

59. Y.P. Yampolskii and V.M. Rybin, Reaction Kinetics and Catalysis Letters, 1, 321(1974).

60. P.D. Pacey and J.H. Purnell, J.Chem.Soc. Faraday Trans., I, 68, 1462(1972).

61. T.C. Clark, T.P.J. Izod and G.B. Kistiakowsky, J.Chem.Phys., 54, 1295(1971).

62. J.R. McNesby, J.Am.Chem.Soc., 64, 1671(1960).

63. M.H.J. Wijnen, J.Chem.Phys., 23, 1357(1955).

64. A.F. Trotman-Dickenson, J.R. Birchard and E.W.R. Steacie, J.Chem. Phys., 19, 163(1951).

65. T.C. Clark and J.E. Dove, Can.J.Chem. 51, 2147(1973).

66. L.M. Quick, D.A. Knecht and M.H. Back, Int.J.Chem.Kin., 4, 61(1972).

67. F.C. Stehling, J.D. Frazee and R.C. Anderson, 8th Combustion Symposium, Cal.Inst.Techn., p. 775 (1960).

68. A. Burcat and A. Lifshitz, J.Chem.Phys, 52, 3613(1970).

69. F.S. Dainton and D.E. McElcheran, Trans.Faraday Soc., 51, 657 (1955). V.N. Kondratiev, Rate Constants of Gas Phase Reactions, translated by L.J. Holtschlag, Office of Standard Reference Data, NBS (1972).

70. I.L. Mar'yasin and P.A.Tesner, Int.Chem.Eng., 2, 303(1962).

71. A.G. Gaydon, Imp.College Chem.Eng., 8, 42(1954).

72. E.C.W. Smith, Proc.Roy.Soc., A 174, 110(1940).

73. A.G. Gaydon and H.G. Wolfhard, Proc.Roy.Soc., A 201, pp. 501, 570(1950).

74. A.G. Gaydon and G. Whittingham, Proc.Roy.Soc., A 189, 313(1947).

75: a. G. Porter, 4th Symp. on Combust., p. 248(1952).

b. G. Porter, Combust.Res. and Rev., AGARD Memorandum (1955) p. 108, U.S. Govt. Printing Office.

76. K. Rummel and P.O. Veh, Arch Eisenchutenwesen, 14, 489(1941).

77. W.G. Parker and H.G. Wolfhard, J.Chem.Soc., 2038(1950).

78. G.L. Johnson and R.C. Anderson, Proc. 5th Biennial Conf. on Carbon, 395(1958).

APPENDIX 1
THE PYROLYSIS OF METHANE
FUNDAMENTAL DATA

Temp (K)	Press (Torr)	Time (Min)	H_2	C_2H_6	C_2H_4
			Yield x 10^8 (mole/l)		
995	741	2.0	-	5.2	-
		3.0	7.8	8.43	-
		5.0	-	9.1	-
		10.0	-	17.3	-
		10.0	-	24.6	-
		10.0	50.3	21.9	-
		20.0	107.0	28.2	13.8
		20.0	-	25.2	7.9
		30.0	-	26.6	19.2
		30.7	-	24.2	20.6
		40.0	-	27.7	33.3
	640	5.0	-	9.2	-
		10.0	-	15.2	-
		20.0	-	20.1	6.7
		30.0	-	29.0	20.6
		40.0	67	30.8	35.3
		50.0	110	31.2	49.8
	540	5.0	-	7.6	-
		10.0	-	11.5	-
		20.0	-	17.3	2.9
		30.0	-	20.9	9.2
		40.0	118	21.3	17.7
		50.0	150	23.6	25.2
	440	10.0	18.9	10.8	-
		20.0	30	17.4	-
		40.0	63	22.0	9.4
		40.0	71	20.4	8.0
		60.0	101	22.2	30.2
		100.0	-	22.7	48.8
		100.0	-	19.0	39.7
		140.0	215	28.6	78.3
		200.0	261	31.0	93
		260.0	1500	72.6	269
		319.0	-	166	579
	333	5.0	-	1.24	-
		5.0	-	2.24	-
		10.0	-	5.95	-
		20.0	-	6.1	-
		30.0	-	6.8	-
		40.0	-	8.3	3.3
		60.0	7.1	7.6	6.2

APPENDIX 1 (CONTINUED)

Temp (K)	Press (Torr)	Time (Min)	H_2	C_2H_6	C_2H_4
			Yield x 10^8 (mole/l)		
995	230	5.1	-	2.0	-
		10.0	-	3.2	-
		20.0	-	3.6	-
		30.0	-	5.7	-
		40.0	-	4.8	-
		50.0	-	5.4	-
		71.2	-	5.4	4.2
		90.0	-	6.4	8.3
	162	10.0	-	2.0	-
		20.0	-	2.1	-
		30.0	-	4.3	-
		40.0	-	3.0	-
		50.0	-	6.1	-
		90.0	-	3.7	-
	108	10.0	-	1.7	-
		20.0	-	1.95	-
		25.0	-	2.76	-
		30.0	-	3.90	-
		50.0	-	3.04	-
		60.0	-	3.66	-
		75.0	-	3.58	-
		100.0	-	3.85	-
	51.2	5.0	-	0.32	-
		10.0	-	0.83	-
		10.0	-	0.35	-
		20.0	-	0.63	-
		30.0	-	0.92	-
		40.0	-	1.86	-
		40.0	-	1.12	-
		50.0	-	1.65	-
		50.0	-	1.44	-
		60.0	-	1.86	-
		80.0	-	1.95	-
		99.0	-	3.96	-

APPENDIX 1 (CONTINUED)

Temp (K)	Press (Torr)	Time (Min)	H_2	C_2H_6	C_2H_4	C_2H_2
			Yield x 10^8 (mole/l)			
1038	741	0.5	8.6	8.6	-	
		1.0	14.7	15.6	-	
		2.0	36.7	29 4	-	
		3.0	64.1	38.8	-	
		4.13	105	47.0	10.8	
		4.1	-	47.1	13.8	
	642	0.5	7.6	6.9	-	
		1.0	13.7	13.2	-	
		2.0	26.5	23.9	-	
		3.0	44.3	31.8	-	
		4.0	64.4	38.3	-	
	542	0.5	7.1	5.8	-	
		1.0	11.8	10.4	-	
		2.0	-	17.9	-	
		2.0	21.6	19.4	-	
		3.0	34.6	23.7	-	
		4.0	50.0	28.7	-	
	441	0.5	-	4.2	-	
		1.0	-	8.0	-	
		1.0	-	8.3	-	
		2.0	13.4	14.5	-	
		2.0	14.8	14.0	-	
		3.0	20.1	19.2	-	
		3.0	21.5	19.5	-	
		3.0	-	21.1	-	
		4.0	30.7	23.6	-	
		4.0	26.1	23.3	-	
		4.0	-	21.6	-	
		4.0	-	23.5	-	
		5.0	-	25.5	16.1	
		6.0	56.9	28.3	11.2	
		8.0	59.0	31.9	23.5	
		12.0	114	32.2	44.3	
		12.0	123	35.7	48.3	
		14.0	145	36.8	58.9	
		16.0	211	40.1	74.8	
		18.0	254	39	84	
		22.0	361	44.9	108	
		26.0	589	56.3	144	2.5
		30.0	809	70.0	196	7.2
		34.0	1436	89	267	12.1
		38.0	2005	102	319	19.5

APPENDIX 1 (CONTINUED)

Temp (K)	Press (Torr)	Time (Min)	H_2 Yield x 10^8 (mole/l)	C_2H_6 Yield x 10^8 (mole/l)	C_2H_4 Yield x 10^8 (mole/l)
1038	338	0.5	2.74	2.76	-
		1.0	5.73	5.11	-
		2.0	8.1	8.9	-
		3.0	12.0	12.6	-
		4.0	19.0	15.2	-
	236	0.5	1.6	1.15	
		1.0	2.8	3.1	
		1.0	2.7	2.6	
		2.0	5.3	9.5	
		2.0	5.6	4.5	
		3.0	7.5	13.4	
		3.0	9.8	6.8	
		4.0	12.4	16.7	
		4.0	12.1	19.8	
		4.0	8.7	11.5	
		4.0	14.3	9.9	
		5.0	17.6	13.0	
		5.0	20.4	10.6	
		6.07	23.9	11.8	
		7.0	25.3	12.5	
		8.0	33.5	13.7	
		9.0	33.7	13.1	
		10.0	39.8	13.0	
		11.0	47.1	14.6	
		12.0	54.0	14.6	
	188	1.0	2.0	2.5	
		1.0	2.4	1.84	
		2.0	3.1	4.3	
		2.0	4.5	-	
		2.0	4.0	-	
		2.0	3.6	4.7	
		2.0	5.9	3.3	
		0.5	-	1.1	
		3.0	6.5	7.4	
		3.0	7.9	4.5	
		4.0	11.8	7.85	
		4.0	11.0	5.93	
		5.0	12.2	9.2	
		5.0	14.3	6.7	
		6.0	16.5	7.6	
		7.0	20.4	8.4	
		8.0	24.7	8.4	
		9.0	28.2	9.0	
		10.2	32.9	9.0	
		12.0	40.1	10.3	

APPENDIX 1 (CONTINUED)

Temp (K)	Press (Torr)	Time (Min)	H_2	C_2H_6	C_2H_4
			Yield x 10^8 (mole/l)		
1038	109	0.4	-	0.3	
		2.0	1.86	-	
		2.0	1.55	1.44	
		3.0	2.49	1.95	
		4.0	2.79	-	
		4.0	3.9	2.0	
		5.0	4.5	2.8	
		6.0	5.3	3.6	
		6.0	4.7	3.3	
		7.0	8.7	3.9	
		8.0	7.0	4.2	
		8.0	7.9	-	
		9.0	11.2	4.8	
		10.0	10.4	3.9	
		10.0	11.3	4.7	
		10.0	10.9	4.7	
		12.0	-	4.7	
		14.0	18.3	5.2	
	96	1.0	0.98	0.94	
		2.0	-	0.92	
		2.0	1.24	1.3	
		3.0	2.22	1.63	
		4.0	3.43	-	
		4.0	2.95	2.85	
		4.0	6.47	2.3	
		6.0	4.9	2.95	
		8.0	6.72	3.77	
	66	2.0	1.36	0.73	
		4.0	2.45	1.15	
		6.0	1.72	1.68	
		6.0	3.95	1.80	
		8.0	5.17	3.77	
	43	3.2	1.24	0.67	
		6.0	-	0.98	
		9.0	1.68	1.36	
		9.0	1.68	1.53	
		12.0	-	1.55	
	32	3.0	-	0.38	
		6.0	-	0.67	
		9.0	-	0.92	
		12.0	1.09	1.07	
		15.0	1.4	1.24	
		20.0	2.5	1.42	
		25.0	3.4	1.78	
		28.0	3.4	1.65	

APPENDIX 1
(CONTINUED)

Temp (K)	Press (Torr)	Time (Min)	H_2	C_2H_6 Yield x 10^8	C_2H_4 (mole/l)	C_2H_2
1068	742	0.5	25.3	28.4	-	-
		1.0	66.5	42.1	9.1	-
		1.5	109	51.6	26.6	-
		2.0	169	65.7	55.6	-
		2.5	231	78.7	76.7	-
		3.0	314	68.8	91.4	-
		4.0	422	75.4	123.1	-
		5.1	-	81.8	170	-
		6.0	961	96.2	223	-
		7.0	1275	112	277	-
	600	0.5	-	21.6	-	-
		1.0	48.8	37.5	4.0	-
		2.0	132	54.1	30.0	-
		2.5	-	61.6	47.4	-
		3.0	201	62.1	62.3	-
		4.0	-	68.8	100	-
		4.5	-	63.9	106	-
	440	0.24	-	5.0	-	-
		0.41	14.9	12.5	-	-
		0.71	-	10.5	-	-
		0.71	-	12.6	-	-
		0.71	-	17.9	-	-
		1.0	-	18.1	-	-
		1.45	28.9	31.6	4.17	-
		2.0	69.5	38.2	15.8	-
		3.0	145	41.5	33.2	-
		5.04	230	44.1	66.8	-
		7.0	487	44.5	98.5	-
		10.0	975	80.9	195	-
		12.0	1649	114.9	310	-
	339	0.5	-	8.54	-	-
		1.0	-	15.9	-	-
		1.5	-	21.1	1.44	-
		2.0	36.3	26.1	3.6	-
		2.5	-	29.0	8.3	-
		3.0	62.3	31.0	13.3	-
		4.0	104	33.6	26.9	-
		5.0	136	36.0	38.2	-
		7.0	-	41.4	65.5	-
		10.0	482	56.5	115	-

APPENDIX 1
(CONTINUED)

Temp (K)	Press (Torr)	Time (Min)	H_2	C_2H_6	C_2H_4	C_2H_2
			Yield x 10^8 (mole/l)			
1068	233	0.5	-	4.86	-	-
		1.0	-	9.3	-	-
		1.5	-	12.2	-	-
		2.0	-	15.6	-	-
		3.03	-	19.3	4.5	-
		4.0	-	17.6	8.7	-
		6.0	-	20.7	21.1	-
		8.0	159	19.8	27.3	-
		10.08	274	25.6	44.9	-
		13.0	611	50.6	115	2.1
		20.0	1853	79.6	235	10.3
		25.0	4556	112	490	29.0
	154	0.5	-	2.78	-	-
		1.02	-	4.9	-	-
		2.0	-	5.2	-	-
		3.0	13.4	11.3	-	-
		4.0	20	13.7	1.82	-
		5.0	32.2	13.9	4.33	-
		6.0	33.3	15.0	7.0	-
		8.0	-	15.6	12.3	-
		10.0	79.6	18.0	19.3	-
		20.0	507	43.3	92.5	-
	104	1.0	-	2.53	-	-
		1.5	-	3.7	-	-
		2.0	-	5.2	-	-
		3.0	-	6.5	-	-
		4.0	-	7.9	0.15	-
		5.0	-	9.3	0.35	-
		6.0	22	-	0.6	-
		6.0	18	8.9	-	-
		8.0	28.5	8.4	2.66	-
		10.0	37.3	8.6	5.63	-
		12.0	54	9.1	8.2	-
		14.0	82	10.3	11.4	-
		18.0	97	11.4	16.0	-
	75.5	2.0	-	2.9	-	-
		4.0	-	5.9	-	-
		6.0	-	6.1	1.3	-
		8.0	17.0	7.9	-	-
		10.0	17.4	6.8	1.84	-
		15.06	36.7	8.5	5.4	-
		20.0	60.7	9.9	11.0	-
		30.0	180	18.5	31.9	-

APPENDIX 1 (CONTINUED)

Temp (K)	Press (Torr)	Time (Min)	H_2	C_2H_6	C_2H_4	C_2H_2
			Yield x 10^8 (mole/l)			
1068	48.6	2.0	-	1.45	-	-
		4.0	-	2.68	-	-
		6.0	2.8	3.29	-	-
		8.0	8.7	4.12	-	-
		12.0	11.45	4.25	-	-
		16.0	16.4	4.71	1.53	-
		20.0	23.6	5.17	2.87	-
		24.0	28.3	5.70	4.19	-
		30.0	-	7.22	6.85	-
	25.2	4.04	-	0.86	-	-
		6.0	-	1.39	-	-
		8.06	-	1.59	-	-
		10.0	-	1.80	-	-
		12.0	-	1.93	-	-
		12.0	-	2.07	-	-
		16.0	-	2.09	-	-
		20.0	-	2.11	-	-
		26.34	-	2.30	-	-
		28.0	-	3.06	-	-
		30.0	-	2.81	-	-
1103	743	0.25	-	52.8	9.2	-
		0.5	-	82.7	17.8	-
		0.75	-	98.5	42.1	-
		1.0	-	107.2	63.0	-
		1.5	-	120.2	125.8	-
	602	0.25	52.6	45.0	-	-
		0.5	214	76.0	-	-
		1.0	-	65.4	-	-
		1.25	-	96.4	-	-
		1.5	-	86.5	-	-
		2.0	-	114	5.9	-
		2.5	-	142	15.7	-
		3.0	-	173	26.0	-
	440	0.24	-	29.3	-	-
		0.5	-	45.9	10.7	-
		0.75	-	57.6	28.6	-
		1.0	-	65.3	50.1	-
		2.0	-	78.9	132.7	-
		2.5	-	89.2	176.2	5.8
		3.0	-	110.2	243	13.3
		3.5	-	131.9	305	18.0
		4.0	-	168.1	422	33.3
		4.5	-	167	472	45.4
		5.0	-	161	517	51.1

APPENDIX .1
(CONTINUED)

Temp (K)	Press (Torr)	Time (Min)	H_2	C_2H_6	C_2H_4	C_2H_2
			Yield x 10^8 (mole/l)			
1103	233	0.51	-	18.0	-	-
		1.00	47.6	28.4	7.7	-
		1.50	-	32.5	22.1	-
		2.00	-	36.5	35.7	-
		3.00	247	44.4	68.5	-
		4.00	-	57.9	112	-
		6.00	-	103	258	24.3
	121	0.51	-	6.5	-	-
		1.00	-	11.4	1.82	-
		2.00	-	17.6	9.6	-
		2.50	45.5	16.5	9.6	-
		3.05	-	18.4	18.6	-
		4.00	-	25.4	36.4	-
		5.00	-	24.5	35.1	-
		7.00	-	39.4	77.6	-
		8.00	-	52.7	122	-
	49	1.00	-	2.38	-	-
		2.00	-	3.69	-	-
		3.00	-	4.88	-	-
		4.00	-	5.00	-	-
		4.18	-	5.72	-	-
		5.00	-	6.01	-	-
		7.00	-	7.68	-	-
		9.00	-	9.21	11.8	-
		11.00	-	12.5	20.0	-
		13.00	-	15.6	28.4	-
		15.00	-	21.4	42.9	-

APPENDIX 1
(CONTINUED)

Temp (K)	Press (Torr)	Time (Min)	C_2H_6	C_2H_4	C_2H_2	C_3H_6	C_3H_4
			Yield x 10^8 (mole/l)				
1038	433	2.00	12.7	1.34	*	*	*
		4.00	20.5	6.53	*	*	*
		6.00	25.2	13.4	*	1.61	*
		6.00	24.9	13.8	*	-	*
		8.00	28.3	25.1	0.51	2.19	*
		10.00	29.0	32.8	0.65	2.78	*
		13.02	31.7	48.6	1.41	7.25	1.07
		18.00	29.7	62.3	2.30	10.7	1.65
		18.00	36.6	73.7	2.58	14.7	2.41
		25.00	50.1	128.1	7.41	34.1	7.04
		30.00	65.9	168	11.7	46.9	9.86
		39.00	105.6	352	31.8	96.5	17.3
		50.00	169.9	801	92.4	201	25.9
		60.00	178	1072	113	196	18.5
		65.00	216	1390	145	243	20.5
		70.00	307	1933	203	302	23.7
	443#	1.00	10.1	0.34	*	*	*
		2.00	17.1	2.2	*	*	*
		2.02	16.2	2.1	*	*	*
		3.02	21.4	4.6	*	*	*
		4.00	24.6	10.3	*	0.49	*
		5.00	27.6	17.0	0.31	0.89	*
		7.00	29.8	28.8	0.76	2.4	*
		9.00	31.3	41.2	1.21	4.94	0.48
		12.00	32.6	56.6	2.01	9.44	0.85
		16.00	38.0	81.3	-	17.9	2.4
		20.00	41.4	109	-	-	-
		24.00	60.5	156	11.7	44.9	7.15
		30.00	93.8	290	27.8	86.0	13.1
		35.05	118	451	47.8	124	16.0

* undetectable
\- not measured
\# with packed vessel, S/V=9.6

APPENDIX 1

(CONTINUED)

Temp (K)	Press (Torr)	Time (Min)	C_2H_6	C_2H_4	C_2H_2	C_3H_6	C_3H_4
			Yield x 10^8 (mole/l)				
1038	13.3	15.00	0.60	*	*	*	*
		30.04	0.86	0.128		*	*
		45.00	1.04	0.302	*	*	*
		60.00	1.17	0.687	*	*	*
		80.00	1.29	0.940	*	*	*
	43.9	5.00	0.90	*	*	*	*
		10.00	1.87	*	*	*	*
		15.00	1.99	0.35	*	*	*
		22.00	2.53	0.81	*	*	*
		26.00	2.53	1.04	*	*	*
		30.00	2.62	1.32	*	*	*
		40.00	2.91	2.45	*	*	*
	100.0	5.00	3.14	0.126	*	*	*
		7.50	4.04	0.503	*	*	*
		10.00	4.61	0.838	*	*	*
		12.59	5.13	1.76	*	*	*
		15.00	5.40	2.05	*	*	*
		20.00	6.26	3.96	*	*	*
		22.50	6.43	5.36	*	*	*
		26.00	6.47	6.58	*	0.49	*
	228.0	2.51	5.84	0.17	*	*	*
		5.00	10.28	1.76	*	*	*
		7.50	12.21	4.52	*	*	*
		10.00	14.45	9.23	*	*	*
		12.52	14.51	12.40	0.24	1.13	*
		17.50	15.96	21.57	0.75	1.97	0.37

APPENDIX 1
(CONTINUED)

Temp (K)	Press (Torr)	Time (Min)	C_2H_6	C_2H_4	C_2H_2	C_3H_6	C_3H_4
				Yield x 10^8 (mole/l)			
1038	595	2.00	19.8	3.85	*	*	*
		4.00	29.9	12.5	*	0.5	*
		6.00	35.9	26.2	0.40	1.86	1.00
		10.00	47.3	70.5	1.76	11.9	1.15
		12.00	43.6	76.3	2.09	13.3	2.17
		14.00	46.5	89.3	2.97	19.5	4.94
		18.00	57.2	130.0	5.70	35.2	10.3
		23.00	77.7	191.0	11.2	58.8	

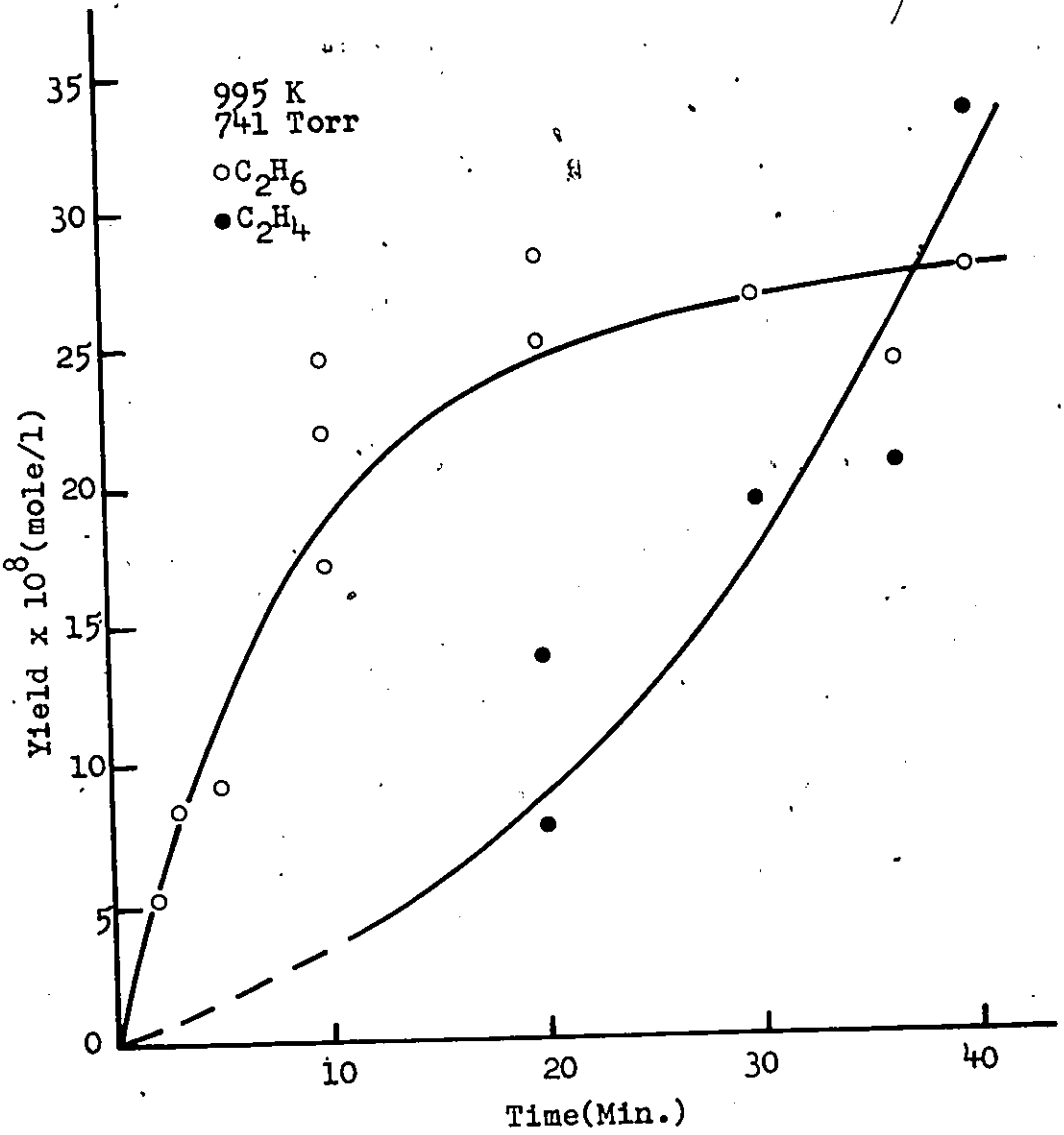
995 K
741 Torr
○ C_2H_6
● C_2H_4
Yield x 10^8(mole/l)
0
5
10
15
20
25
30
35
10
20
30
40
Time(Min.)

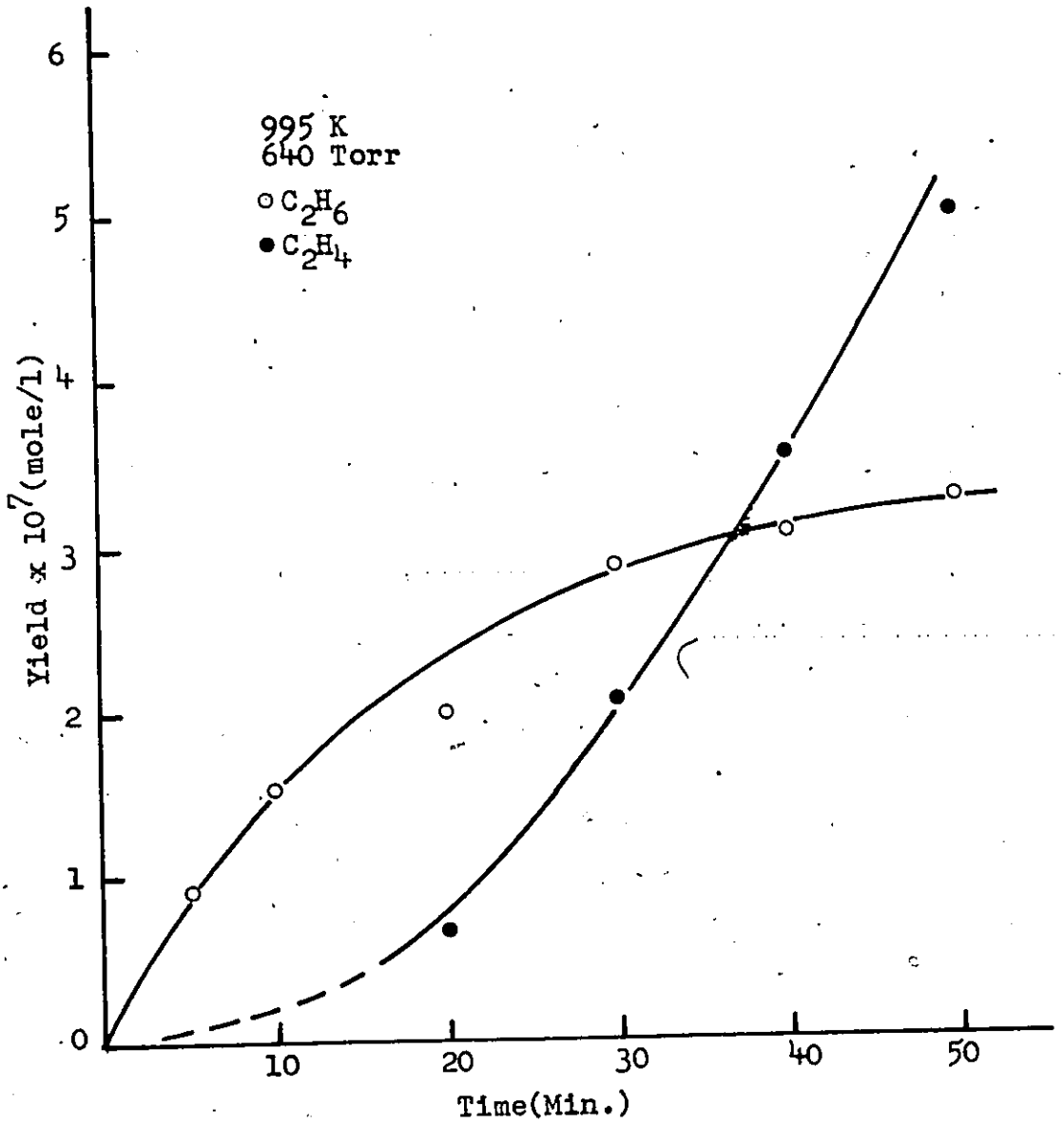
995 K
640 Torr
○ C_2H_6
● C_2H_4
Yield x 10^7(mole/l)
0
1
2
3
4
5
6
10
20
30
40
50
Time(Min.)

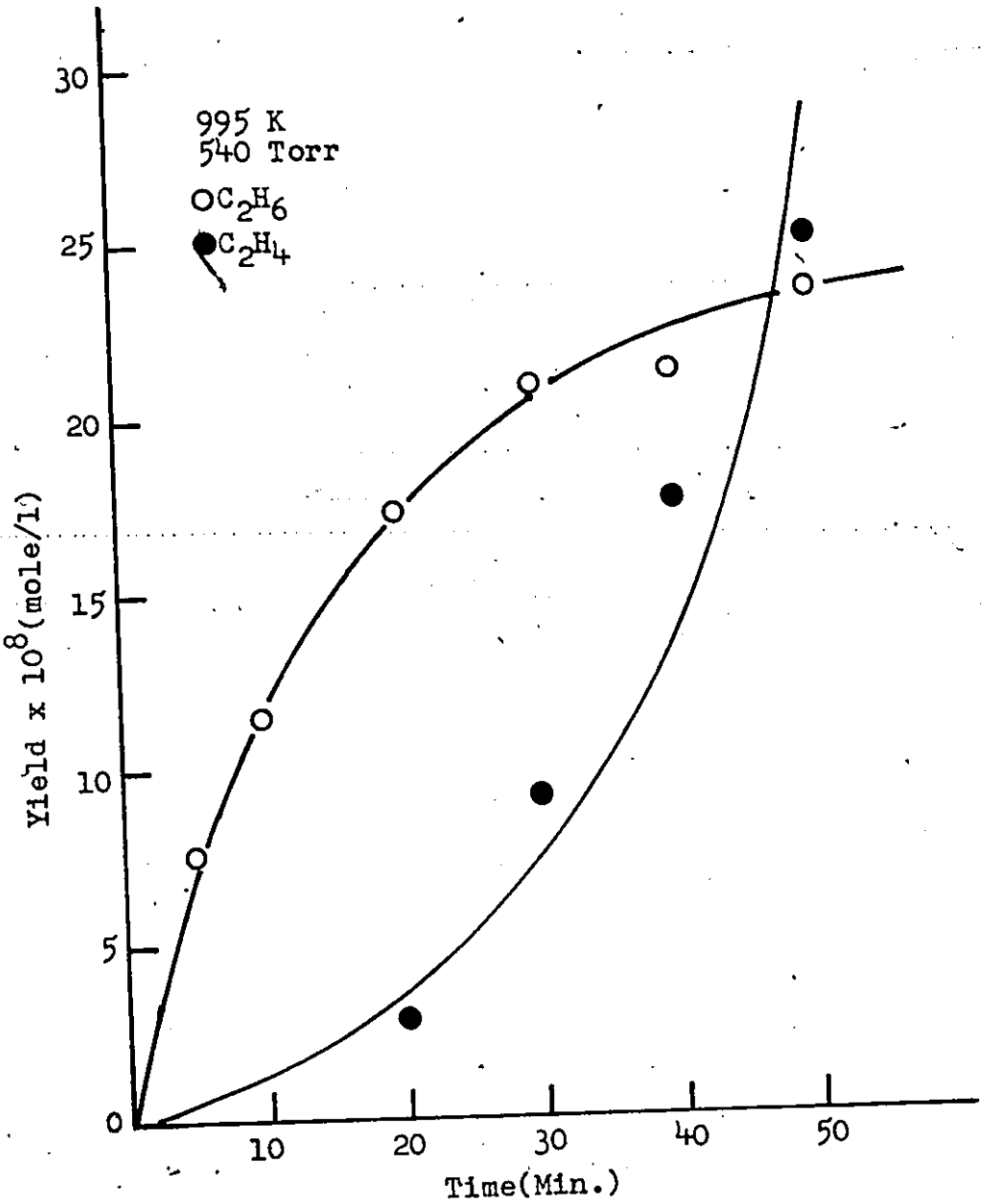
995 K
540 Torr
O C_2H_6
● C_2H_4
Yield x 10^8(mole/l)
Time(Min.)
0
5
10
15
20
25
30
10
20
30
40
50

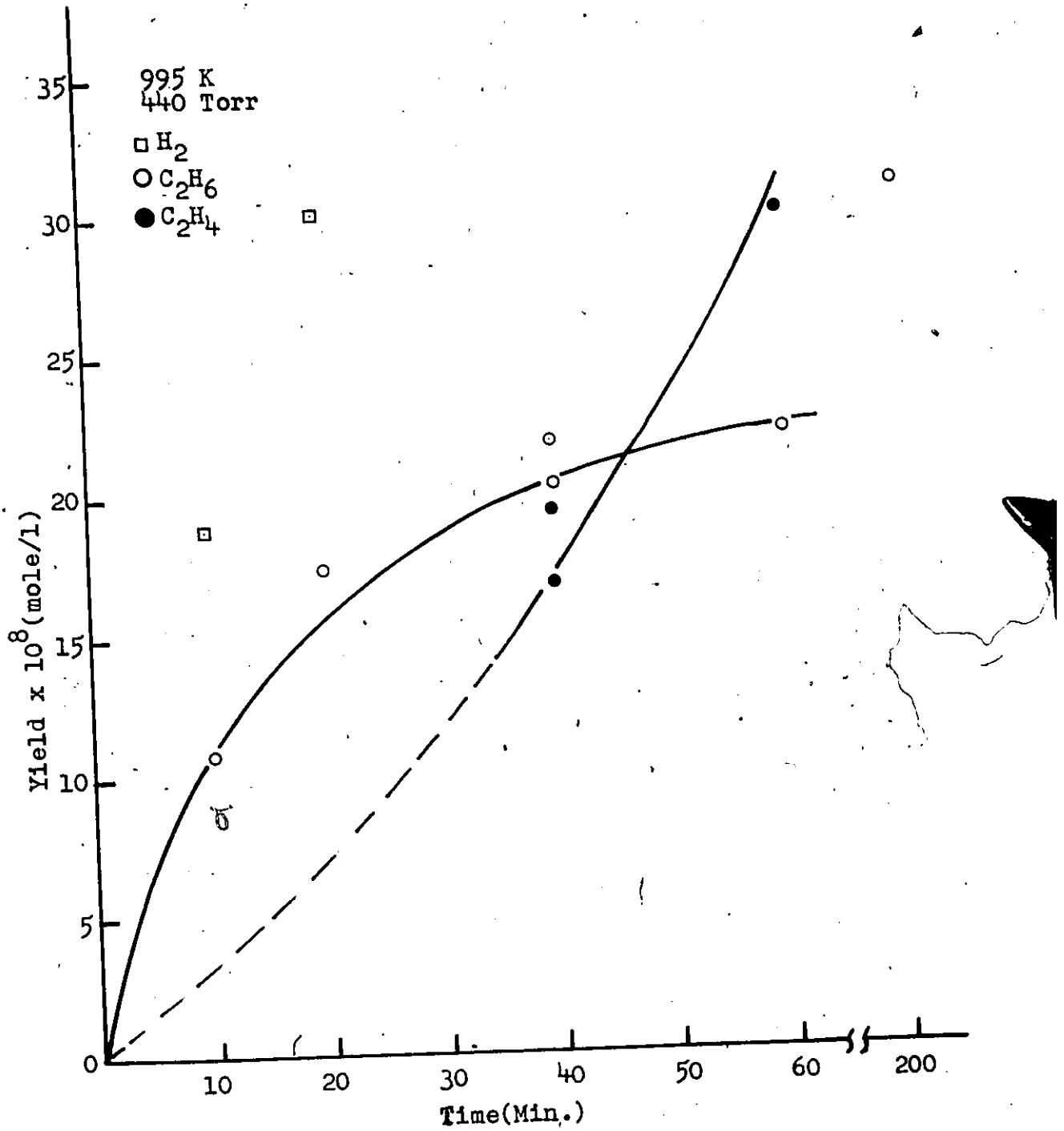
995 K
440 Torr
H2
C2H6
C2H4
Yield x 10^8 (mole/l)
Time(Min.)
0
5
10
15
20
25
30
35
10
20
30
40
50
60
200

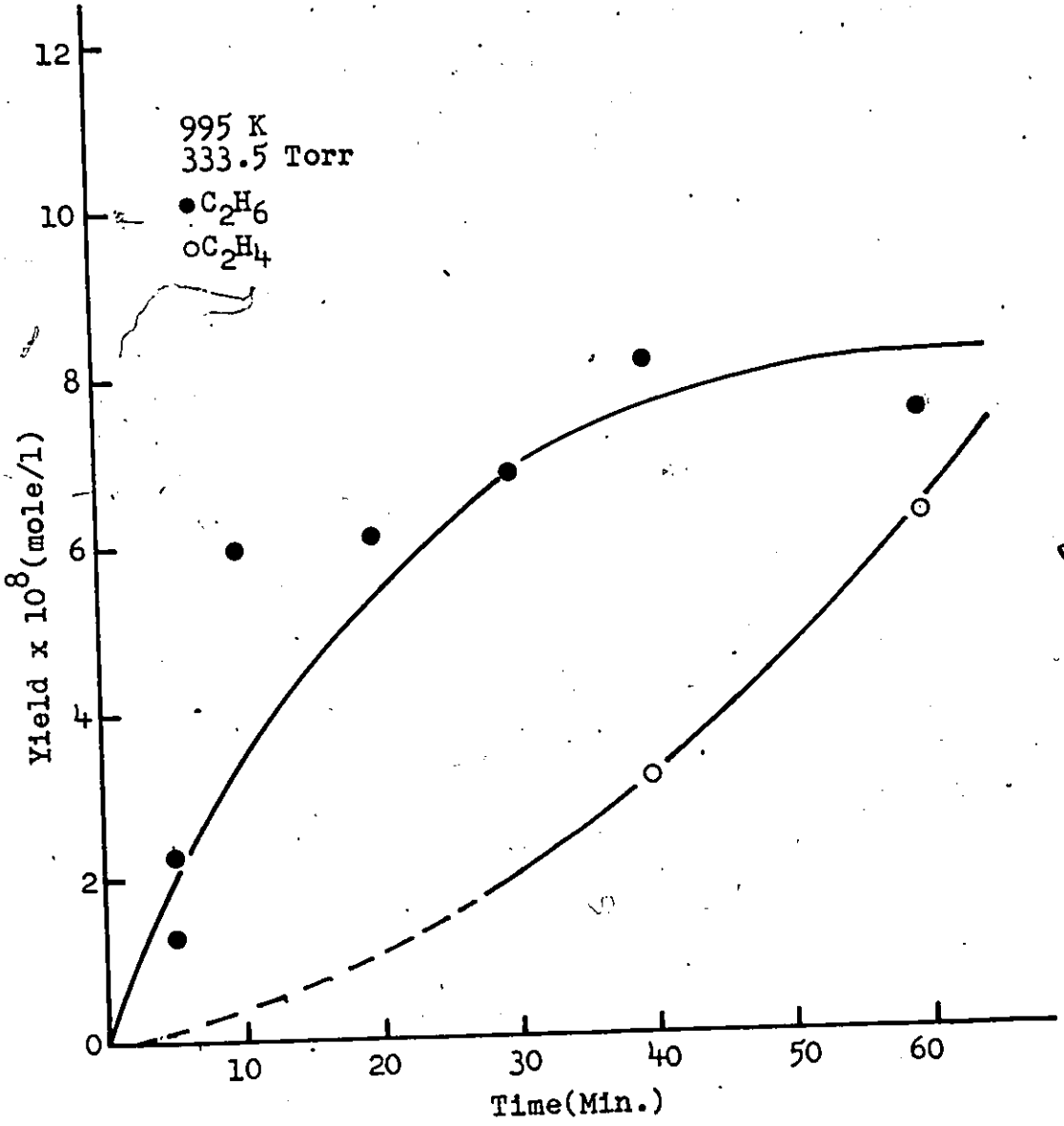
995 K
333.5 Torr
●C_2H_6
○C_2H_4
Yield x 10^8(mole/l)
0
2
4
6
8
10
12
10
20
30
40
50
60
Time(Min.)

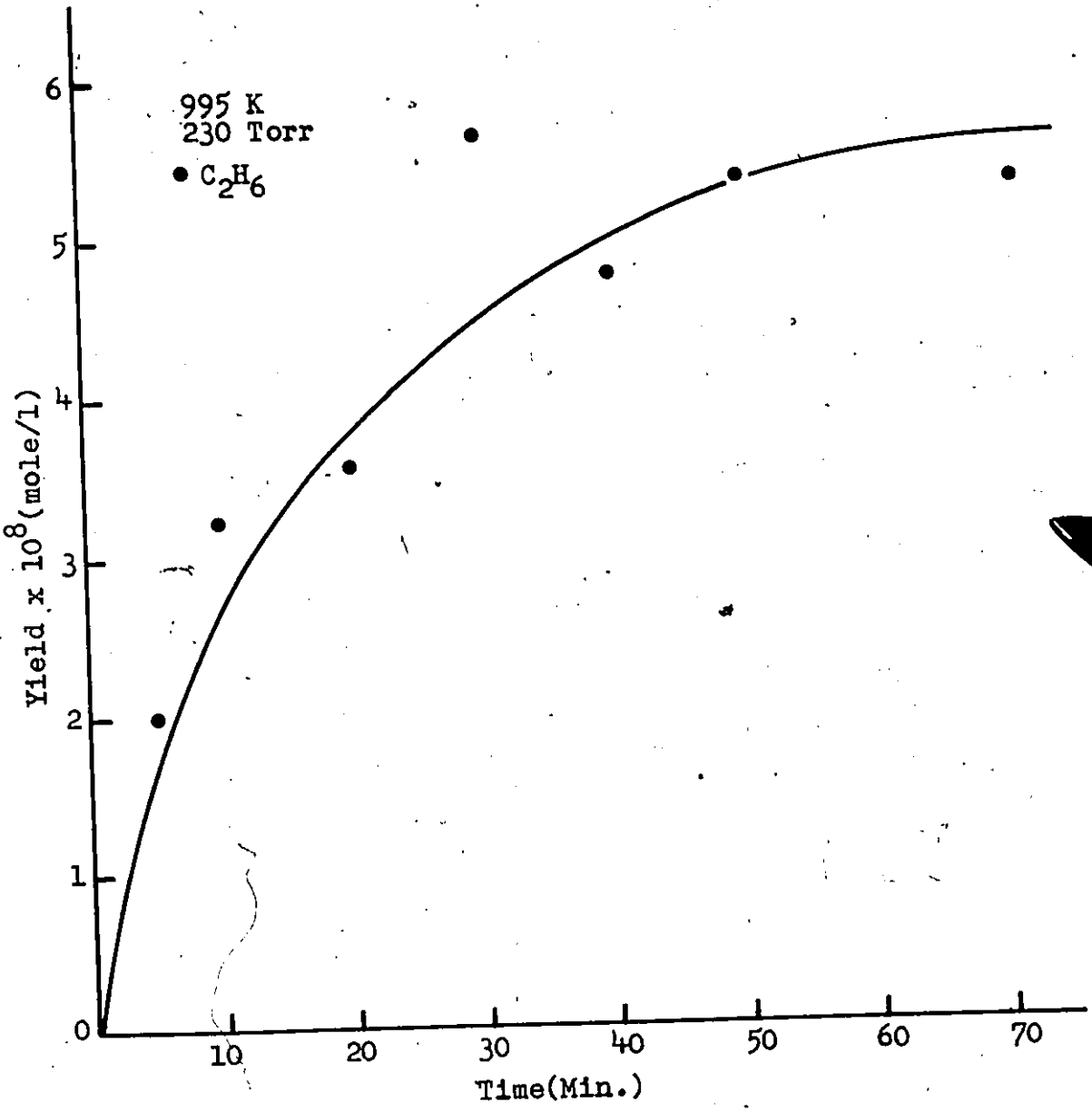
995 K
230 Torr
● C_2H_6
Yield x 10^8(mole/l)
0
1
2
3
4
5
6
10
20
30
40
50
60
70
Time(Min.)

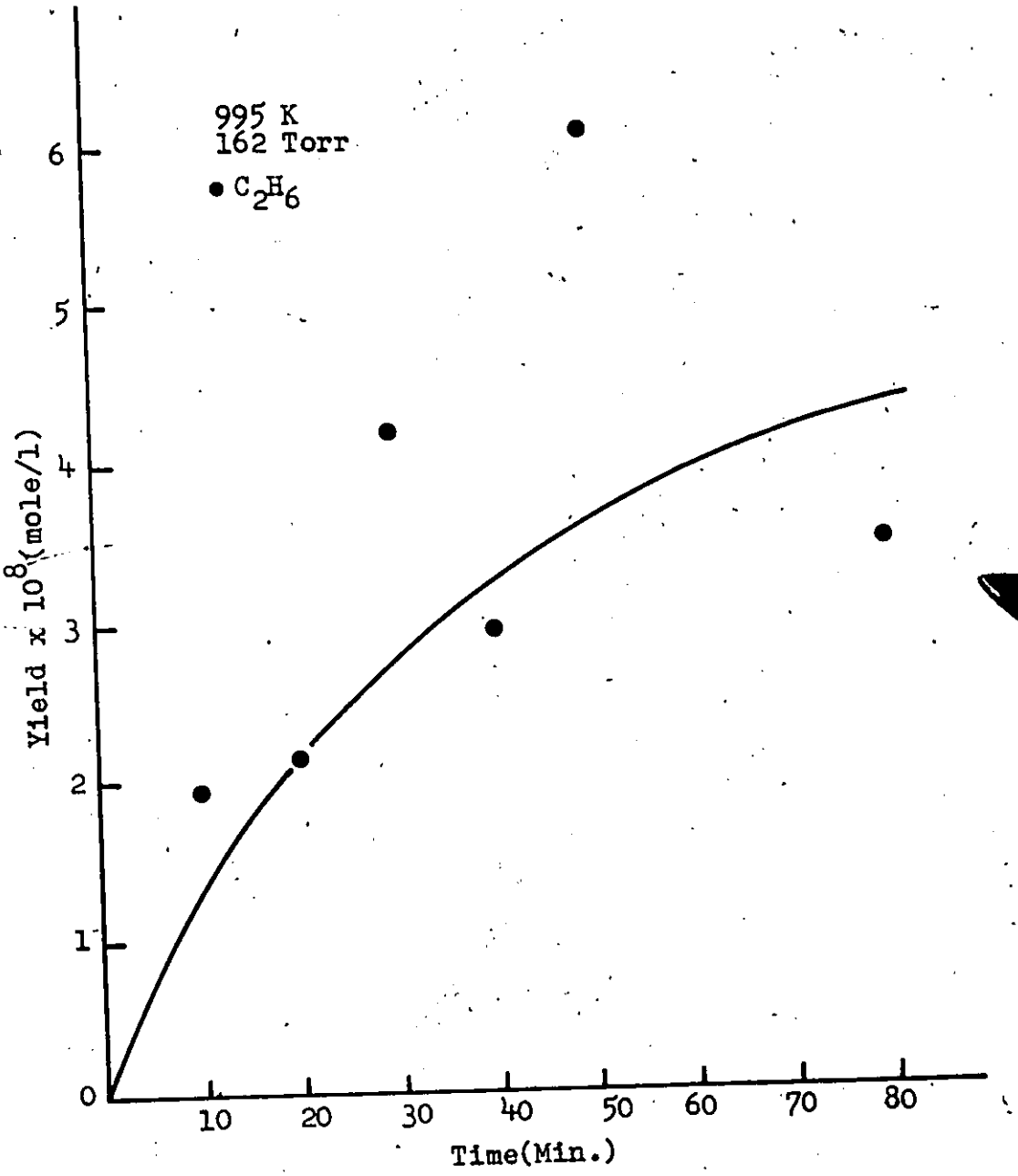
995 K
162 Torr
● C_2H_6
Yield x 10^8(mole/l)
0
1
2
3
4
5
6
10
20
30
40
50
60
70
80
Time(Min.)

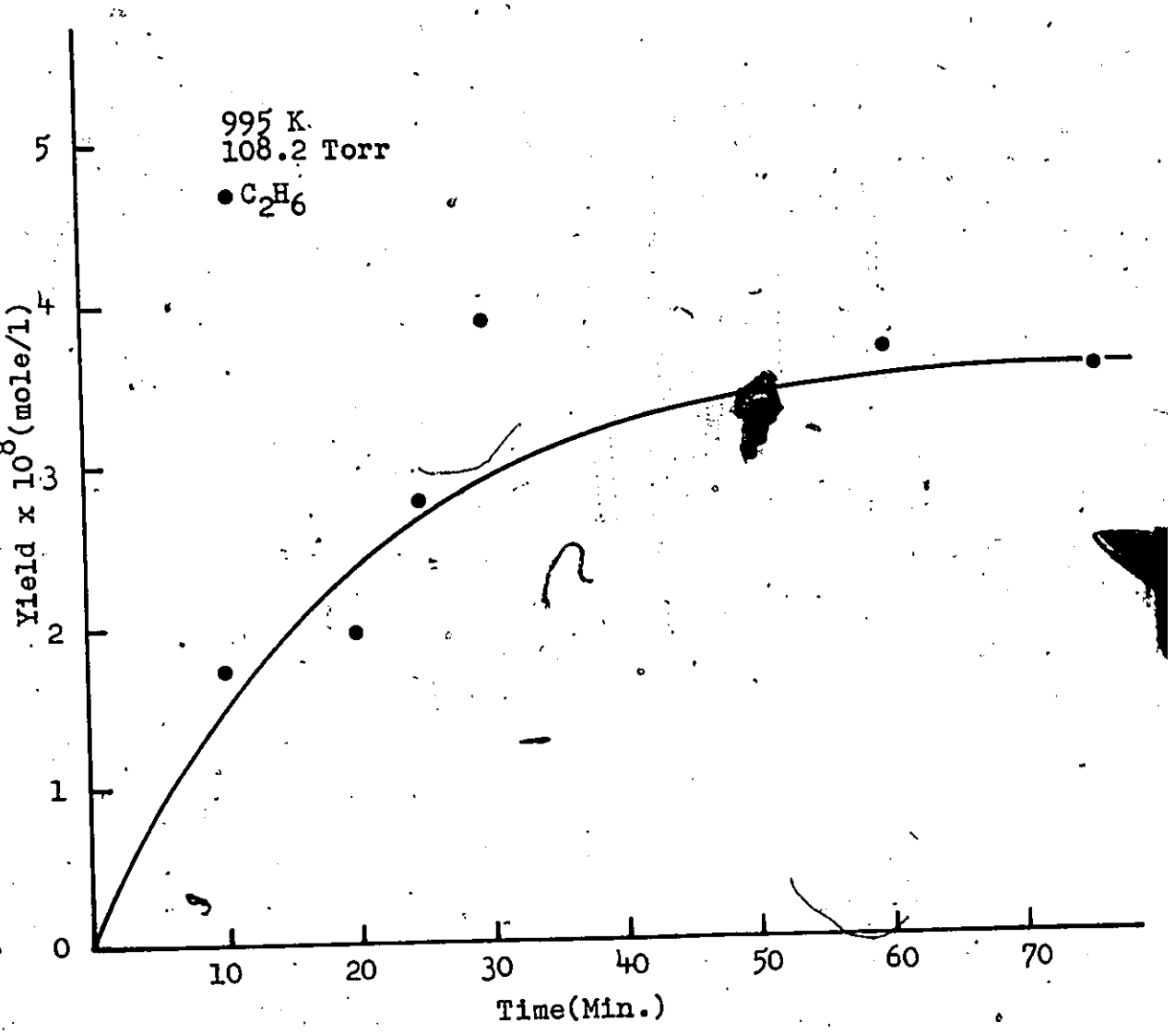
995 K
108.2 Torr
● C_2H_6
Yield x 10^8(mole/l)
0
1
2
3
4
5
10
20
30
40
50
60
70
Time(Min.)

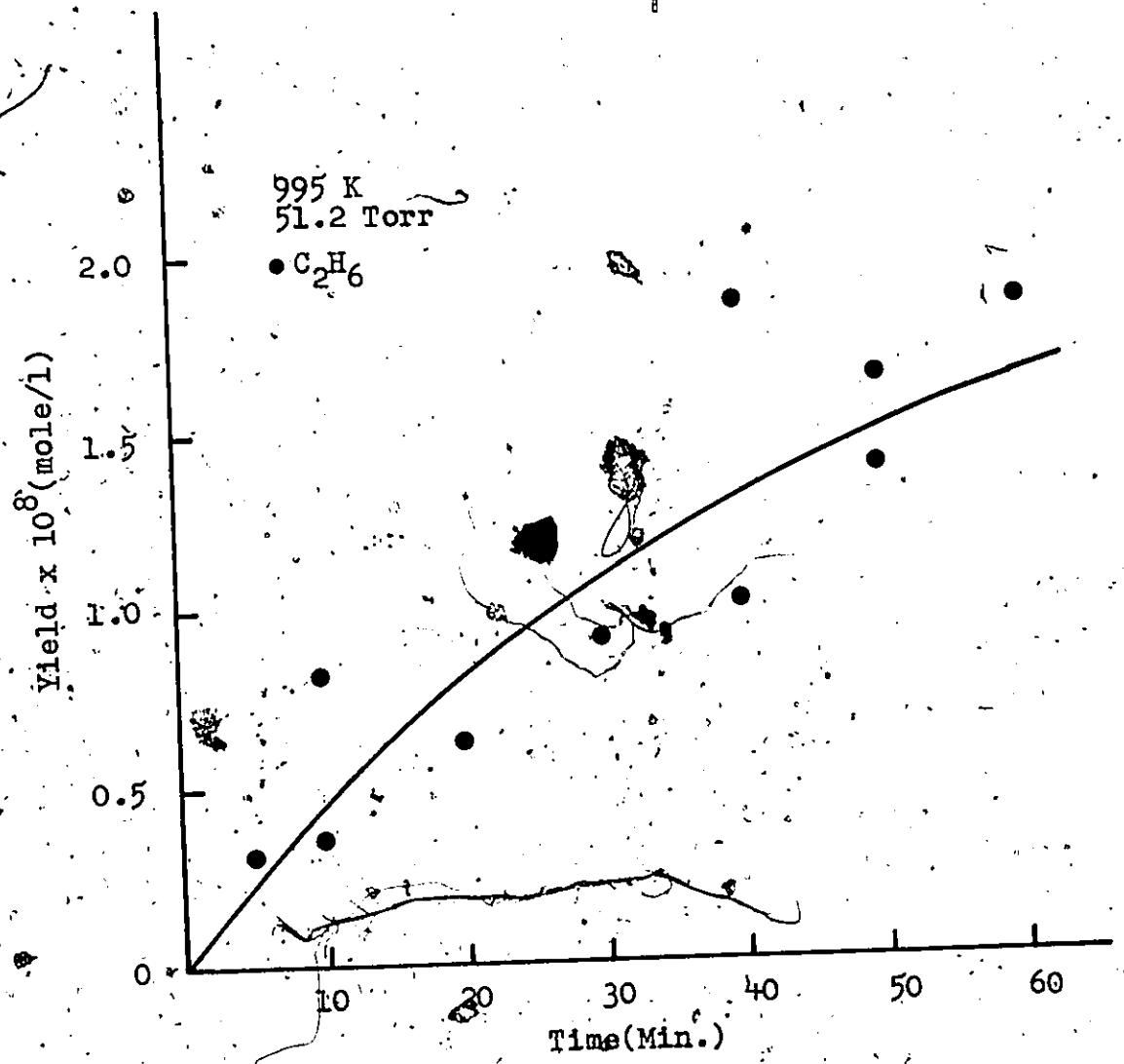
995 K
51.2 Torr
● C_2H_6
Yield x 10^8(mole/l)
2.0
1.5
1.0
0.5
0
10
20
30
40
50
60
Time(Min.)

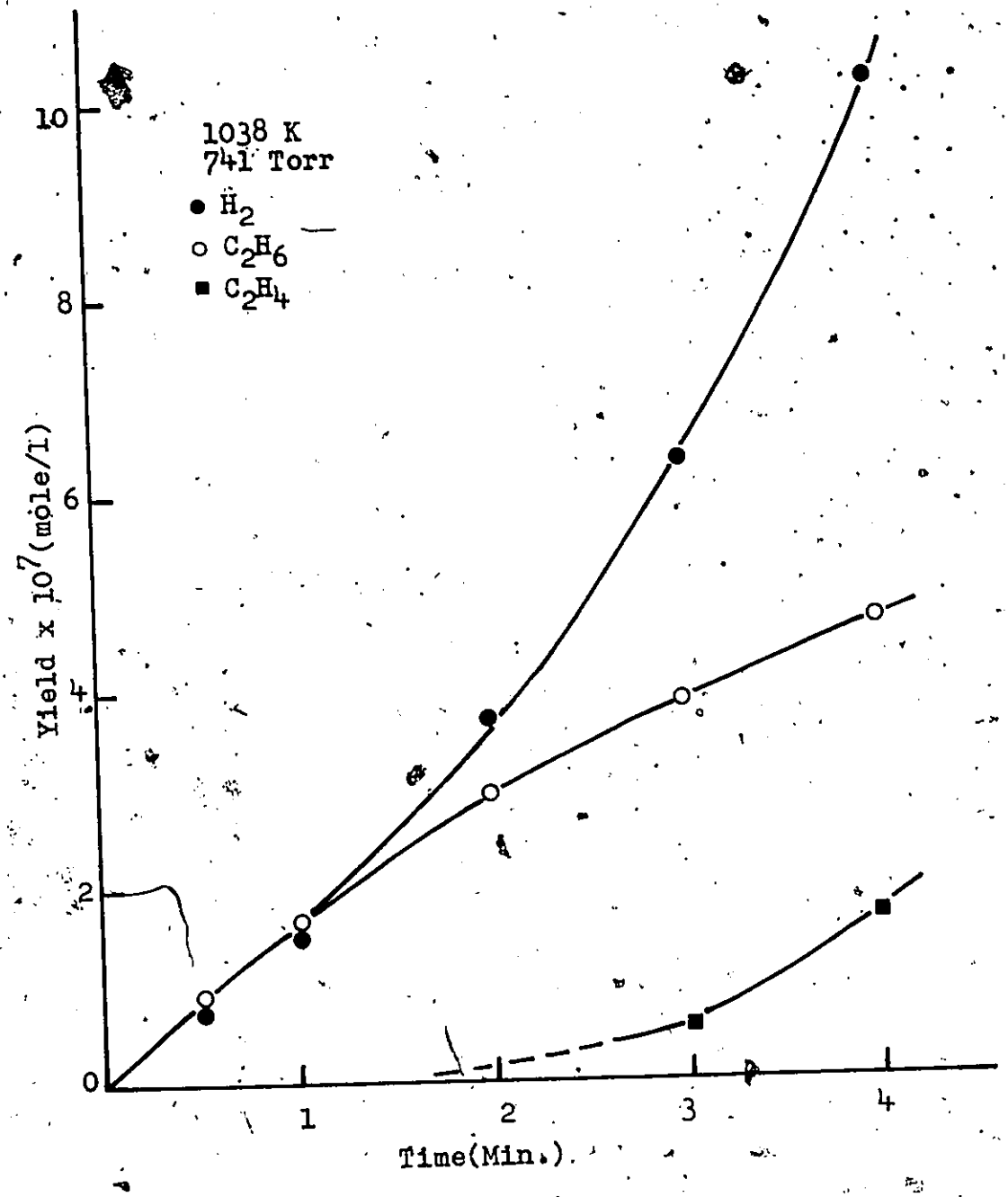
1038 K
741 Torr
● H_2
○ C_2H_6
■ C_2H_4
Yield x 10^7(mole/l)
0
2
4
6
8
10
1
2
3
4
Time(Min.)

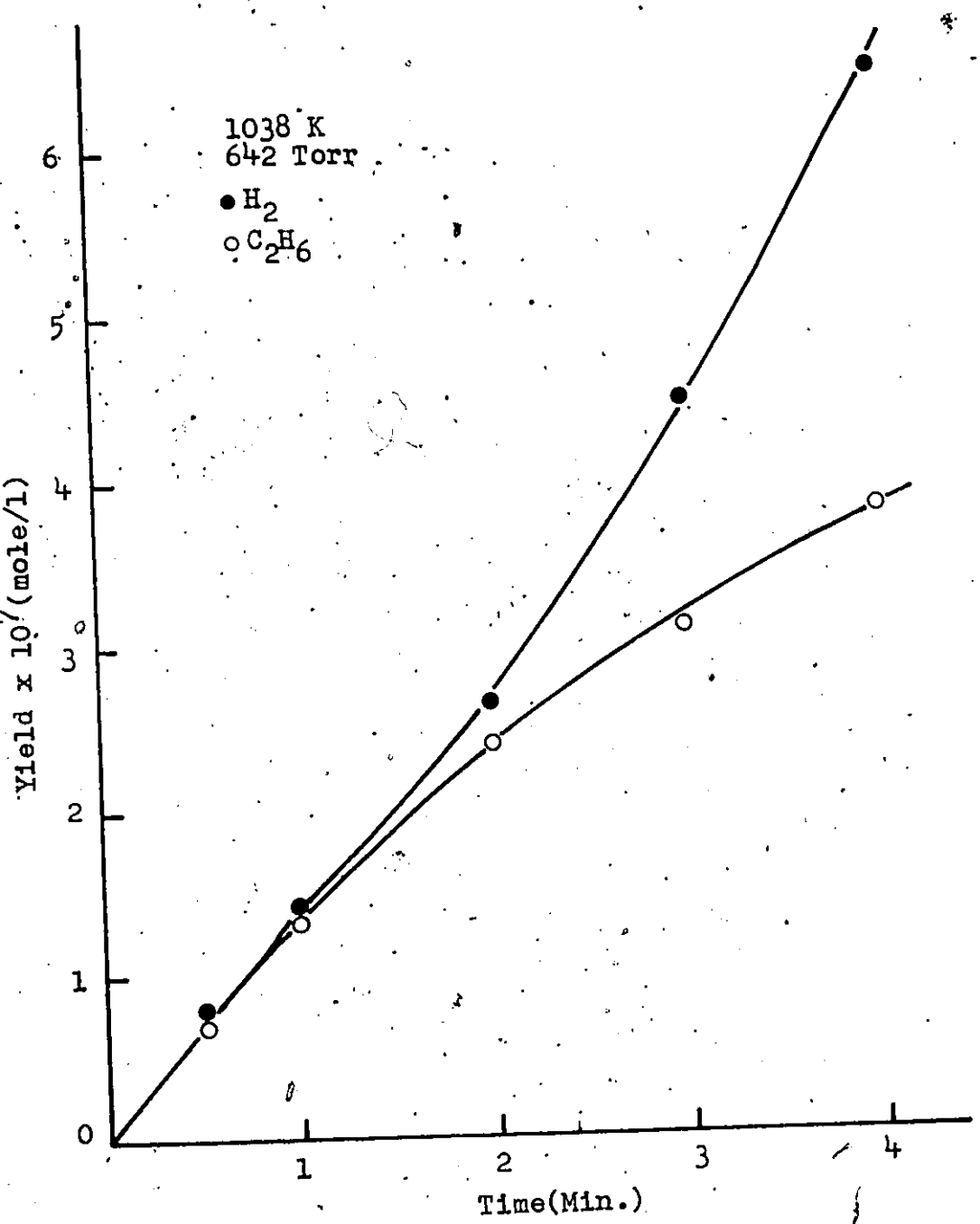
1038 K
642 Torr
● H_2
○ C_2H_6
Yield x 10^7(mole/l)
0
1
2
3
4
5
6
1
2
3
4
Time(Min.)

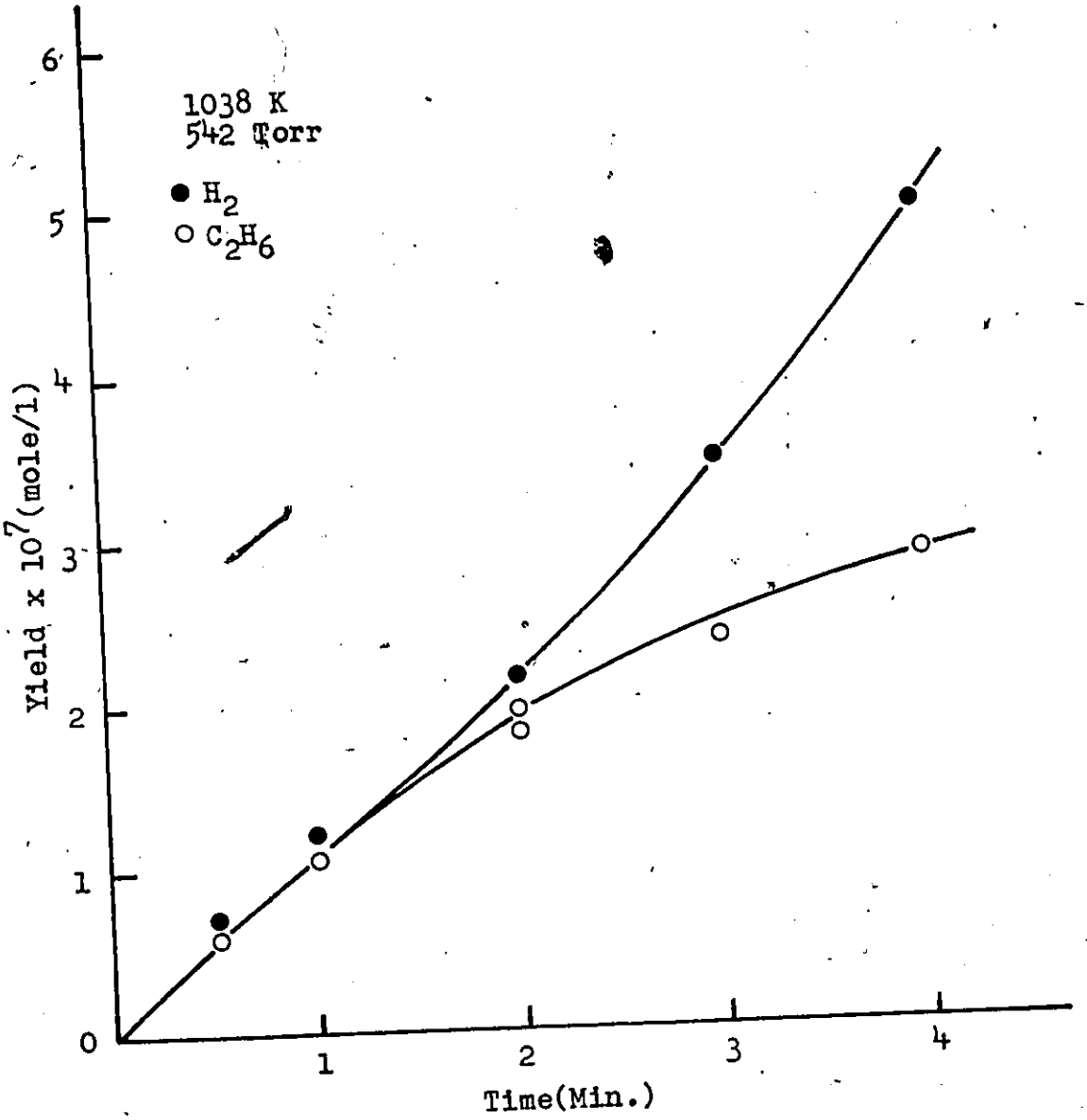
1038 K
542 Torr
● H_2
○ C_2H_6
Yield x 10^7(mole/l)
0
1
2
3
4
5
6
1
2
3
4
Time(Min.)

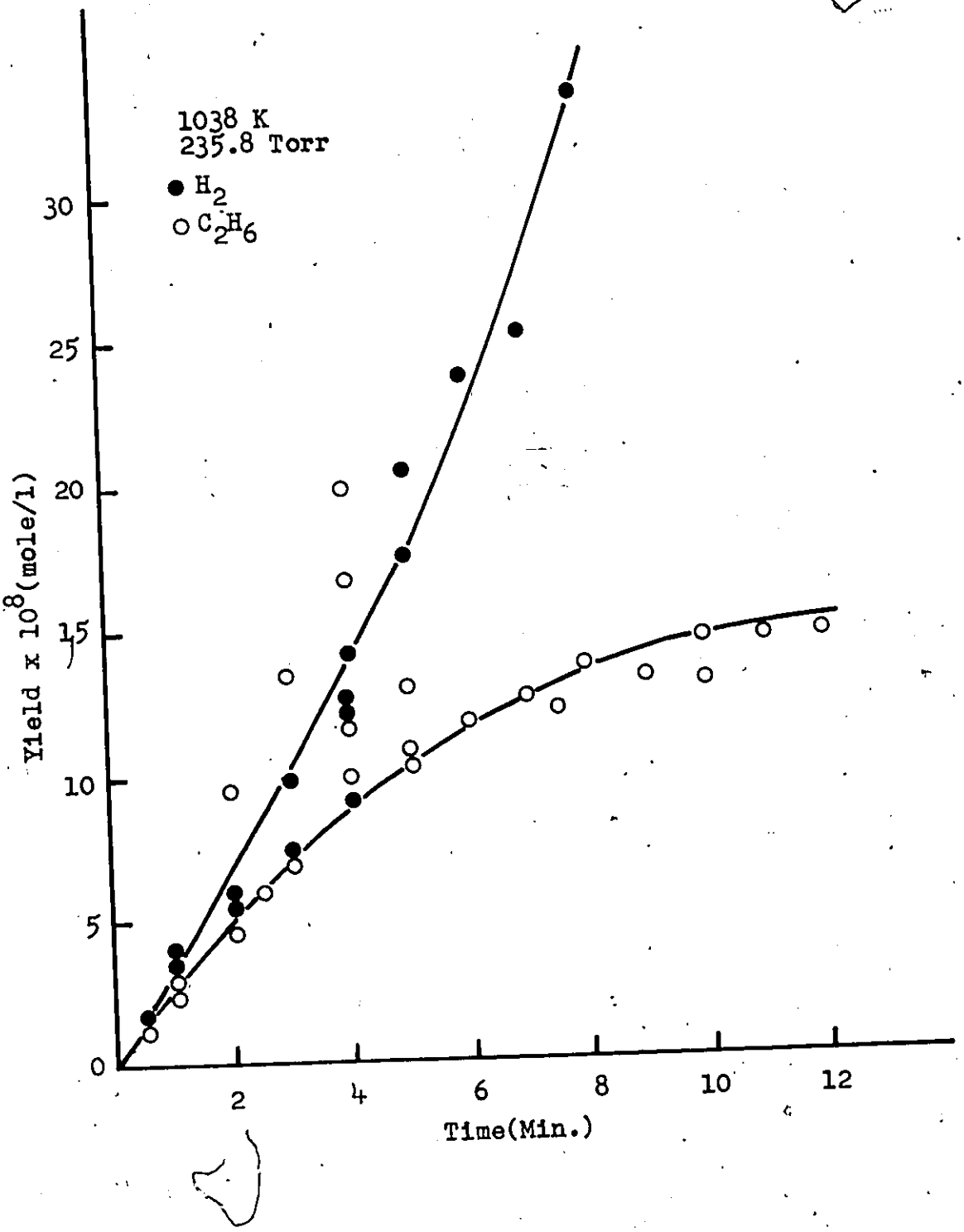
1038 K
235.8 Torr
● H_2
○ C_2H_6
Yield x 10^8(mole/l)
0
5
10
15
20
25
30
2
4
6
8
10
12
Time(Min.)

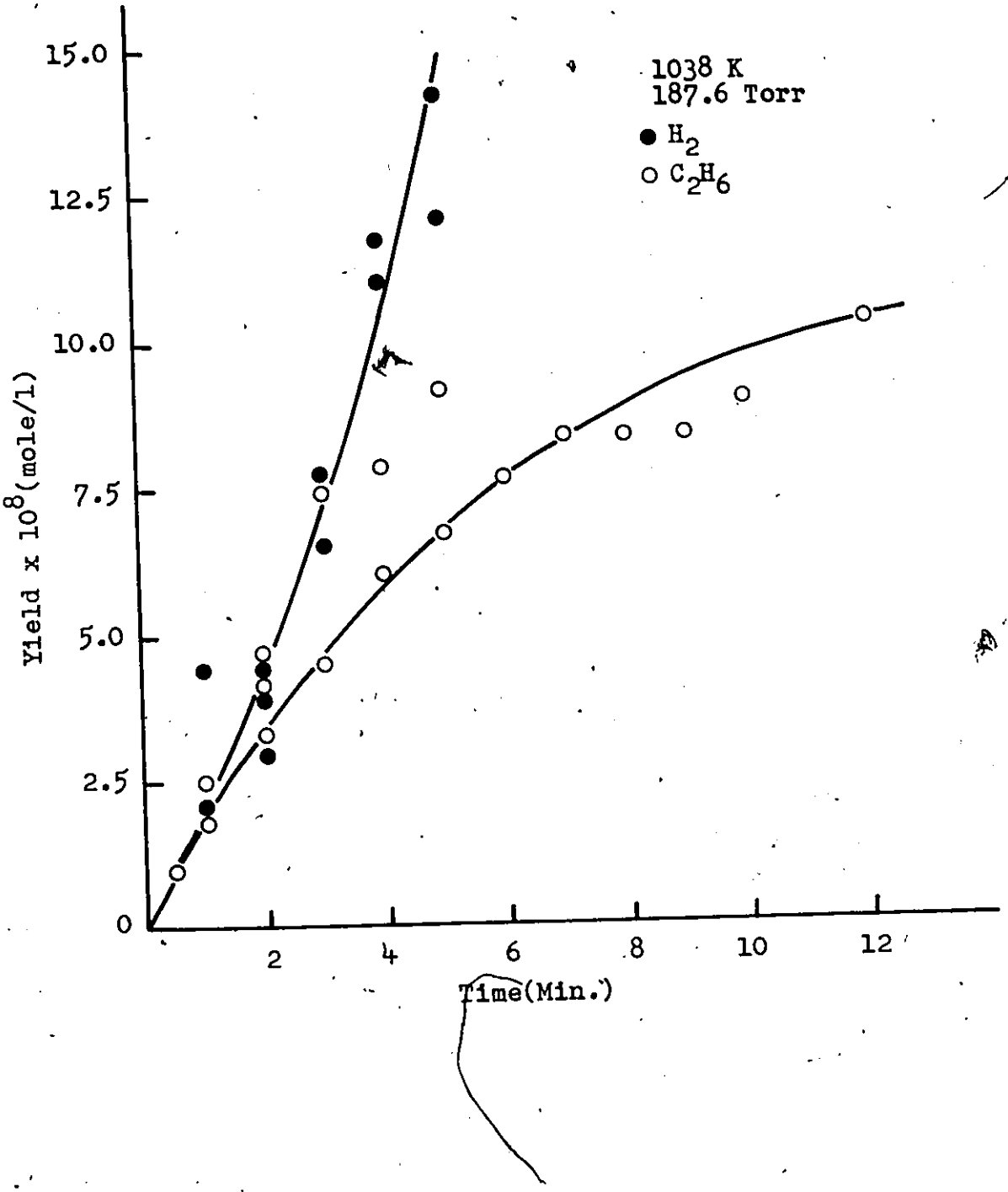
1038 K
187.6 Torr
● H_2
○ C_2H_6
Yield x 10^8(mole/l)
15.0
12.5
10.0
7.5
5.0
2.5
0
2
4
6
8
10
12
Time(Min.)

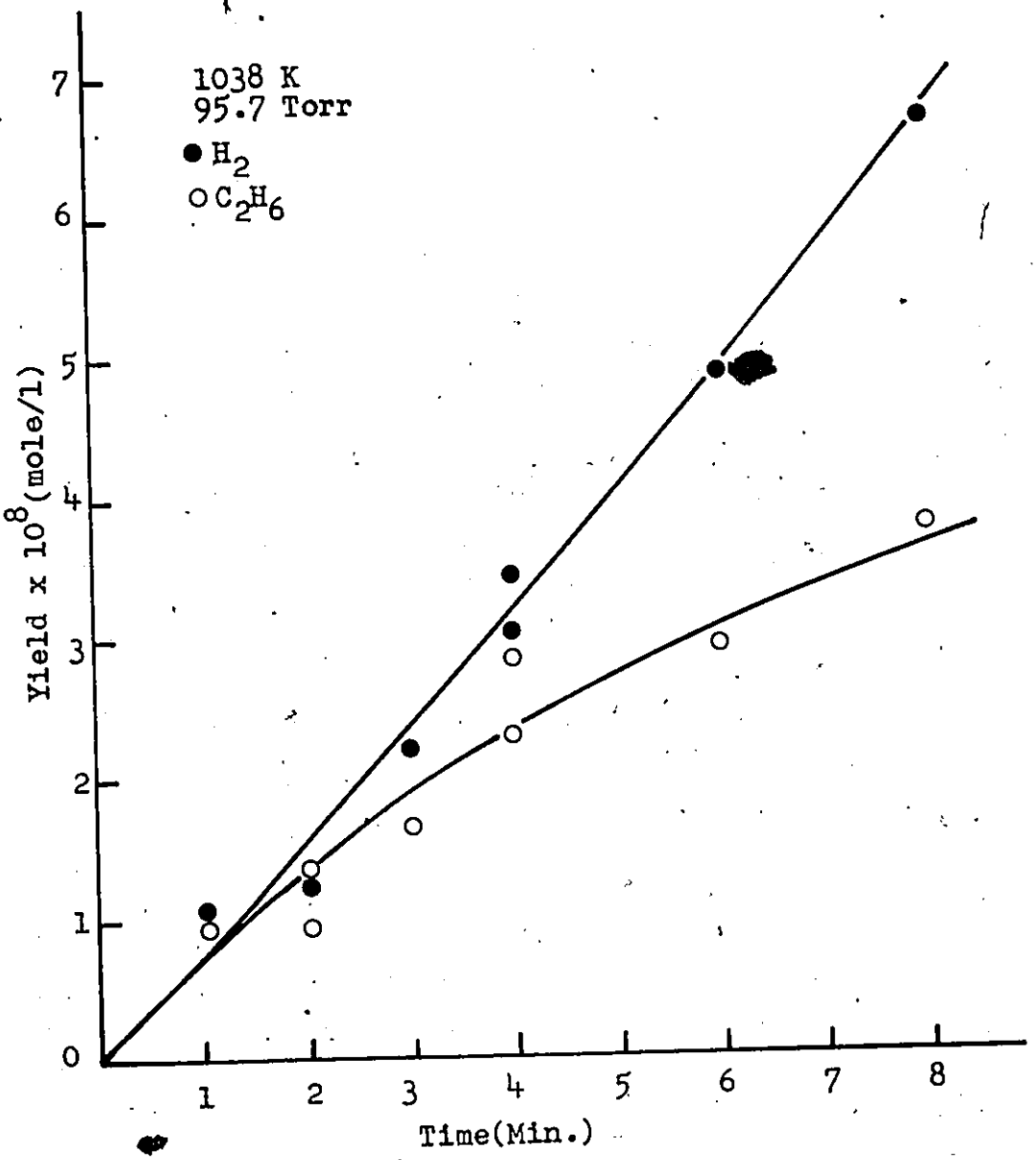
1038 K
95.7 Torr
● H_2
○ C_2H_6
Yield x 10^8(mole/l)
0
1
2
3
4
5
6
7
1
2
3
4
5
6
7
8
Time(Min.)

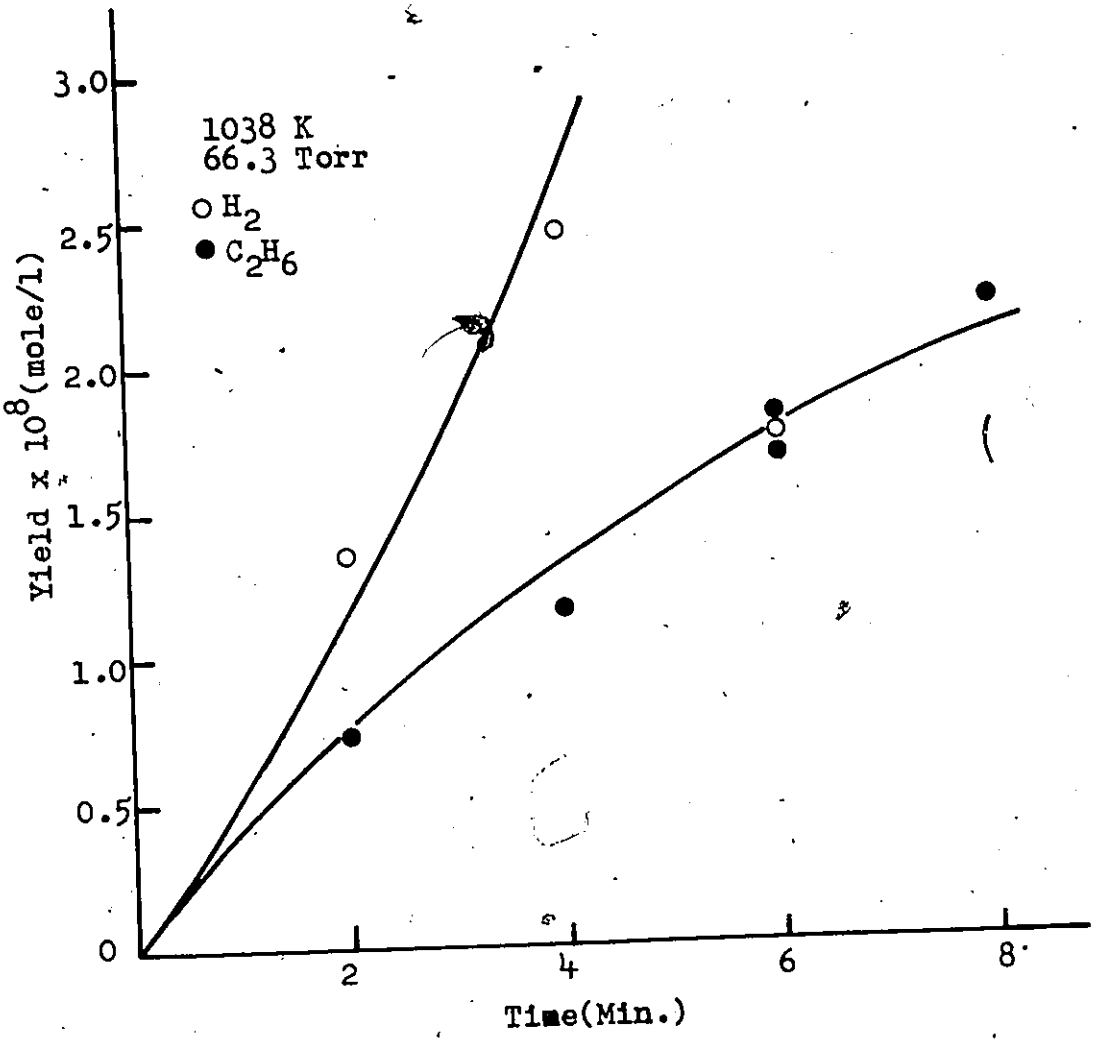
1038 K
66.3 Torr
○ H_2
● C_2H_6
Yield x 10^8(mole/l)
3.0
2.5
2.0
1.5
1.0
0.5
0
2
4
6
8
Time(Min.)

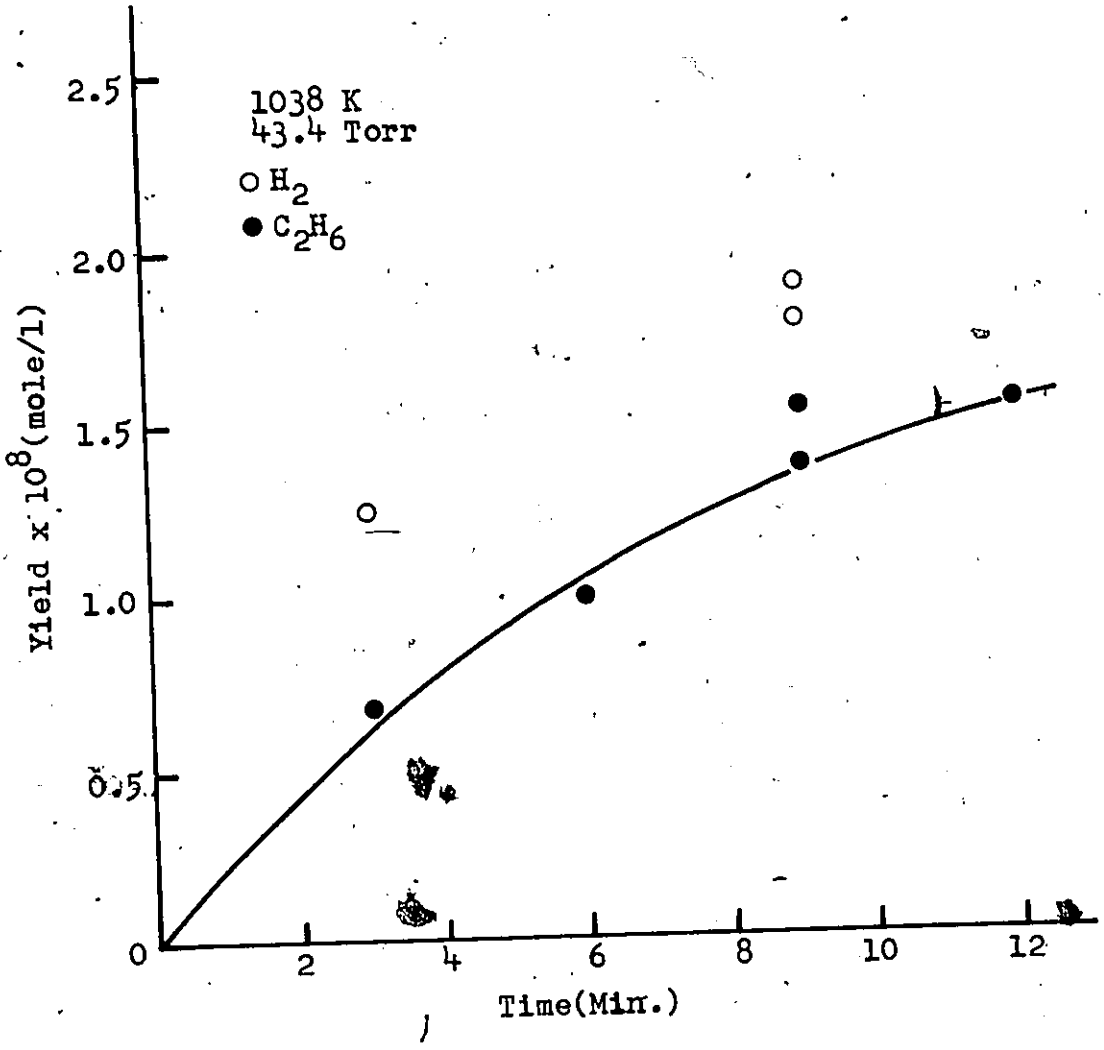
1038 K
43.4 Torr
○ H_2
● C_2H_6
Yield x 10^8(mole/l)
2.5
2.0
1.5
1.0
0.5
0
2
4
6
8
10
12
Time(Min.)

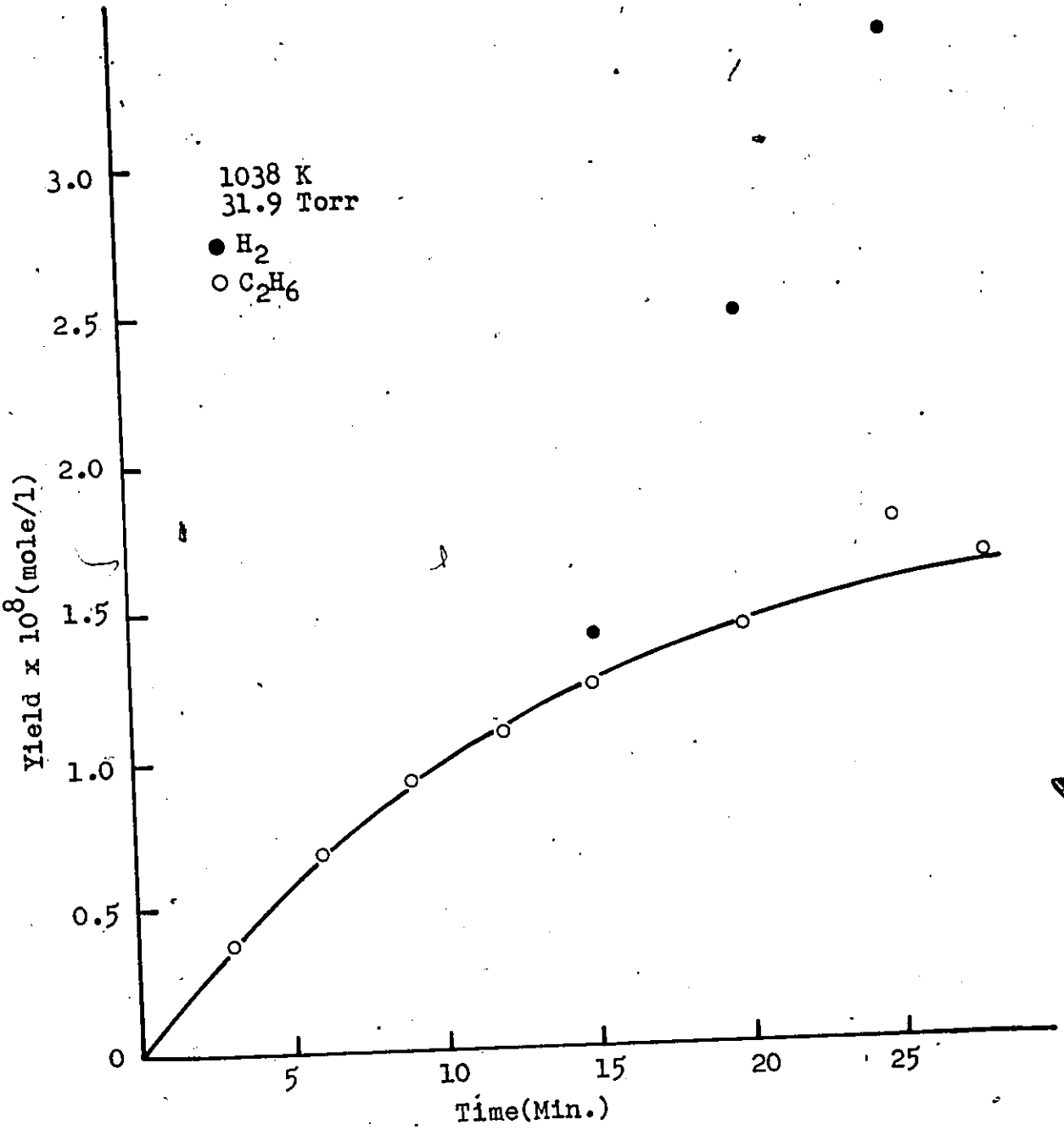
1038 K
31.9 Torr
● H_2
○ C_2H_6
Yield x 10^8(mole/l)
3.0
2.5
2.0
1.5
1.0
0.5
0
5
10
15
20
25
Time(Min.)

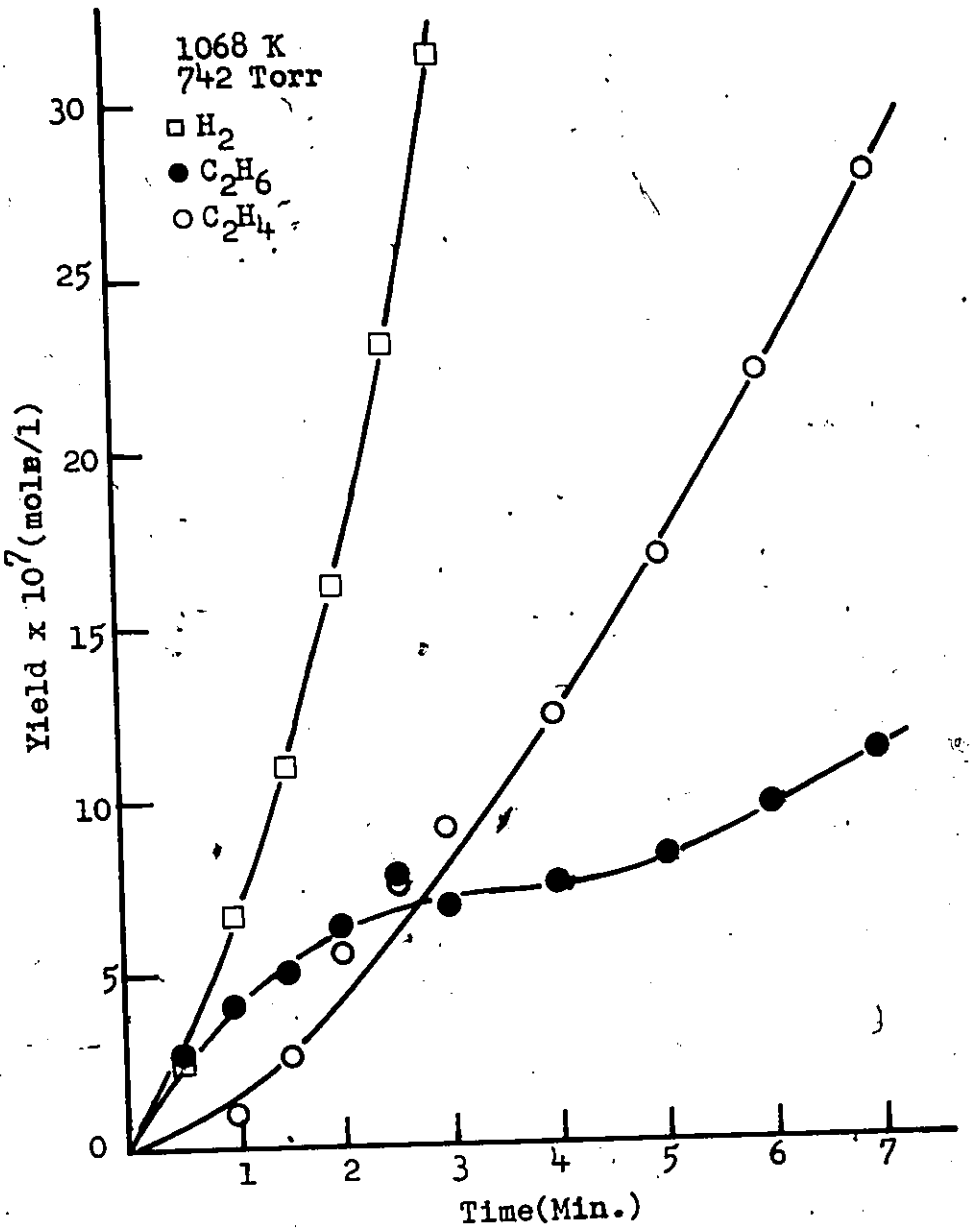
1068 K
742 Torr
□ H_2
● C_2H_6
○ C_2H_4
Yield x 10^7(mole/l)
30
25
20
15
10
5
0
1
2
3
4
5
6
7
Time(Min.)

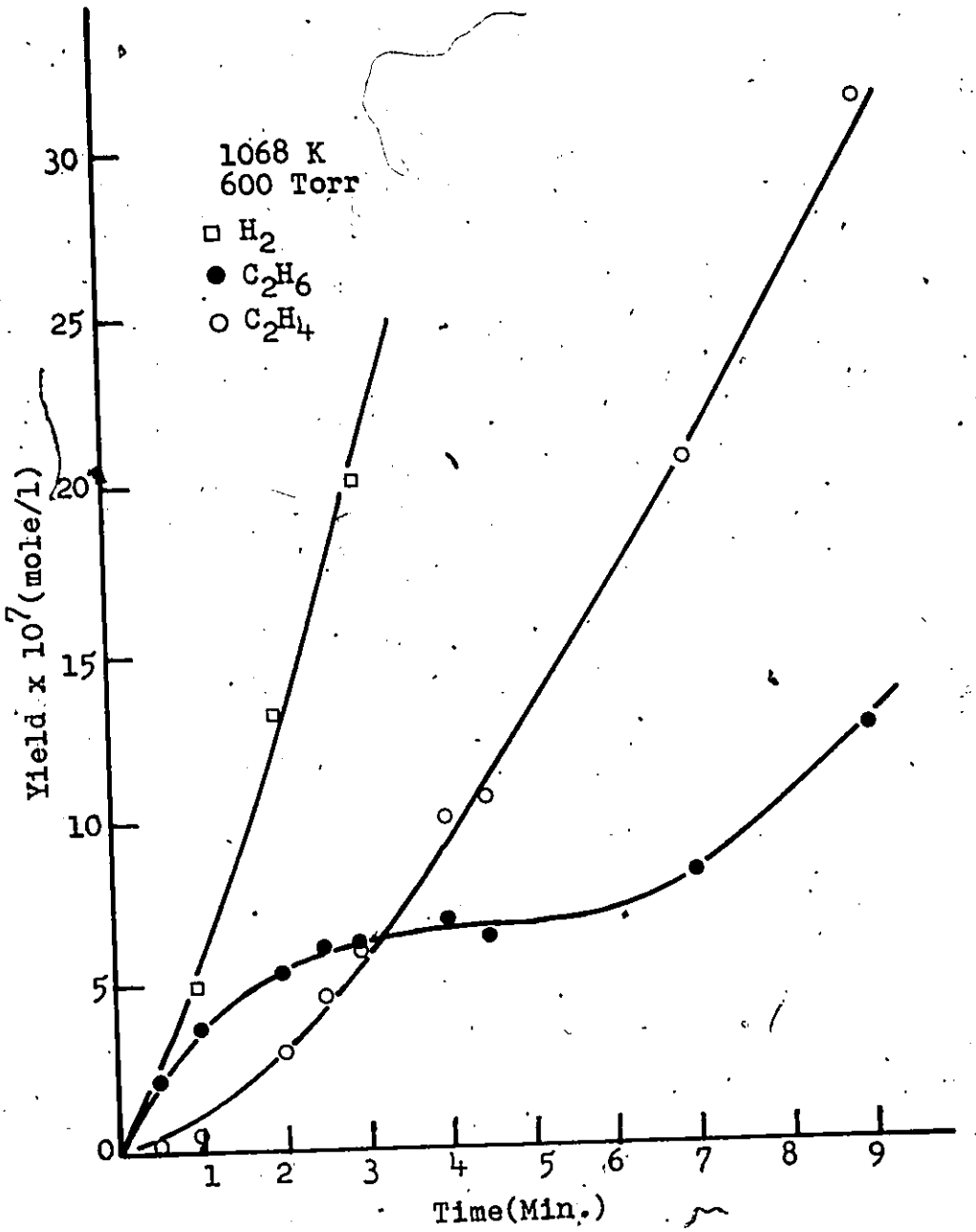
1068 K
600 Torr
□ H_2
● C_2H_6
○ C_2H_4
Yield x 10^7(mole/l)
0
5
10
15
20
25
30
1
2
3
4
5
6
7
8
9
Time(Min.)

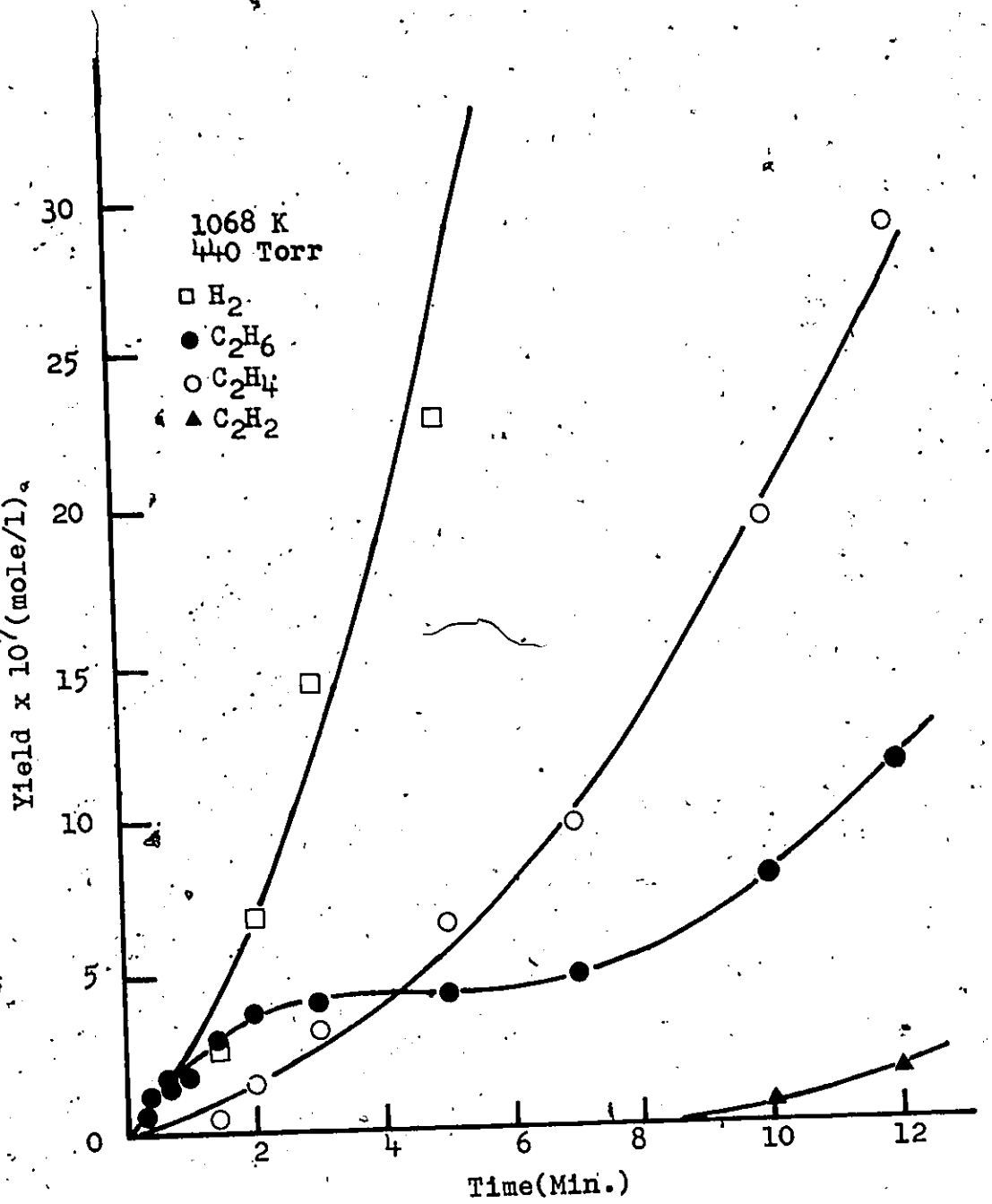
1068 K
440 Torr
□ H_2
● C_2H_6
○ C_2H_4
▲ C_2H_2
Yield x 10^7(mole/l)
Time(Min.)
0
5
10
15
20
25
30
2
4
6
8
10
12

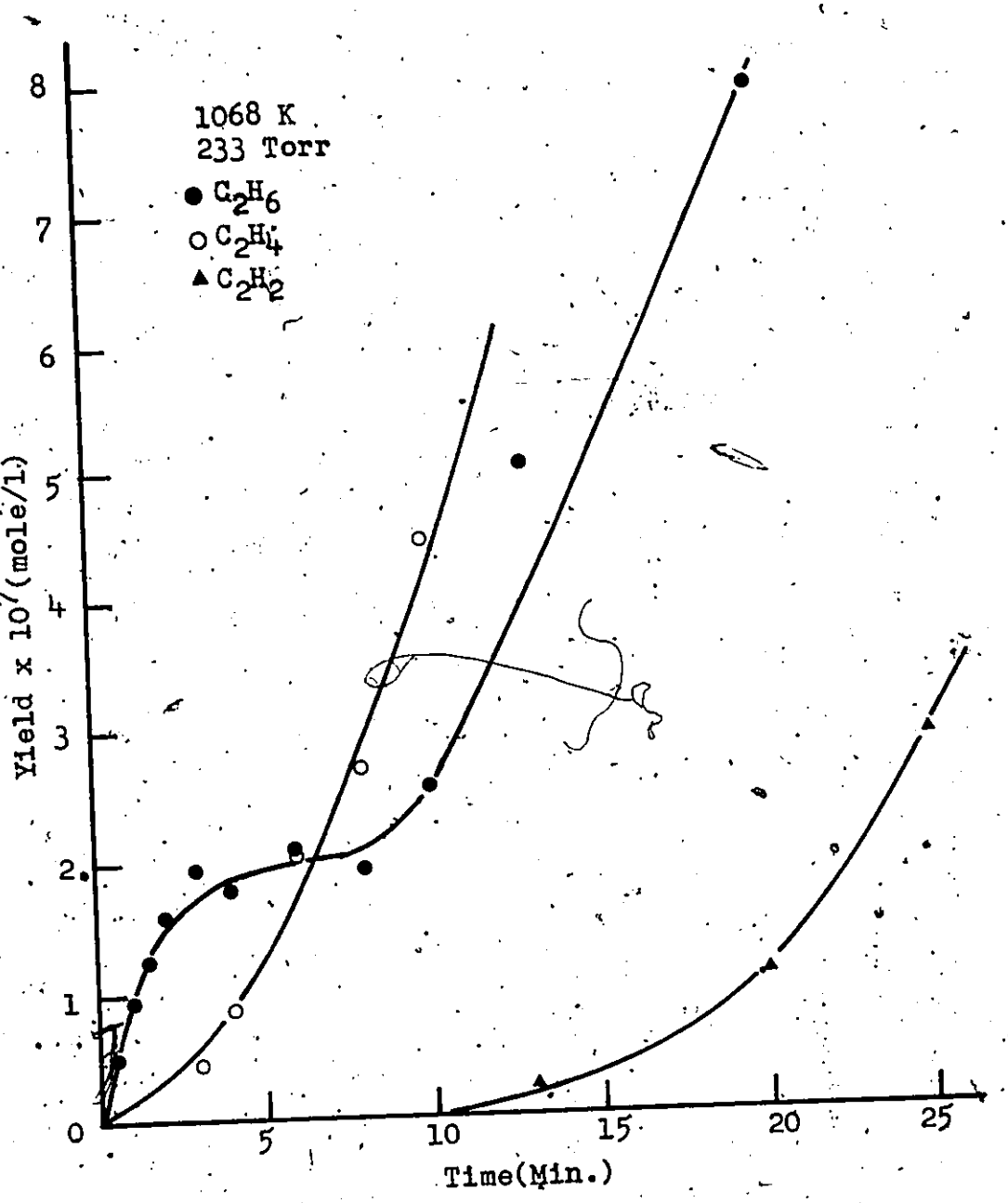
1068 K
233 Torr
● C_2H_6
○ C_2H_4
▲ C_2H_2
Yield x 10^7(mole/l.)
0
1
2
3
4
5
6
7
8
5
10
15
20
25
Time(Min.)

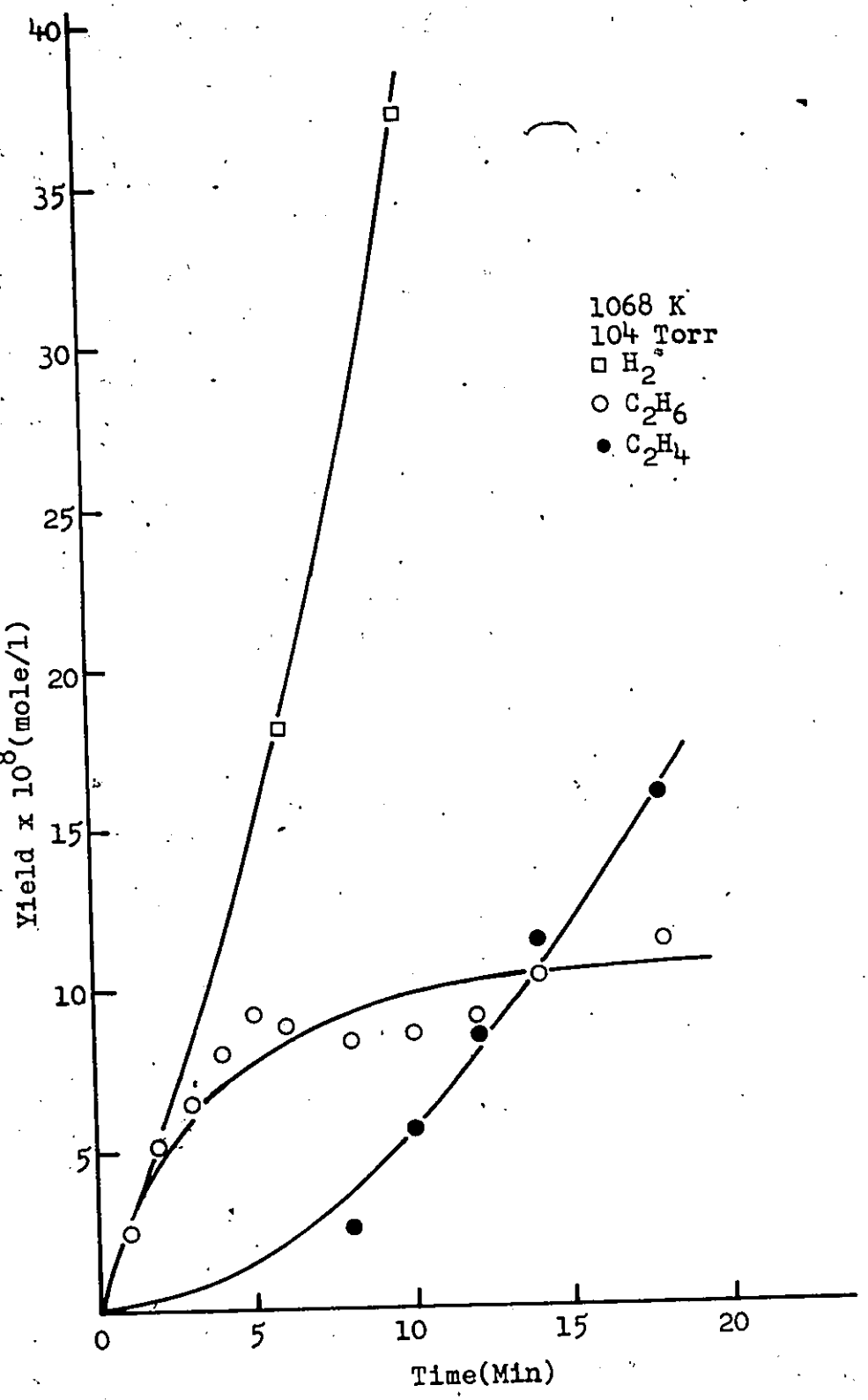
40
35
30
25
20
15
10
5
0
5
10
15
20
Yield x 10^8(mole/l)
Time(Min)
1068 K
104 Torr
□ H_2
○ C_2H_6
● C_2H_4

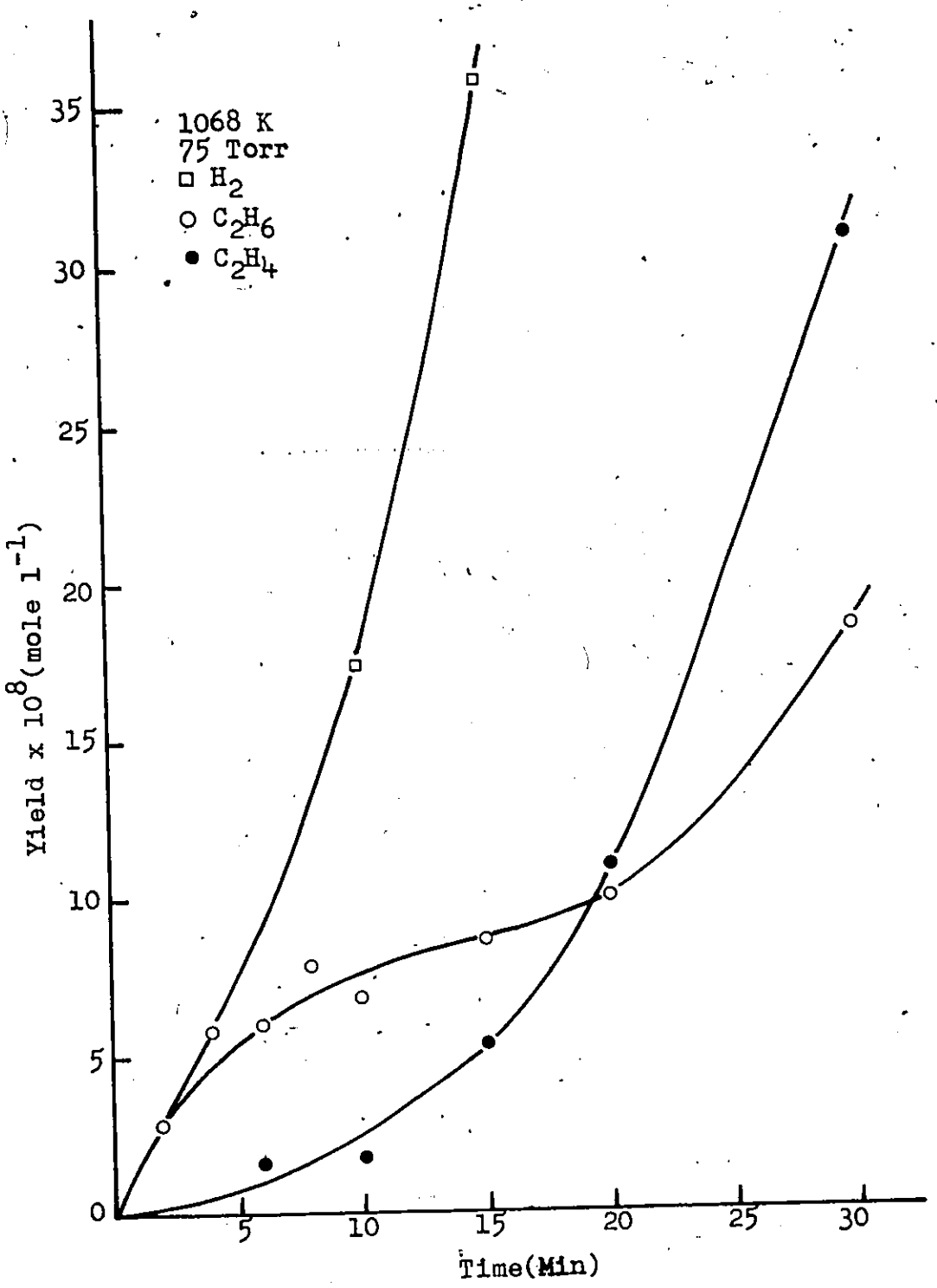
1068 K
75 Torr
□ H_2
○ C_2H_6
● C_2H_4
Yield x 10^8(mole l^{-1})
Time(Min)
0
5
10
15
20
25
30
35

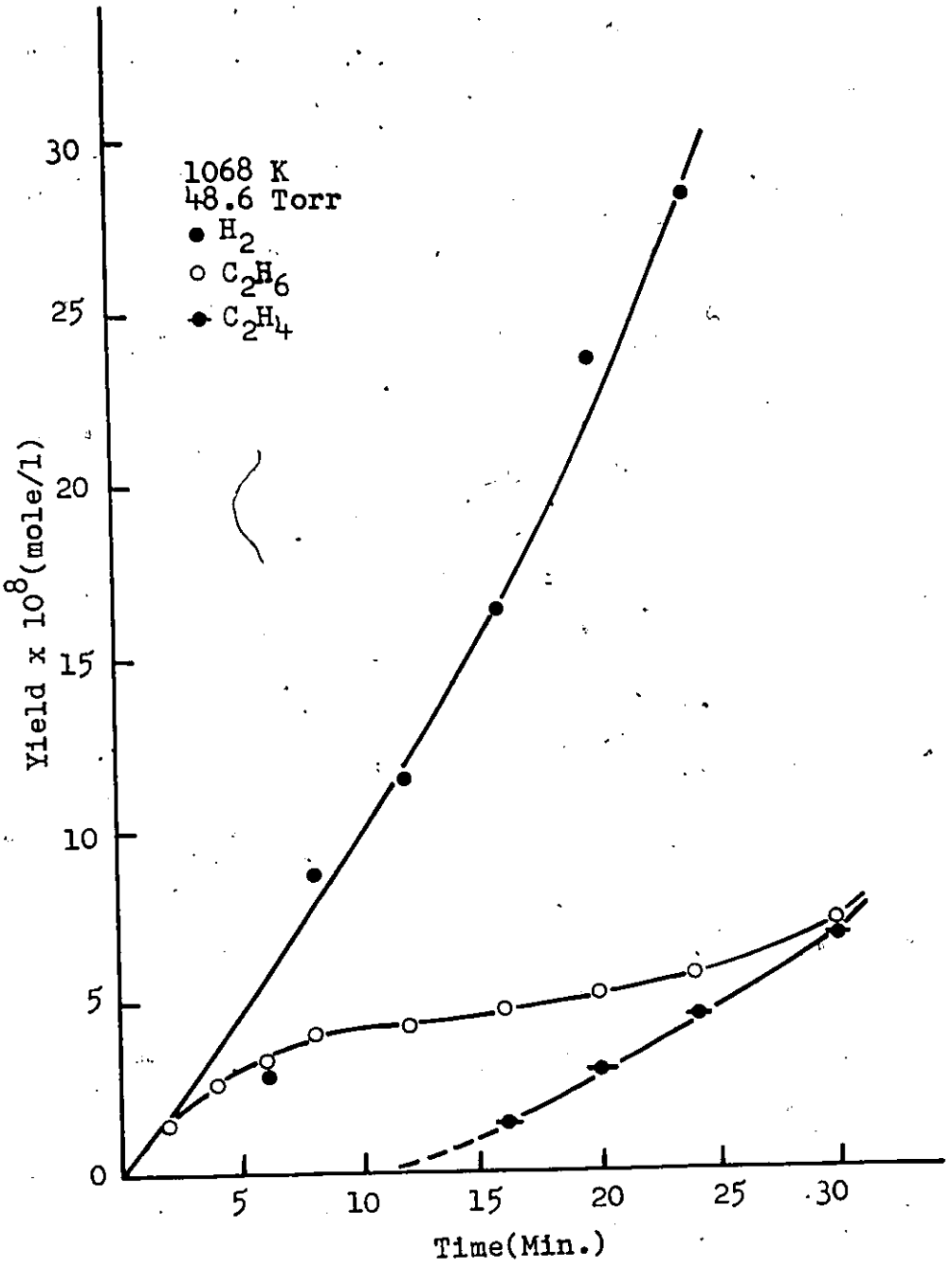
1068 K
48.6 Torr
● H_2
○ C_2H_6
● C_2H_4
Yield x 10^8(mole/l)
0
5
10
15
20
25
30
Time(Min.)

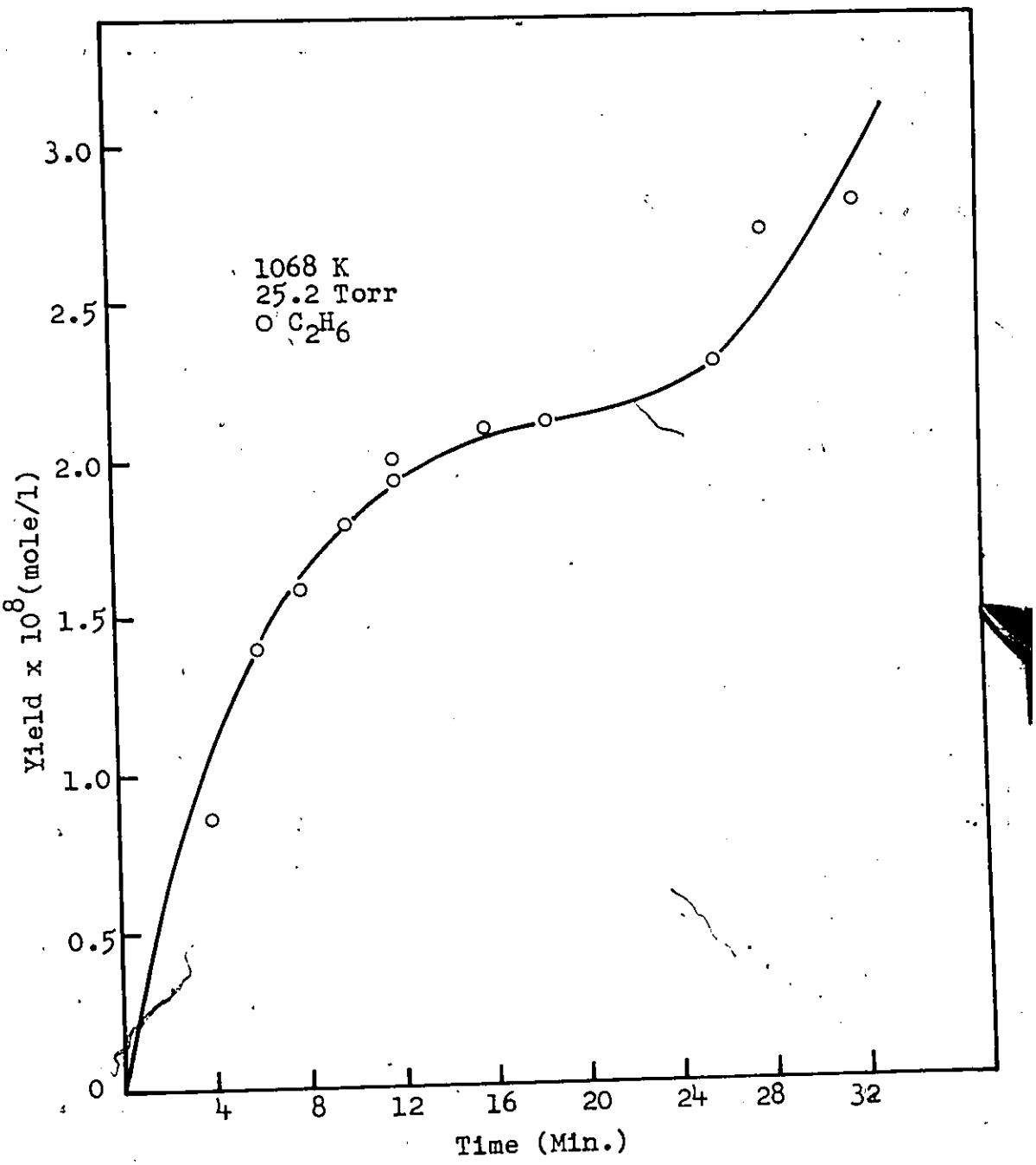
1068 K
25.2 Torr
○ C_2H_6
Yield x 10^8(mole/l)
3.0
2.5
2.0
1.5
1.0
0.5
0
4
8
12
16
20
24
28
32
Time (Min.)

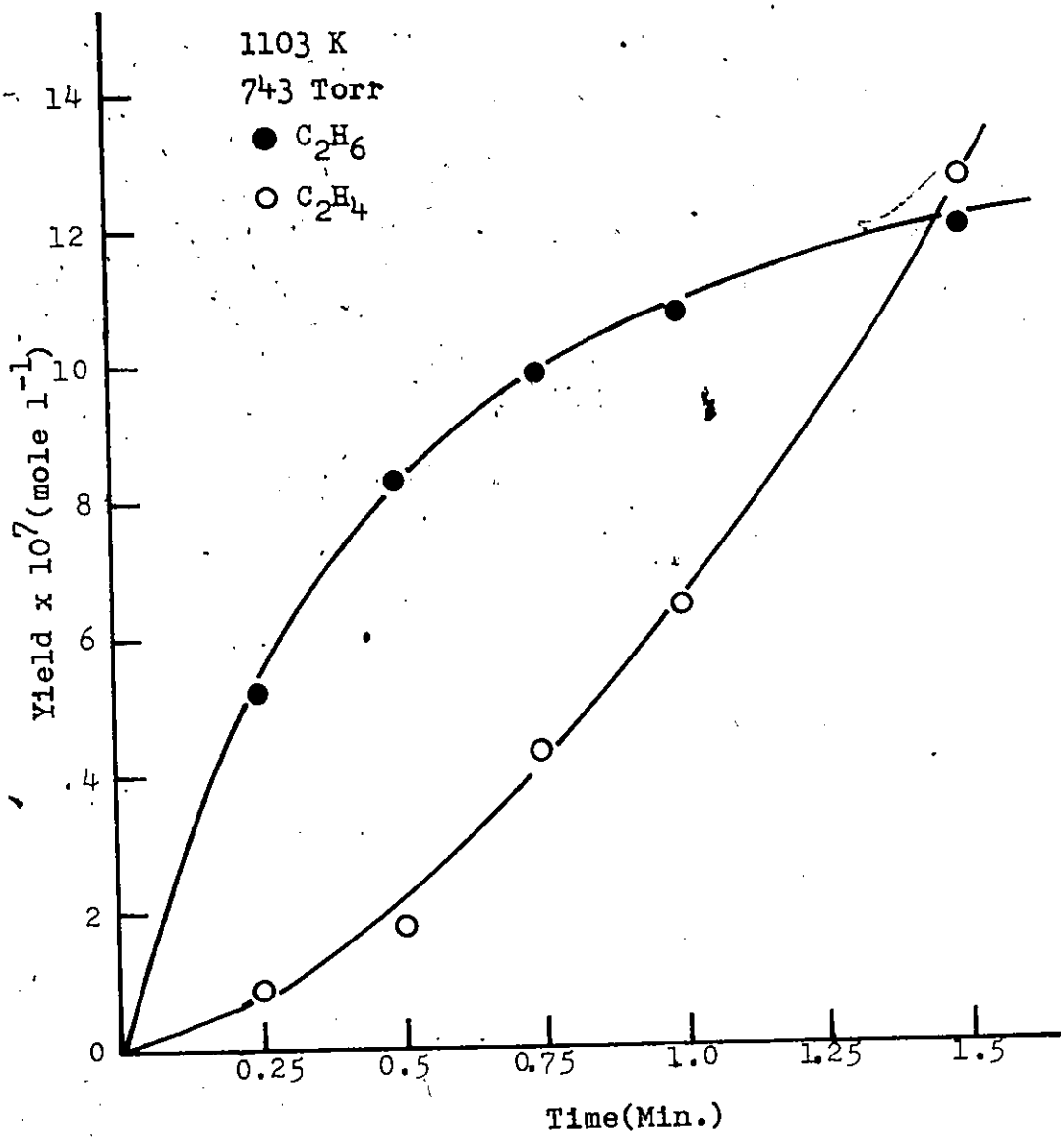
1103 K
743 Torr
● C_2H_6
○ C_2H_4
Yield x 10^7(mole l^{-1})
0
2
4
6
8
10
12
14
0.25
0.5
0.75
1.0
1.25
1.5
Time(Min.)

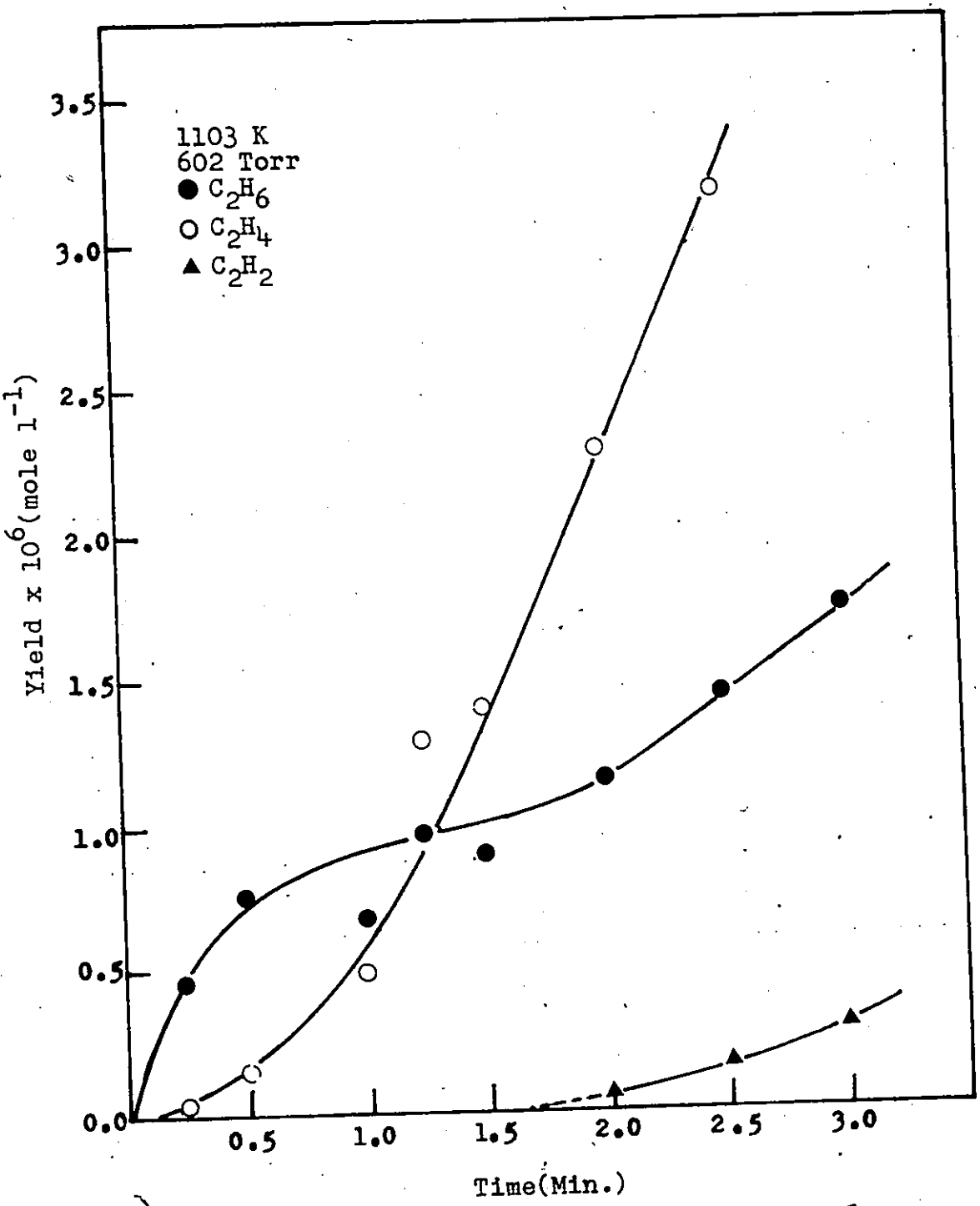
1103 K
602 Torr
● C_2H_6
○ C_2H_4
▲ C_2H_2
Yield x 10^6(mole l^{-1})
Time(Min.)
0.0
0.5
1.0
1.5
2.0
2.5
3.0
3.5

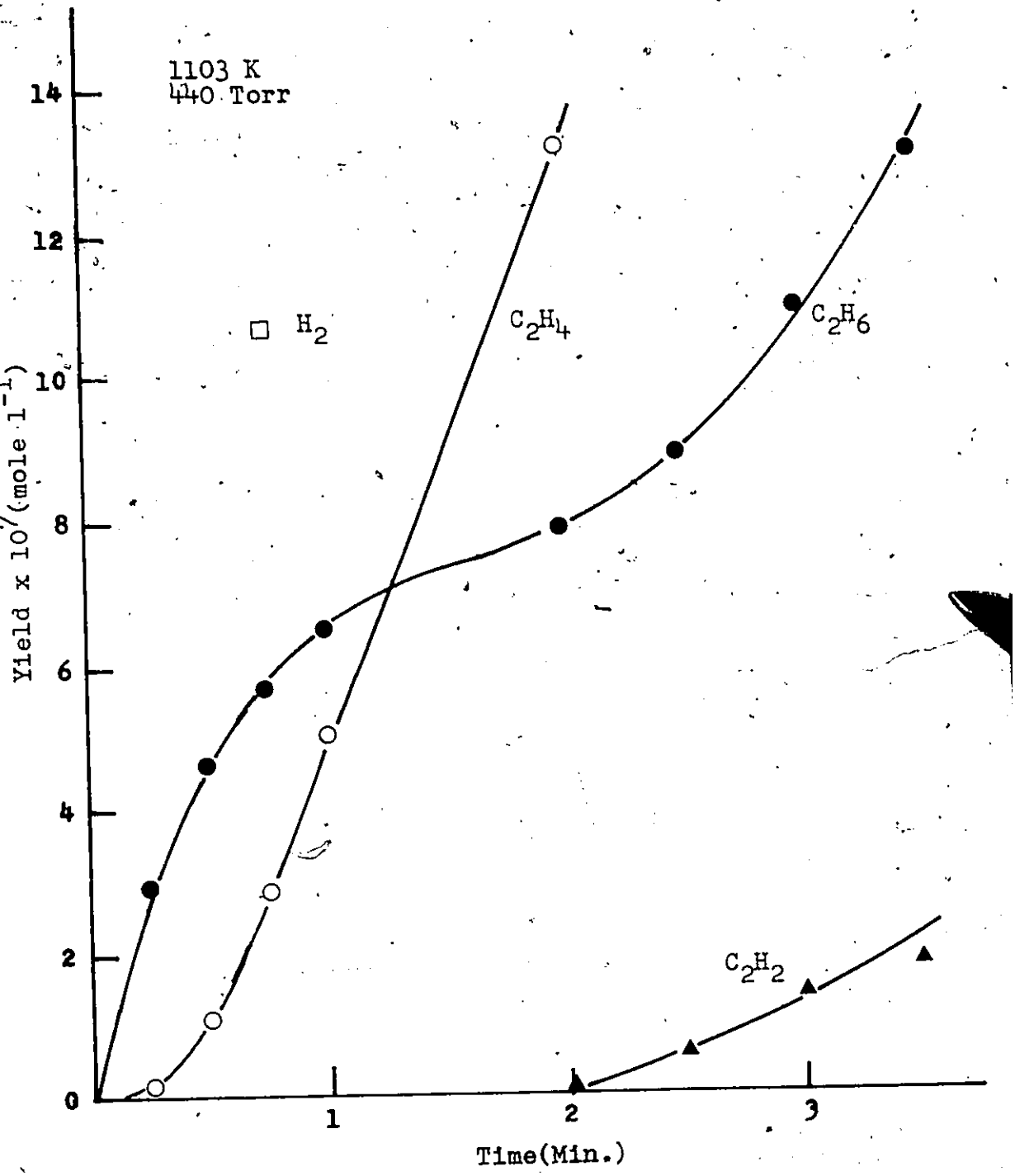
1103 K
440 Torr
□ H_2
C_2H_4
C_2H_6
C_2H_2
Yield x 10^7(mole l^{-1})
0
2
4
6
8
10
12
14
1
2
3
Time(Min.)

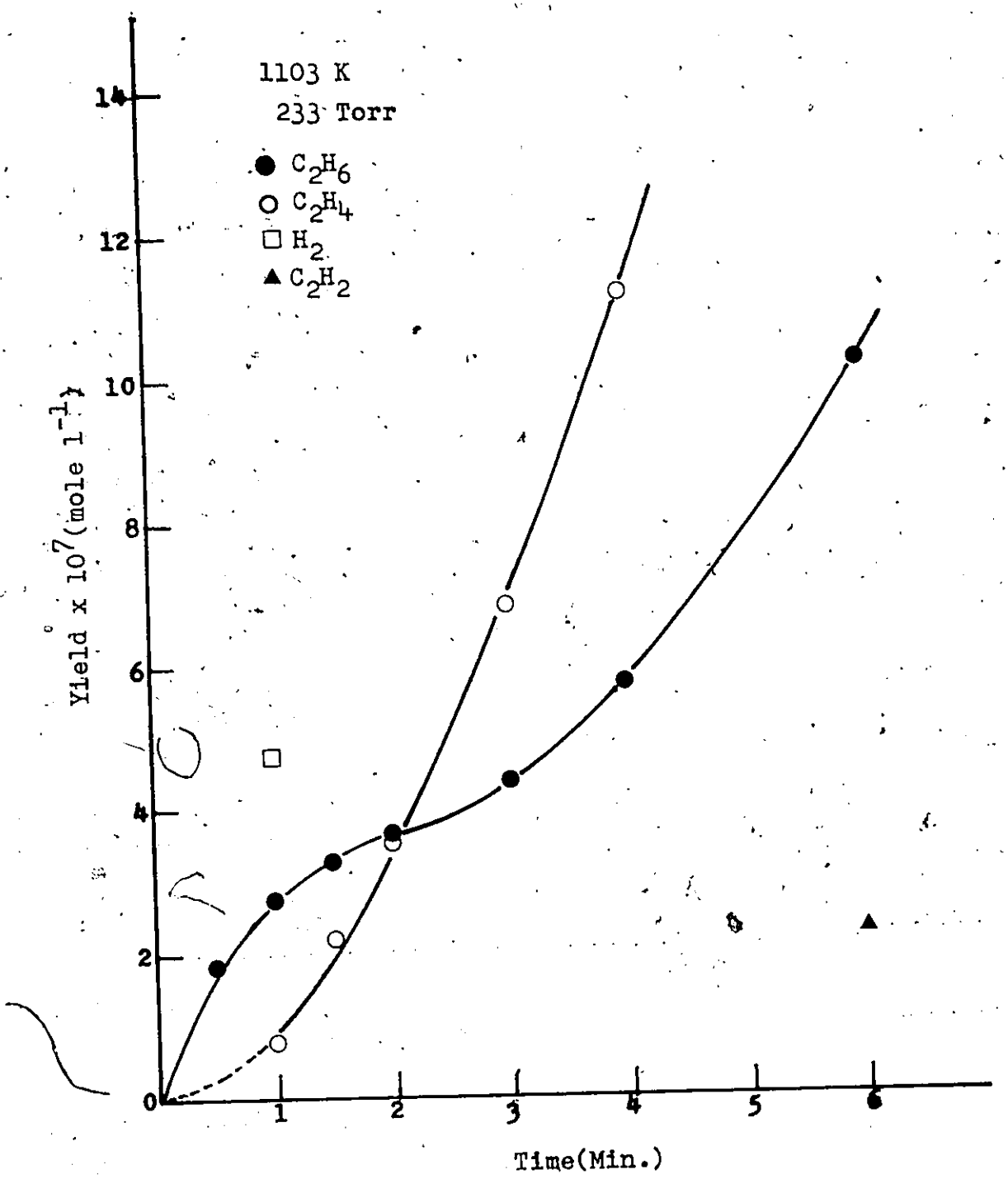
1103 K
233 Torr
C_2H_6
C_2H_4
H_2
C_2H_2
Yield x 10^7(mole l^{-1})
0
2
4
6
8
10
12
14
1
2
3
4
5
6
Time(Min.)

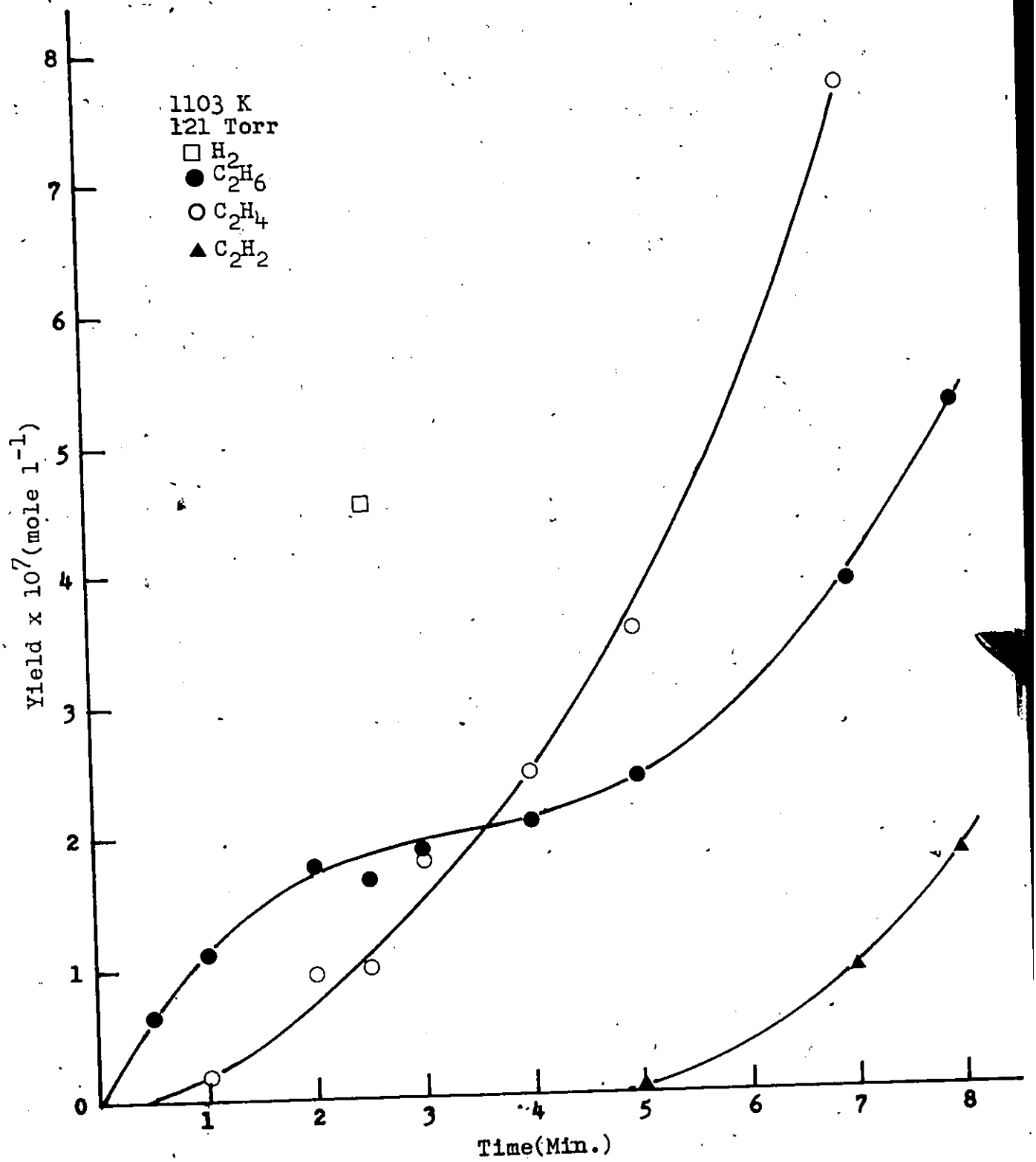
1103 K
121 Torr
□ H_2
● C_2H_6
○ C_2H_4
▲ C_2H_2
Yield x 10^7(mole l^{-1})
Time(Min.)
0
1
2
3
4
5
6
7
8

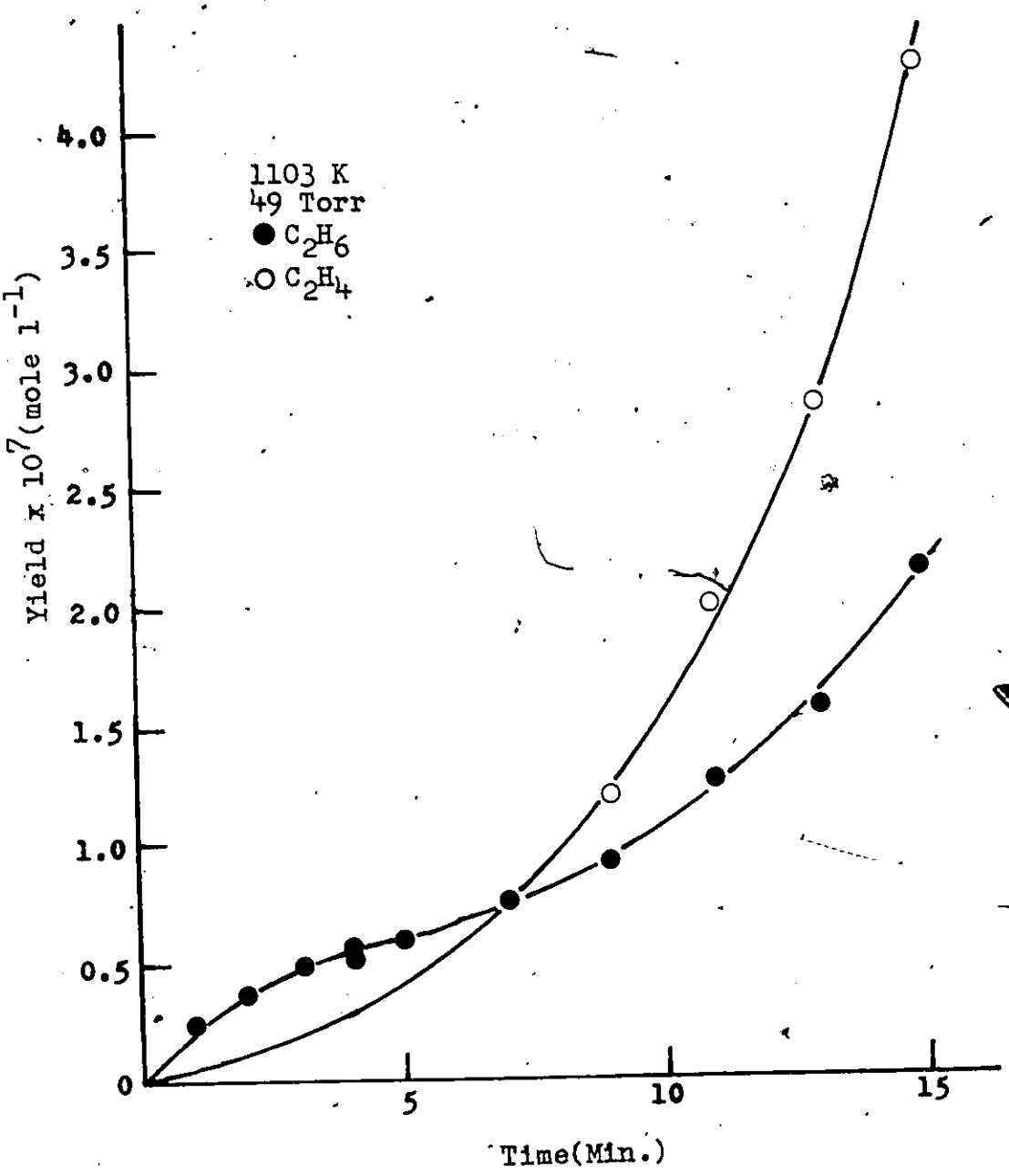
1103 K
49 Torr
● C_2H_6
○ C_2H_4
Yield x 10^7(mole l^{-1})
4.0
3.5
3.0
2.5
2.0
1.5
1.0
0.5
0
5
10
15
Time(Min.)

APPENDIX 2

INTERVAL EXPERIMENT[a]

Temp (K)	Press (Torr)	Time (Min)	C_2H_6	C_2H_4	C_2H_2	C_3H_6	C_3H_4
			Yield x 10^8 (mole/l)				
1038	443	6.00	28.7	18.0	0.18	0.84	*
		6.00	28.2	16.8	0.28	0.80	*
		6.00	28.1	16.8	0.20	0.69	*
		6.00	28.1	16.3	0.18	0.78	*
		6.00	28.2	17.3	-	0.64	*
		6.00	28.2	16.4	0.23	0.69	*
		6.00	28.3	16.1	0.23	0.62	*
		6.00	28.4	17.1	0.23	0.70	
	442	12.00	35.1	50.9	1.48	7.64	0.96
		12.00	35.0	51.3	1.42	7.35	0.81
		12.15	34.7	51.0	1.41	7.43	0.87
		12.00	34.5	50.1	1.48	7.04	0.85
	443	24.00	56.2	130.7	7.77	36.8	7.25
		24.00	58.3	138.2	7.62	38.0	7.29
		24.00	57.4	132.8	7.50	35.8	6.78
		24.00	57.7	135.3	8.04	37.6	7.22
	443	36.00	120.8	376.5	35.1	111.9	19.7
		36.00	122.9	392.6	37.8	117.1	20.6
		36.00	124.1	397.3	38.2	117.6	20.8
		36.00	123.2	393.3	33.9	115.4	20.7

a (Interval experiment) means that any possible carbon deposit was not burned off after each experiment.

APPENDIX 3

CH_4-CD_4 ISOTOPE EXCHANGE FUNDAMENTAL DATA

T (K)	Time (Min.)	m/e 20	19	18	17	16	15	14
880	5	1248	45.3	769.8	34.6	1555.3	1035.4	42.45
		(CD_4:CD_3H:CH_3D:CH_4 = 24.56: 0.0213: - : 30.22)						
	10	1430	54.3	890.1	44.7	1651.6	188.9	48.1
		(CD_4:CD_3H:CH_3D:CH_4 = 26.42: 0.089: 0.0937: 28.19)						
	20	1192	54.7	706.6	48.0	1505.4	990.2	40.5
		(CD_4:CD_3H:CH_3D:CH_4 = 24.2: 0.273: 0.140: 30.2)						
	30	1205	59.0	757.4	57.2	1553	1063	42.0
		(CD_4:CD_3H:CH_3D:CH_4 = 23.9: 0.343: 0.424: 30.12)						
	40	995.8	50.8	610.4	51.2	1245.1	815.5	33.54
		(CD_4:CD_3H:CH_3D:CH_4 = 24.3: 0.432: 0.344: 29.7)						
	50	1215	68.6	739	69.9	1544	1002	41.2
		(CD_4:CD_3H:CH_3D:CH_4 = 24.0: 0.525: 0.423: 29.84)						
	61.5	859	41.5	522	38.0	1105	731	30.8
		(CD_4:CD_3H:CH_3D:CH_4 = 24.0: 0.33: 0.193: 30.3)						
957	0	353	12.6	256	12.7	415	288.4	12.6
		(CD_4:CD_3H:CH_3D:CH_4 = 25.4: 0: 0: 29.4)						
	20	418	24.1	241.3	27.3	502.1	342	14.7
		(CD_4:CD_3H:CH_3D:CH_4 = 24.8: 0.585: 0.623: 28.8)						
	40	664	43.4	475.5	54.6	802.6	539.5	24.6
		(CD_4:CD_3H:CH_3D:CH_4 = 24.54: 0.769: 0.934: 28.6)						
	60	383	32	258	40.2	460.7	308.4	14.0
		(CD_4:CD_3H:CH_3D:CH_4 = 24.36: 1.21: 1.26: 28.0)						
	80	458	50	312	67.7	570	358	17.2
		(CD_4:CD_3H:CH_3D:CH_4 = 23.6: 1.76: 1.91: 27.6)						

APPENDIX 3
CONTINUED

T (K)	Time (Min.)	m/e 20	19	18	17	16	15	14
995	10	428	33.4	314	44.8	535	358	15.7
			(CD_4:CD_3H:CH_3D:CH_4 = 23.9: 1.05: 1.28: 28.5)					
	20	396	51.1	302	71.6	527	342	15.0
			(CD_4:CD_3H:CH_3D:CH_4 = 22.5: 2.14: 1.79: 28.3)					
	30	376	62.3	288	89.2	491	316	13.8
			(CD_4:CD_3H:CH_3D:CH_4 = 22.3: 2.93: 3.14: 26.5)					
	40	334	71.8	273	110.7	470	299	13.4
			(CD_4:CD_3H:CH_3D:CH_4 = 20.8: 3.77: 4.34: 25.9)					
	50	336	85.7	281	132.7	476	296	13.6
			(CD_4:CD_3H:CH_3D:CH_4 = 20.6: 4.55: 5.03: 24.6)					
1038	4	18.6	2.2	14.4	2.45	24.9	16.1	0.8
			(CD_4:CD_3H:CH_3D:CH_4 = 23.1: 0.87: 1.48: 29.4)					
	8	16.4	2.8	15.2	4.0	23.8	15.8	0.6
			(CD_4:CD_3H:CH_3D:CH_4 = 21.3: 1.95: 3.15: 28.4)					
	16	56.0	17.1	49	23.7	82.0	52	2.4
			(CD_4:CD_3H:CH_3D:CH_4 = 19.9: 4.49: 5.06: 25.3)					
	24	16.6	7.72	14.0	12.4	27.6	16.1	0.94
			(CD_4:CD_3H:CH_3D:CH_4 = 17.2: 6.63: 8.51: 22.5)					

APPENDIX 3
CONTINUED

T (K)	Time (Min.)	m/e 20	19	18	17	16	15	14
1068	0.5	14.9	0.55	16.0	1.75	20.1	13.5	0.6
			(CD_4:CD_3H:CH_3D:CH_4 = 23.2: 0.15: 1.90: 29.5)					
	1.0	17.7	1.84	15.5	2.15	24.6	15.4	-
			(CD_4:CD_3H:CH_3D:CH_4 = 22.3: 1.64: 1.11: 29.7)					
	2.0	28.3	2.54	8.89	4.33	30.0	25.6	1.48
			(CD_4:CD_3H:CH_3D:CH_4 = 22.1: 1.31: 1.95: 29.4)					
	3.5	21.7	3.93	28.4	5.78	32.2	20.2	1.0
			(CD_4:CD_3H:CH_3D:CH_4 = 20.6: 3.10: 3.18: 27.9)					
	5.0	27.5	6.69	29.6	10.1	42.2	26.3	1.5
			(CD_4:CD_3H:CH_3D:CH_4 = 19.6: 4.18: 4.33: 26.7)					
1103	0.26	85.2	5.0	57.2	6.0	119.2	73.8	2.67
			(CD_4:CD_3H:CH_3D:CH_4 = 22.71: 0.64: 0.71: 30.7)					
	0.4	59.8	4.2	43	6	83.2	54	1.8
			(CD_4:CD_3H:CH_3D:CH_4 = 22.6: 0.90: 1.03: 30.2)					
	0.5	80	6.9	53.5	9.5	110.6	71.6	3.0
			(CD_4:CD_3H:CH_3D:CH_4 = 22.5: 1.27: 1.30: 29.7)					
	0.77	35.6	4.5	23.0	6.3	49.2	30.7	1.8
			(CD_4:CD_3H:CH_3D:CH_4 = 21.25: 2.2: 2.1: 29.2)					
	1.0	90.5	11.3	-5.1	20.4	127.3	81.2	2.9
			(CD_4:CD_3H:CH_3D:CH_4 = 21.27: 2.66: 2.92: 27.9)					
	1.5	38.4	7.33	5.12	13.3	57.3	35.3	1.0
			(CD_4:CD_3H:CH_3D:CH_4 = 19.89: 3.80: 4.45: 26.66)					

Appendix 4

$$CH_4 \underset{-1b}{\overset{1b}{\rightleftharpoons}} CH_2 + H_2$$

ΔH_f	-17.9	93	0
S^o	44.5	43.3	31.2
C_p	12.87	9.3	7.05

ΔH^o = 110.9 kcal/mole

ΔS = 30.0 e.u.

ΔC_p = 3.48 cal/deg mole

$$\Delta H_{1000} = \Delta H_{298} + \Delta C_p \Delta T$$

$$= 113.3$$

$$\Delta S_{1000} = \Delta S_{298} + \Delta C_p \ln \frac{T_2}{T_1}$$

Change from pressure units to concentration units.

$$\Delta H_c = \Delta H_p - \Delta nRT = 111.3 \text{ kcal/mole}$$

$$\Delta S_c = \Delta S_p - \Delta nR - \Delta nR \ln RT$$

$$= 23.46 \text{ cal/mole}$$

$$k_{1b}/k_{-1b} = K = e^{\Delta S/R} e^{-\Delta H/RT}$$

$$k_{-1b} = 10^{9.62}$$

$$k_{1b} = 10^{14.76}\ 10^{-1130/2.3RT}$$

at 1000°K $\log k_{1b} = -9.61$

Appendix 5

Expression for the rat e of formation of ethane with the alternative initiation step [1b]..

1b	$CH_4 \longrightarrow CH_2 + H_2$
2	$CH_2 + CH_4 \longrightarrow C_2H_6^*$
3	$C_2H_6^* \longrightarrow 2\ CH_3$
4	$C_2H_6^* + M \longrightarrow C_2H_6 + M$
5	$2CH_3 \longrightarrow C_2H_6$

Steady state in Radical	Equation
CH_2	$[CH_2] = k_{1b}/k_2$
$[C_2H_6]^*$	$[C_2H_6]^* = \dfrac{k_{1b}[CH_4]}{k_3 + k_4[CH_4]}$
CH_3	$2k_3[C_2H_6]^* = k_5[CH_3]^2$

Rate of formation of ethane $= k_5[CH_3]^2 + k_4[C_2H_6]^*[M]$

$$= \frac{k_3k_{1b}[CH_4]}{k_3 + k_4[CH_4]} + \frac{k_4k_{1b}[CH_4][M]}{k_3 + k_4[CH_4]}$$

In this case $[M] = [CH_4]$,

therefore $R^o_{C_2H_6} = k_{1b}[CH_4]$